INCREASED THERAPEUTIC INDEX OF TYROSINE KINASE INHIBITORS IN CML THROUGH MEMBRANE TRANSPORTER UPTAKE

A THESIS SUBMITTED TO THE UNIVERSITY OF MANCHESTER

FOR THE DEGREE OF MASTER OF PHILOSOPHY

IN THE FACULTY OF BIOLOGY, MEDICINE AND HEALTH

2017

Arezoo Shajiei

Faculty of Biology, Medicine and Health

School of Biological Sciences

TABLE OF CONTENTS

The final word count: 27,866 words

LIST OF FIGURES

LIST OF TABLES

ABSTRACT

The University of Manchester

Author: Arezoo Shajiei

Degree title: MPhil in Epidemiology

Thesis title: Increased therapeutic index of tyrosine kinase inhibitors in CML through membrane transporter uptake

Year: 2016

Chronic myeloid leukaemia (CML) is a hematopoietic stem cell disease, distinguished by the BCR-ABL gene and the presence of the Philadelphia chromosome. Recent studies have revealed that CML resistance is due to up regulation of the membrane and drug transporters ABCB1 and ABCG2, which have a critical role in drug resistance. Indeed, there is strong evidence suggesting drug transport occurs mainly via proteinaceous carriers. In this regards, the MayBridge Rule of 3 Fragment Library (May Ro3) is a relatively small collection of chemical moieties that are pharmacophore rich and 'metabolite-like'. As a result, in the current project we demonstrate the application of 'binary weapons' which are small non-toxic molecular agents with high affinity to both transporters and imatinib. The interaction between the binary weapon and imatinib enhances the anti-cancer impact of imatinib. In this research study, the first 500 fragments from the Maybridge Fragment (MBF) library was screened to find suitable candidates for enhancing the imatinib effect on K562 cell line while the MBFs alone possessed no toxic effect. Firstly the screenings were performed by pooling fragments, in which we tested the K562 cell enhanced toxicity of imatinib plus MBFs via MTT assays and then those selected pools were analysed in single MBF screenings. Then titration assays of those selected single hits were performed to find the most effective concentration for selected hits. Finally, the selected single hits were used in qPCR to check the effect on expression of candidate membrane associated transporters that were identified from literature review. Moreover, in all experiments SH-SY5Y cells and the drug cisplatin were employed as controls for K562 and imatinib.

In pooled screens for K562 and imatinib, 40 fragments were selected and these pools were further investigated using single MBF screenings and 6 of the 40 MBFs showed the desired effect. Following titration experiments, 2 MBFs were shown to carry the least toxicity even in the highest concentrations, so they were selected as candidates for investigation of the impact on the expression of transporters genes. The expression of transporter mRNAs was investigated and showed some significant dys-regulation of influx or efflux transporters. Compared to the control group, when K562 cells were treated with MBFs (161 or 247), all transporters, efflux and influx, showed downregulation. However, treatment with imatinib and MBF No. 161 for 1 hour showed downregulation for ABCB10, BCR-ABL and SLCO1A2SLCO1A2(P-value = 0.001). However, the expression for other transporters were not dysregulated (no upregulation no downregulation) (P value=0.001), showing the same expression with the control group. Moreover, treatment of K562 cells with imatinib and MBF hit No. 247, all influx and efflux transporters were downregulated significantly. Lastly, the BCR-ABL expression in all different conditions showed downregulation.

In this research programme, K562 served as target cells and as a model of CML while SH-SHY5Y were employed as non-target cells. Through using the 2 selected candidate MBFs in conjunction with imatinib, the cytotoxicity of imatinib was shown to prevail within K562 cells and not SH-SHY5Y cells; in essence increment of the therapeutic index of imatinib was demonstrated.

DECLARATION

No portion of the work referred to in the thesis has been submitted in support of an application for another degree or qualification of this or any other university or other institute of learning.

COPYRIGHT

The following four notes on copyright and the ownership of intellectual property rights must be included as written below:

i. The author of this thesis (including any appendices and/or schedules to this thesis) owns certain copyright or related rights in it (the "Copyright") and s/he has given The University of Manchester certain rights to use such Copyright, including for administrative purposes.

ii. Copies of this thesis, either in full or in extracts and whether in hard or electronic copy, may be made only in accordance with the Copyright, Designs and Patents Act 1988 (as amended) and regulations issued under it or, where appropriate, in accordance with licensing agreements which the University has from time to time. This page must form part of any such copies made.

iii. The ownership of certain Copyright, patents, designs, trademarks and other intellectual property (the "Intellectual Property") and any reproductions of copyright works in the thesis, for example graphs and tables ("Reproductions"), which may be described in this thesis, may not be owned by the author and may be owned by third parties. Such Intellectual Property and Reproductions cannot and must not be made available for use without the prior written permission of the owner(s) of the relevant Intellectual Property and/or Reproductions.

iv. Further information on the conditions under which disclosure, publication and commercialization of this thesis, the Copyright and any Intellectual Property University IP Policy (see http://documents.manchester.ac.uk/display.aspx?DocID=24420), in any relevant Thesis restriction declarations deposited in the University Library, The University Library's regulations (see http://www.library.manchester.ac.uk/about/regulations/) and in The University's policy on Presentation of Theses.

ACKNOWLEDGEMENTS

I would like to thank my supervisors, Dr. Philip Day, Dr. Malkhey Verma and Professor Douglas Kell, for their guidance, support, great patience, and confidence in me over the course of this project.

Problems that at times seemed insurmountable have always been overcome with reference to one person: Mrs. Fiona Marriage and I cannot thank her enough for imparting her experience and knowledge, solves any logistical/technical challenges.

Dr. Howbeer Muhamad Ali and Dr. David Ellis were also kind enough to give sage advice and help when necessary, for which I am very grateful.

I am lucky to have met so many friendly and supportive people in the lab environment and I am proud to call them my friends: Justine, Sunil, Ming, Caro and Alejandro.

Finally, I am also grateful to Dr. Neil Dixon my adviser for his constant support.

Last and most importantly, I thank my parents, for their support through some tough times, their belief in me, and endless love. I would not have become the person I am without them; I am a very fortunate daughter.

DEDICATION

This thesis is dedicated to:

To my lovely parents for their support, worship and encouragement from thousand miles away.

ABBREVIATIONS

ABC	ATP-binding cassette superfamily
ABCB1	ATP-Binding Cassette, Sub-Family B member 1
ABCC1	ATP-Binding Cassette, Sub-Family C member 1
ABCG2	ATP-binding cassette sub-family G member 2
ABL	Abelson
ACTB	Beta-Actin
AP	Accelerated Phase
ATCC	American Type Culture Collection
ATP	Adenosine triphosphate
B2M	βeta 2 micoglobulin
BCR	Breakpoint cluster region
BCRP	breast cancer resistance protein
BLAST	Basic Local Alignment Search Tool
cDNA	Complementary DNA
CML	Chronic myeloid leukaemia
CMPK1	Cytidine monophosphate kinase 1
CP	Chronic Phase
Cq	Cycle Quantification
dATP	Deoxyadenosine triphosphate
dCDP	Deoxycytidine diphosphate
ddI	Didanosine
dFdU	Inactive 2'-2'-difluorodeoxyuridine
dGTP	Deoxyguanosine triphosphate
DHEA-s	Dehydroepiandrosterone sulfate
DHFR	Dihydrofolate reductase
DMEM	Dulbecco's modified eagle's medium
dNDP	Deoxynucleotide diphosphate
dNTP	Deoxynucleotide triphosphate
EGF	Epidermal growth factor
ERK	Extracellular Regulated Kinases
Ev	Efficiency Value
FBS	Foetal bovine serum
FDA	Food and drug administration
GAPDH	Glyceraldehyde 3 phosphate dehydrogenase
H	Hour
HMBS	Hydroxymethyl-bilane synthase
HPRT1	Hypoxanthine phosphoribosyl transferase 1
IFN- α	Interferon-gamma
IGF	insulin-like growth factor
K562	Human chronic myelogenous leukaemia blast crisis cell line
KD	kilo Dalton
LNA	Locked nucleic acid
LNT	Linear no-threshold

MACCS	Molecular ACCess System
May Ro3	MayBridge Rule of 3 Fragment Library
MBF	Maybridge Ro3 2500 Diversity Fragment Library
MDR	Multi drug resistant
Min	Minute
MRD	Minimal residual disease
Micro Litter	ML
mRNA	Messenger RNA
MRP	Multidrug resistance proteins
MRP1	Multi-drug Resistance-associated Protein
MTT	Microculture Tetrazolium Assay
NCBI	National Centre for Biotechnology Information
NDP	Ribonucleotide diphosphate
NMTS	Nearest metabolite Tanimoto similarity
NT5Cs	Cytosolic 5'-nucleotidases
OATPs	Organic anion transporter polypeptides
OCT-1	Organic Cation Transporter 1
Oligo	Oligonucleotide
PBS	Phosphate buffered saline
PCR	Polymerase chain reaction
PDGF	Platelet-derived growth factor
P-gp	P-glycoprotein
PH+	Philadelphia chromosome–positive
PI3K	Phosphoinositide 3-kinase
RIN	RNA Integrity Number
RNA	Ribonucleic acid
Ro3	Rule of Three
RPL13A	Ribosomal protein L13a
RPL32	Ribosomal protein L32
rpm	Revolutions per minute
RPMI	Roswell park memorial institute
RT-qPCR	Quantitative Real time polymerase chain reaction
S	Second
SCLO	Solute carrier organic anion
SD	Standard deviation
SDHA	Succinate dehydrogenase complex, subunit A
SH-SY5Y	Human neuroblastoma cell
SLC	Solute carrier superfamily
SNP	Single nucleotide polymorphism
TDF	Tenofovir
TK	Tyrosine kinase
TKI	Tyrosine kinase inhibitor
TMDs	Transmembrane domains
TS	Thymidilate synthase
VGEF	Vascular growth endothelial factor

CHAPTER 1

INTRODUCTION

1.1 CHRONIC MYELOID LEUKAEMIA (CML)

Chronic myeloid leukaemia (CML) is a myeloproliferative disorder of hematopoietic pluripotent stem cells and is one of the most extensively studied neoplasms(1). CML accounts for approximately 15% of all new cases of leukaemia and affects about 1-2:100,000 adults per year. In this disorder, a slight male predominance has been observed (1.4/ 1.3) with a median age at diagnosis of 57-60 years (2-5). CML is characterized by the increased proliferation of mature granulocytes and their originators (6-9). It is genetically characterized by the presence of the reciprocal translocation t(9;22); the Abelson proto-oncogene (abl) on chromosome 9 is translocated to the Breakpoint Cluster Region (bcr) on chromosome 22, forming a fusion gene in which ABL-related tyrosine kinase (TK) activity is constitutively activated(6, 10, 11) (See Figure 1.1).

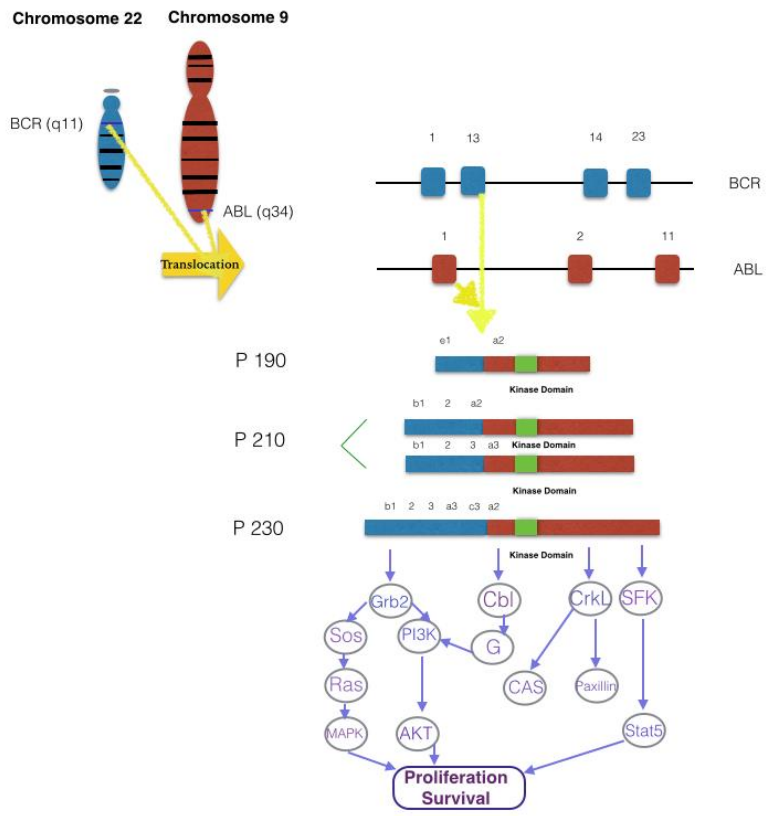

Figure.1.1 A schematic image of translocation between chromosomes 9 and 22

The structure of the breakpoint cluster region (BCR)-proto-oncogene tyrosine-protein kinase (ABL1) gene and protein. The breakpoints of the translocation usually involve the intron 13 or 14 of BCR, named major breakpoint, intron 1 of BCR, named minor breakpoint, and exon 23 of BCR. For ABL1, the breakpoint always involves the region between exons 1b and 2. So the BCR-ABL1 protein contains the kinase domain. Three possible variations of BCR-ABL are possible, so the different breakpoints that generate the p230, p210, and p190 isoforms are shown. In addition, main pathways regulated by the BCR-ABL1 protein. The downstream pathways regulated by BCR-ABL1 protein associated with cell survival, cell proliferation, cell cycle, cell differentiation, apoptosis, and the microenvironment of leukaemia stem cells such as: STAT5 signal transducers and activators of transcription 5, CRKL Crk-like protein,PI3 K phosphatidylinositol 3-kinase, GRB2 the adaptor protein growth factor receptor-bound protein 2, SOS son of seven less, MEK mitogen-activated protein kinase, ERK extracellular signal-regulated kinases and the RAS-to-MAPK (mitogen-activated protein kinase) pathways. Figure modified from Mughal and Goldman (2004)(12).

The balanced translocation between chromosomes 9 and 22 forms a characteristically short chimeric chromosome termed the Philadelphia chromosome (Ph^+), which occurs in >90% of CML patients. This is the hallmark of CML (9, 13, 14) and encodes the BCR-ABL fusion oncoprotein with a molecular weight within the range of 190 and 230 kD, depending on the exact location of the breakpoint, and possesses constitutive tyrosine kinase activity (15). The

fusion BCR-ABL protein is a constitutive tyrosine kinase that activates multiple downstream signalling pathways, resulting in the survival and proliferation of CML cells and positively affects cellular differentiation, growth, apoptosis and adhesion (15-19) (See Figure 1.1).

1.2 DIAGNOSIS OF CML

The cause of CML is mainly unknown, with ionizing radiation being the only established risk factor for CML in atomic bomb survivors (5). About 40% of CML patients are asymptomatic and diagnosis is established during routine blood tests (20). However, the majority of patients present with symptoms such as fatigue, weight loss, night sweats and abdominal discomfort due to splenomegaly (21). The natural history of CML may be progressed through three distinct clinical stages termed chronic phase (CP), accelerated phase (AP) and blast crisis (BC) (8, 22-25) (see Figure 1.2)

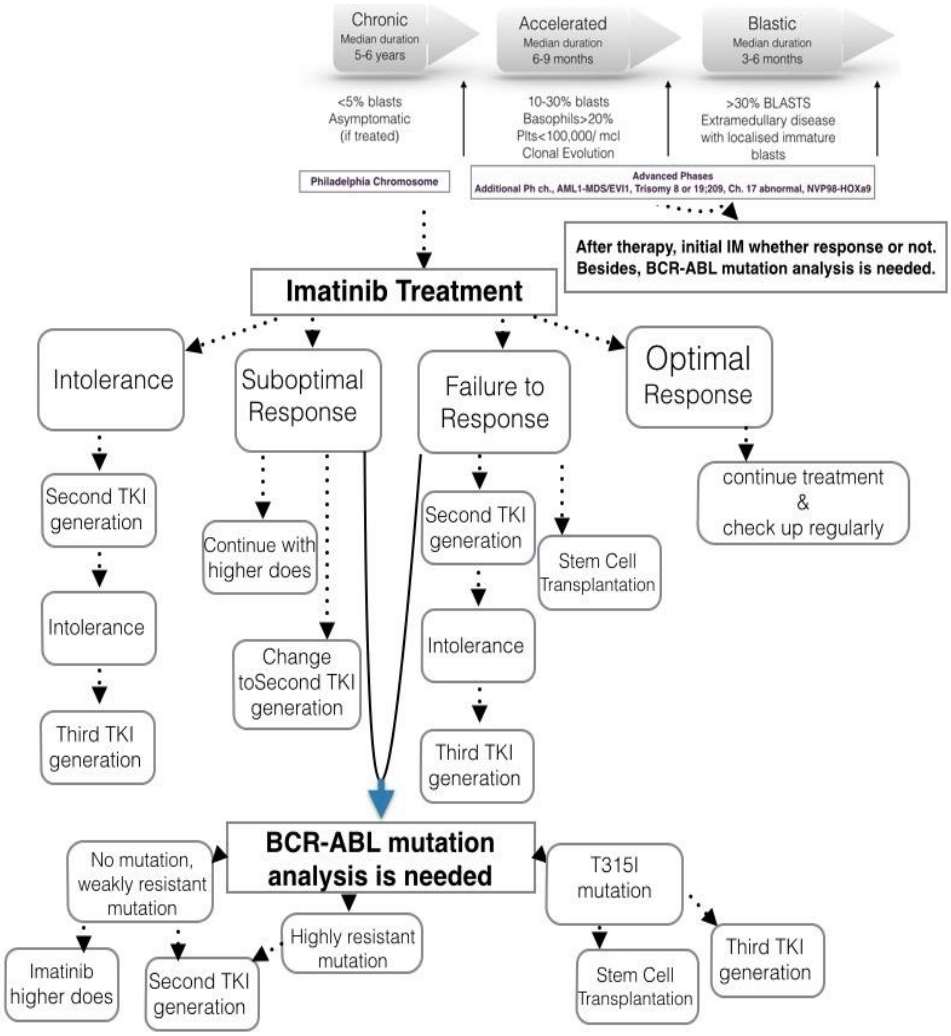

Figure 1.2 A schematic of treatment with imatinib and other TKIs generations and CML disease progression

Treatment with imatinib has four types of responses: i) intolerance, ii) suboptimal response, iii) failure to response and finally, iv) optimal response all of which are based on clinical observations. For each response the continuation of treatment with imatinib or later generation TKIs will be assessed. Moreover, the three stages of CML diseases are defined based on the presentation of blast cells and the duration of disease. (Figure modified from Zaharieva and Amudov (2013))(26).

1.3 CML TREATMENT

Clearly the main objective of CML treatment is to achieve a complete cytogenetic (molecular) response, which refers to the absence of detectable Ph^+ related translocations in the bone marrow or peripheral blood (27). The presence of any remaining leukemic cells evading the detection sensitivity of conventional diagnostic methods is termed minimal

residual disease (MRD) (28). The use of MRD enables better and more effective approaches to the quantification of CML and plays a critical role in the early detection of impending haematology relapse (29). Usually for monitoring MRD, RT-qPCR for CML patients is used (30). Bringing all these together, there always remains a concern about imatinib, as despite the demonstration of clear disease improvement, most patients have undetectable amounts of BCR-ABL and still undergo a rapid relapse (31). The use of MRD in CML should prove useful for the general implementation of strategies for stratified medicine, as therapy lead by quantitative molecular measurements are likely to become more commonplace (9). Analysis of RT-qPCR data from CML patients treated with imatinib and who reach complete molecular response disclosed a biphasic response; the first phase is a rapid drop in the BCR-ABL level followed by a second phase with a shallower gradient (32, 33), see Figure 1.3.

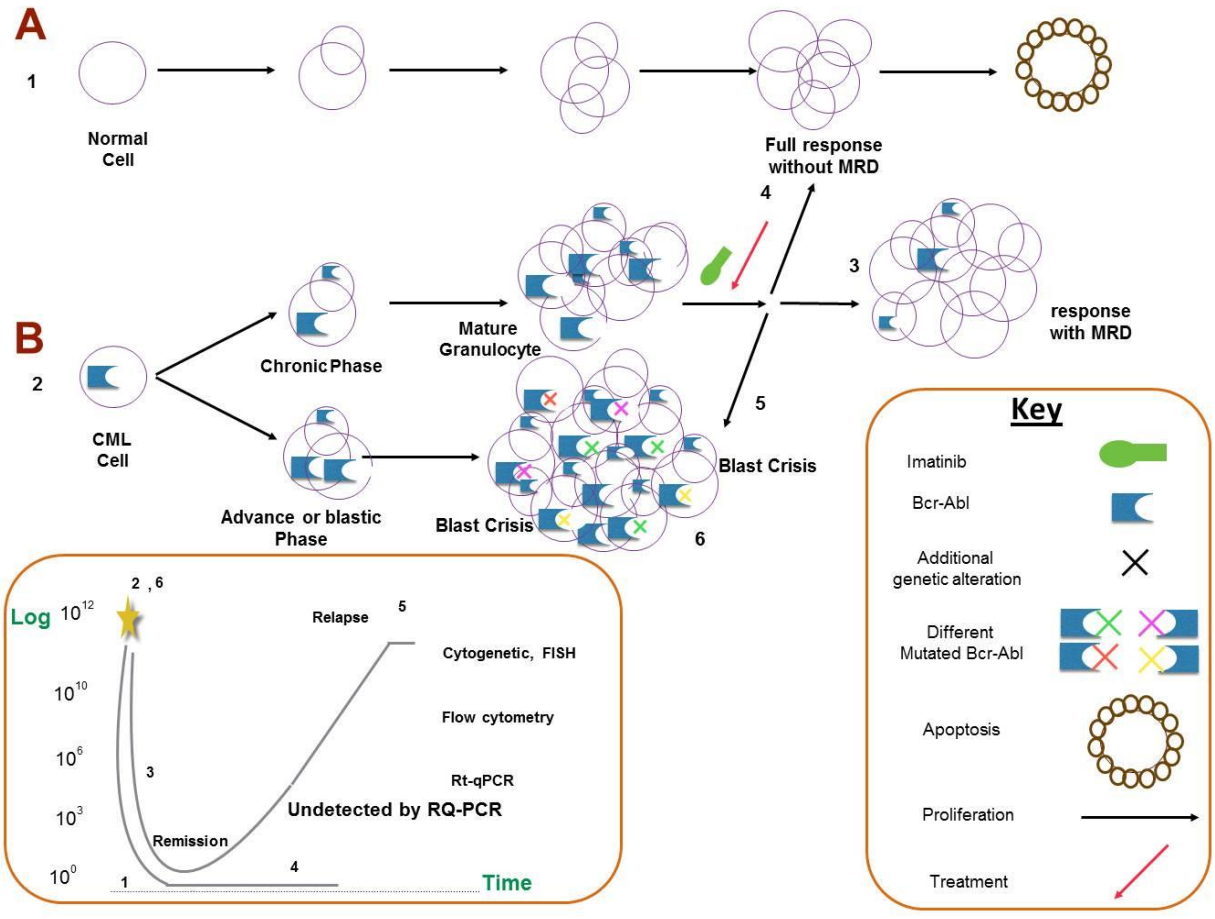

Figure 1.3 Clonal expansion of CML and treatment procedure with potential mutations arising during treatment.

A) Depicts the usual cell cycle where after several cell divisions ends with apoptosis and normal cell death. B) Shows the CML cell cycle, and those cells with the BCR-ABL translocation can progress towards either mature granulocyte or blast crisis with more mutations in Ph^+ cells. By commencing imatinib therapy, cells can show different responses: full response with no MRD, response with MRD and resistance to therapy, and blast crisis. All numbers in A and B correspond to numbers in the graph showing the diagnostic procedure based on the amount of BCR-ABL or the response of the disease.

Since 1850, many treatment options were recognised for CML disease which categorised in three classes: potentially curative therapy, palliative and targeted therapy and combination therapy- personalized medicine. Based on this categorization TKIs are classified in targeted therapy, presented in figure 1.4 (34).

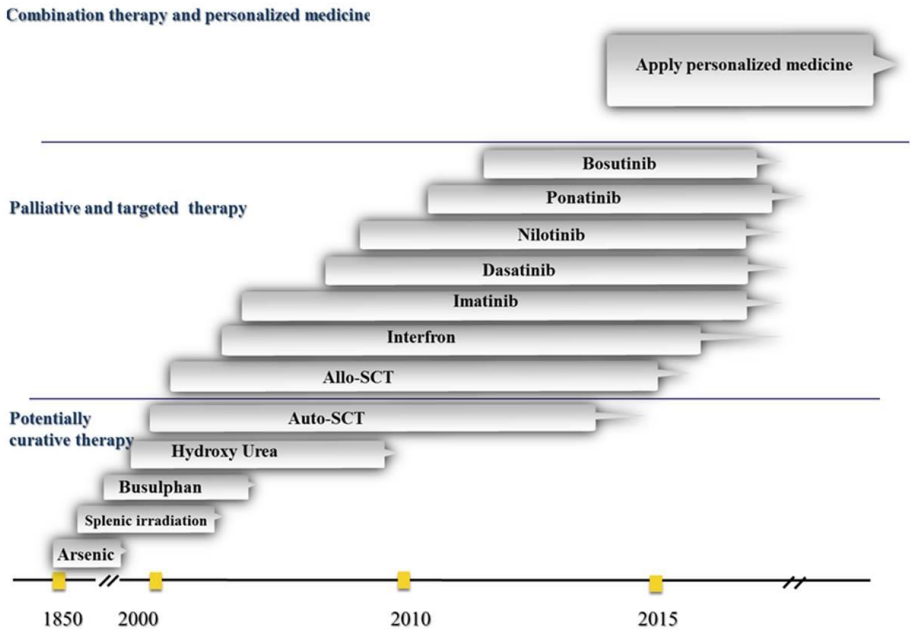

Figure 1.4 Therapy options for CML disease

The figure shows three therapeutic classes which have started from 1850; potentially curative therapy, palliative and targeted therapy and the recent combination and personalized therapy. Figure modified from Pavlu et al (2011)(34).

1.3.1 BCR-ABL TYROSINE KINASE INHIBITORS

Tyrosine kinases are a large and diverse category of enzymes that can catalyse the transfer of a phosphate group from adenosine triphosphate (ATP) to phosphorylate target proteins and which play vital roles in cell signal transduction pathways that regulate cell proliferation, differentiation, anti-apoptosis signalling and programmed cell death (35). Advances in the field of molecular targeted therapies have revolutionized cancer treatment. The implementation of TKI therapy could be considered as a prototype for the successful treatment of cancer (36, 37). In total, five TKIs are approved for the treatment of CML in the United States including imatinib, dasatinib, nilotinib, bosutinib and ponatinib (32, 38) as shown in Table 1.1 (chemical structures for TKIs generations were demonstrated in appendix 3). In 1996, Druker et al. reported the first *in-vitro* data on CML cell lines regarding the effect of highly selective 2-phenylaminopyrimidine (formerly known as signal transduction inhibitor 571, or STI 571), now known by its trade name as imatinib or imatinib mesylate (2, 36).

TKIs Generations	Main Target	Chemical Structure	Binding Site/ Inhibitor type	Date of approval
First generation; Imatinib	Inactive BCR-ABL, PDGFR,ARG, KIT, VEGF, DDR1, NQO2	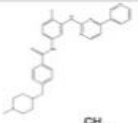	ATP-binding site/ ATP-competitive	2001
Second generation; Dasatinib	Active and inactive BCR-ABL, ARG, TEC, BTK, PDGFR, SRC, EPHA2, DDR1	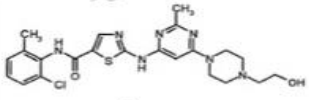	ATP-binding site/ATP competitive	2006
Nilotinib	Inactive BCR-ABL, PDGFR, ARG, KIT, VEGR, DDR1, NQO2	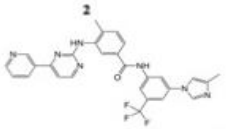	ATP-binding site/ATP competitive	2007
Third generation; Bosutinib	BCR-ABL, SRC, TEC, CAMK2G, PDGFR, C-KiT	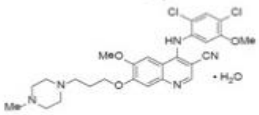	ATP-binding site/ATP competitive	2012
Ponatinib	All mutated forms of BCR-ABL, including T315I, FGFRs, VEGFRs, TIE2, Flt3	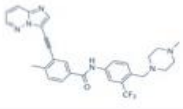	ATP-binding site/ATP competitive	2012

Table 1.1 TKI generations and their related primary targets and chemical structures.
Three generations of TKIs with approval date, main chemical structure, targets and binding sites, plus their mode of inhibition, are shown (modified from(26)).

With the use of TKIs, the overall survival of CML patients has dramatically increased. In the years prior to the introduction period of imatinib (during 1975 - 1977), by developing in CML therapy the five-year overall survival rate was 24%, which increased steadily to 39% during the period 1966-1998. However, during 1999-2006, the five-year survival rate increased to 56.8% and the overall survival was estimated at 85% (2, 6, 39). Conversely, lack of adherence to TKIs inevitably results in disease progression and treatment resistance (39, 40). . Overall, TKIs have transformed CML from a life-threatening leukaemia (with a 10-20% mortality rate per year) to a chronic disease, managed by oral medications (with a 1-2% mortality rate per year) (20).

Imatinib (STI571) as the first and most popular TKI that can offer an effective and durable therapy for CML including complete hematologic remission, long-term survival and molecular response (13, 41). In 2001, imatinib therapy became the first TKI, approved by the Food and Drug Administration (FDA) as a standard treatment, replacing IFN-α (6, 42). Imatinib is a relatively specific inhibitor of BCR-ABL, ABL and ARG TK activities (43, 44). Despite durable cytogenetic responses in CML patients, approximately 75% of CML patients treated with imatinib do not achieve complete cytogenetic response and require alternative treatments (45-47). The rate of resistance to imatinib within four years was up to 20%, increasing to 70-90% in patients with AP/BP CML (43, 46, 48).

Imatinib binds to the ATP binding site within the catalytic site of ABL1 and stabilizes the inactive form of kinase, with the A-loop in a closed conformation and the ATP-binding P-loop in a distorted conformation (44). Additionally, structural data suggest that imatinib acts as a competitive inhibitor at the ATP-binding site of BCR-ABL protein, leading to a closed or

inactive configuration and the inhibition of enzyme activity in proteins (49, 50). ATP prevents tyrosine phosphorylation and downstream signalling, leading to growth arrest and apoptosis (Figure 1.5) (35, 51).

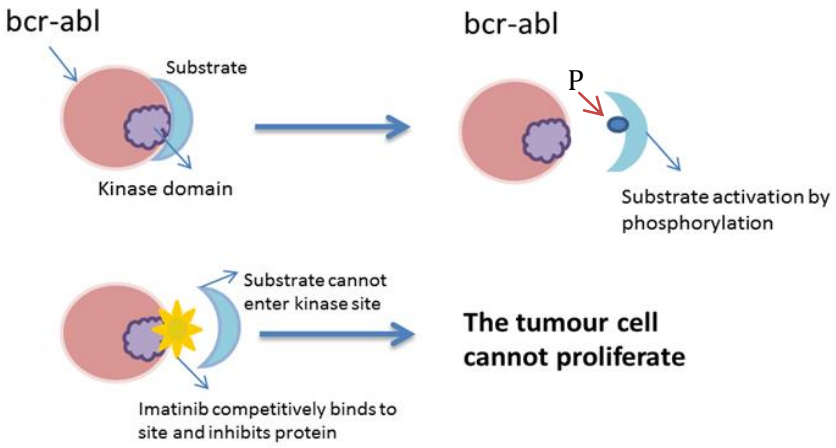

Figure 1.5 Mechanism of imatinib action.

Structural data suggest that imatinib acts as a competitive inhibitor at the BCR-ABL protein ATP-binding site, leading to a closed or inactive configuration and the inhibition of TK activity. Imatinib binds to the amino acids of the BCR/ABL tyrosine kinase ATP binding site and stabilizes the inactive, non-ATP-binding form of BCR/ABL, thereby preventing tyrosine auto phosphorylation and, in turn, phosphorylation of its substrates. This process ultimately results in "switching-off" the downstream signalling pathways that promote leukemogenesis.

1.3.2 THE MECHANISM OF TKI ACTIVITY

There is substantial evidence that malignant alterations of hematopoietic cells by BCR-ABL protein rely on its TK activity (9). In cancer, mutant kinases frequently act as oncogenes that promote tumour cell survival, growth or replication by causing aberrancies in proliferation, apoptosis resistance (or genomic instability), angiogenesis (or cell migration) and adhesion through interference with β-integrin signalling and multiple downstream pathways during metastasis (14, 52).

Increased knowledge about CML and the discovery of TK molecular pathways have led to the development of a "smart drug", which specifically inactivate BCR-ABL kinase (52). To date, three main strategies have been proposed for inhibiting signalling by BCR-ABL oncoproteins: i) using ATP-competitive; ii) allosteric and BCR-ABL pathway inhibitors; and iii) BCR-ABL inhibitors are dominated by ATP-competitors (41, 43),(9, 53). TKI block the activation of the BCR-ABL pathway and prevents disease progression by inhibiting BCR-ABL kinase activity and decreasing the number of malignant cells (45). BCR-ABL kinase is necessary for deregulated growth of leukemic cells, and can lead to treatment inhibition in CML and other Ph^+ leukaemia in clinical trials (8).

1.4 THE MECHANISM OF RESISTANCE TO BCR-ABL INHIBITORS

Clinical and *in-vitro* evidence have shown that cells treated with TKIs tend to acquire genetic modifications to overcome the inhibitory effects of these agents (54). It is assumed that through disease progression and in the chronic phase of CML, the initiating BCR-ABL translocation event may cause genetic instability and extra genetic abnormalities in genes involved in cellular proliferation, differentiation and apoptosis (33). Naturally, chromosomal abnormalities including trisomy 8 and translocation of other oncogenes occur and these extra abnormalities result in resistance to TKI and impaired treatment (52, 55). Based on the clinical course of the disease, resistance to treatment is divided into primary and secondary sub-types. Primary resistance occurs when the expected responses are not achieved by the frontline therapy (41). In contrast, secondary resistance develops after a targeted response to the frontline therapy was achieved but subsequently lost (Figure 1.6) (45, 56, 57).

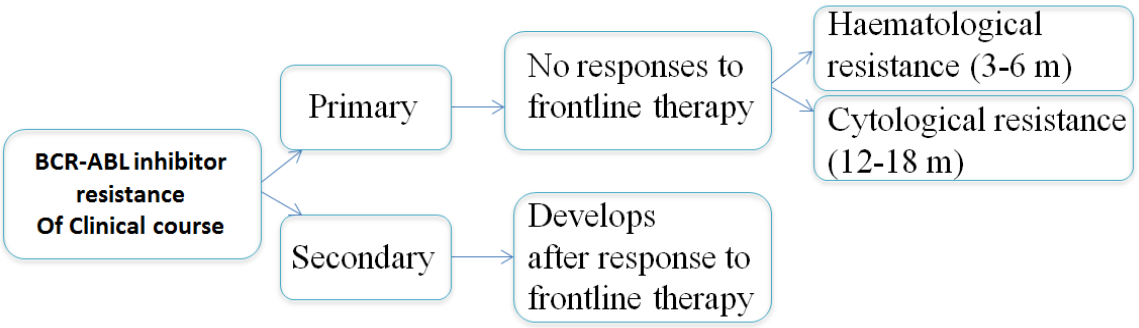

Figure 1.6 From a clinical perspective of BCR-ABL inhibitor resistance the response can be divided into primary and secondary groups.

Primary resistance is defined as no emerging response to frontline therapy which is further sub-divided into haematological resistance and cytological resistance. Secondary resistance develops after a period of response to the frontline therapy. m = month.

According to many pre-clinical and clinical studies, from a mechanistic perspective, the emergence of resistance to treatment can be categorized into BCR-ABL-dependent and independent processes (57). BCR-ABL-dependent mechanisms include BCR-ABL mutations and amplification, along with impaired signalling pathways. BCR-ABL-independent mechanisms include drug efflux, mediated by ATP-binding cassette (ABC) -deficient base excision repair for chromosomal abnormalities. Overall, understanding the underlying causes of resistance is a crucial step towards combating CML (41). The mechanism of TKI resistance observed in a number of CML patients can be either dependent or independent of BCR-ABL. BCR-ABL–dependent mechanisms are characterized by the emergence of mutations in the tyrosine kinase domain, including T315I mutation and/or BCR-ABL protein overexpression, caused by gene amplification (58). On the other hand, mechanisms independent of BCR-ABL are characterized by deregulations in drug transport (Figure1.7) (47).

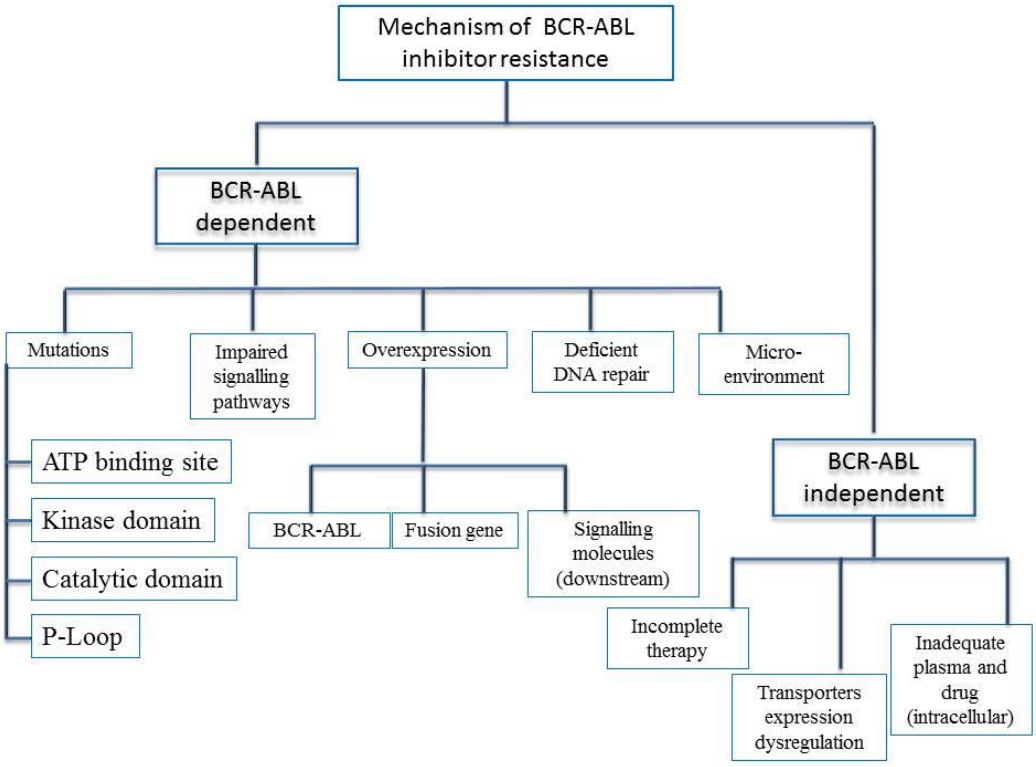

Figure 1.7 Schematic for the mechanism for BCR-ABL inhibitor resistance

The development of TKI resistance is classified into two groups; BCR-ABL dependent and BCR-ABL independent. Each group is further sub-divided in other classes, in which mutations impaired signalling pathways, over-expression, deficient DNA repair and micro-environment are categorized for the dependent group. However, mechanisms including inadequate intracellular plasma drug level, dysregulation of transporter expression and incomplete therapy are grouped as independent factors related to BCR-ABL mechanisms.

1.5 EVIDENCE FOR TRANSPORTERS USED BY DRUGS IN THE TREATMENT OF CML

A general theory of drug movement through biological membranes is that they can pass membrane via passive diffusion at a level related to their lipophilicity. Though, it is becoming obvious that membrane transporters are likewise important elements of *in vivo* drug disposition, therapeutic efficacy, and adverse drug reactions (59).

In this regards, transporters are important mediators of specific cellular uptake and thus, many researchers have shown that the cellular concentrations of imatinib and other TKIs are

influenced by membrane-bound drug transporters. The amount of imatinib, present in target cells, is determined by the balance between proteins mediating the inward and outward (efflux) transport of imatinib (60). Furthermore, Multidrug resistance (MDR) in cancer cells is a phenotype whereby cells display reduced sensitivity to anticancer drugs, based on a variety of mechanisms including those related to membrane and transporters, including; an increase in drug efflux, and the reduction of drug uptake (61).

A potential solution to the deficiencies of imatinib therapy may involve strategies to increase the effective intracellular drug concentration. Work in this field has focused on cell surface drug transporters (62). Recently membrane and drug transporter proteins have gained increasing interest across numerous therapeutic areas and have been found to play importance in TKIs resistance (63). As noted in figure 1.6, these resistance mechanisms are categorized as independent mechanism for TKIs. Moreover, it is known that one of the most common mechanisms that produce MDR in cancer cells is the presence of ABC transporters, ubiquitous membrane-bound proteins, which can generate energy from ATP hydrolysis to transport compounds across the membrane (64). The overexpression of transporters confers cross-resistance to multiple drugs through actively effluxing cytotoxic drugs. Several members of ABC protein family have been found to determine the resistance of BCR-ABL inhibitors (61, 63, 65). Based on established studies, TKIs act as both substrates and inhibitors of ABC drug transporters, depending on the concentration of inhibitor used and its affinity to the transporter (66). These findings indicate that analysis of drug-transport activity, or markers thereof, might be useful predictors of response to imatinib (67). MDR mediated by multidrug efflux ABC transporters is a critical issue in the treatment of leukaemia with permeability P-gp (P-glycoprotein, ABCB1), MRP1 (multi-drug resistance-associated protein, ABCC1) and BCRP (breast cancer resistance protein, ABCG2) are efflux transporters and are now recognized to have an important role in the absorption, distribution,

excretion and toxicity of drugs (xenobiotics) and were shown to be the key effectors of MDR in cell line studies (68). Moreover, ABCC10 (MRP7) has only been recently classified as a member of the ABC superfamily that confers the MDR phenotype to cancer cells. However, TKIs are transported out of the cells by ABC transporters, resulting in drug resistance phenotype in cancer patients so this outcome may be the result of an altered expression pattern or activity of drug transporters (66),(69) (Figure 1.8 and table 1.2).

Also, with regard to TKI influx, organic cation transporter 1 (OCT-1) is involved in the maintenance of intracellular imatinib concentration in which certain polymorphisms in OCT-1 gene are correlated with response to imatinib therapy (70) (Table 1.2).

Nonetheless, solute carrier (SLC) membrane transport proteins control essential physiological functions, including nutrient uptake and waste removal that have been identified as passive transporters, ion coupled transporters, and exchangers, such as SLCO1A2 and SLC22A1 (69) (62, 71).

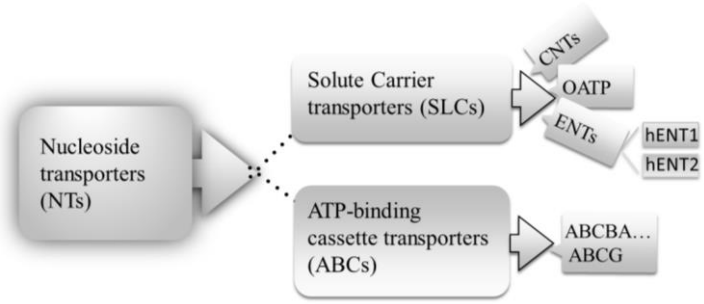

Figure 1.8 Nucleoside transporters: showing the classification of NT super families divided to SLC and ABS sub-families.

Nucleosides transporters are integral member proteins that regulate the transportation of nucleosides, nucleobases and nucleoside analogue drugs across cell membranes. These transporters in humans can be classified into two major super families namely the solute carrier (SLC) and the ATP-binding cassette (ABC) (modified from (72).

Fortunately, resistance mechanisms are illustrated in several ways, and novel agents with theoretically good tolerability, targeting multiple signalling pathways, have been introduced

to sensitize cancer cells to BCR-ABL inhibitors (73-75). Moreover, TKIs are new and fast growing group of anticancer drugs which acting as a substrate or inhibitors of some ABC transporters and metabolizing enzymes. As a result, they create a complex condition in resistance and effective dose selection. Molecular analysis of the functional interactions between such novel drugs and ABC transporters suggests the usefulness of investigating them to predict resistance (76-78).

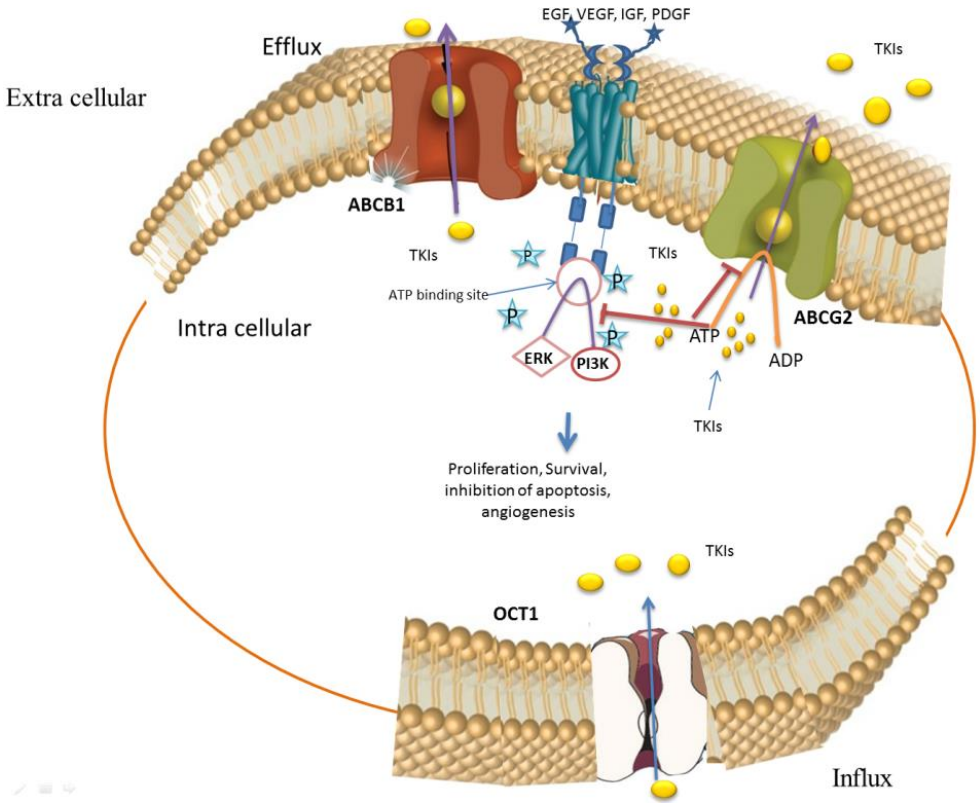

Figure 1.9 ABC drug transporter-mediated MDR "pump".

TKIs are taken into cells through influx transporters such as SLC22A1. Once inside cells, TKIs block the ATP-binding site of receptor TKs and prevents downstream phosphorylation events, thus inhibiting cell proliferation and survival networks such as those related to ERK, PI3K, EGF, VEGF, IGF and PDGF. Adversely, some TKIs also bind to the substrate-binding pocket of the transporter and are effluxed by the hydrolysis of ATP molecules, thereby reducing the intracellular TKI concentration. Therefore, there are some recognized efflux transporters for TKIs among ABC transporters family such as ABCB1 and ABCG2 that cause MDR and decrease the amount of TKIs in the cells.

Transporters	Definition
ABCC1	ABCC1 or multidrug resistance-associated protein 1 (MRP1). A uni-directional efflux transporter with a ubiquitous tissue distribution and wide substrate specificity including important therapeutics.
ABCB1	The ATP-binding cassette, subfamily B (MDR/ATP), a member gene (ABCB1/MDR1) encodes the cell surface P-glycoprotein (PgP) acting as an energy-dependent multidrug efflux pump.
ABCG2	ATP-BINDING cassette, subfamily G, member2 also known as breast cancer resistance protein.
ABCB10	ABCB10 (also known as ABC mitochondrial erythroid). Essential for erythropoiesis and for protection of mitochondria against oxidative stress.
SLC22A1 (OCT1)	Organic cation transporter 1 (OCT1, SLC22A1, important for the disposition of clinically important drugs, metabolites and signalling molecules.
SLCO1A2 (OATPA1)	Organic anion transporter poly peptides (OATPs). A drug uptake transporter with broad substrate specificity.

Table1.2 the list and definition of transporters that were investigated in the current project.

ABCC1, ABCB1, ABCG2 and ABCC10 subfamilies of ABC transporters. SLC22A1 and SLCO1A2 subfamilies of SLC transporters. These transporters have effect in imatinib drug resistance for CML disease.

1.6 MAYBRIDGE FRAGMENTS AND THEIR EFFECTS ON DRUG DISCOVERY

Drug finding is divided into many stages, nonetheless largely it normally starts with a screening phase, in which a set of structurally diverse drug-like small-molecule compounds are screened against a selected target assay to generate ‘hits’. A selection phase then follows, in which one or more hits with the most desirable reactions are identified and validated (79) (Figure 1.9). In this regards, the MayBridge Rule of 3 Fragment Library (May Ro3) is a relatively small collection of chemical entries that are pharmacophore rich (80). In 2014, based on the fact that any bioactive molecule in the human cells to cross the cellular membrane to exert its effects intracellularly; O’Hagan et al. hypothesized that successful drugs are more likely to be ‘metabolite-like’. It states that for a drug to exert is cytotoxic effects efficiency, the Tanimoto distance, is the most widely used distance formula as a mathematical representation of the idea of a similarity between two molecules based on the number of common molecular fragments, between the drug and a known human metabolite is more likely to be 0.5 or greater in molecular Access system (Maccs) fingerprint space, provided that the molecular is not excessively halogenated (81). As a result, it seems that the

interaction between imatinib transporters needs more investigation and research even through by working on transporters and changing their expression, then the outcome for TKIs and especially imatinib therapy will go better.

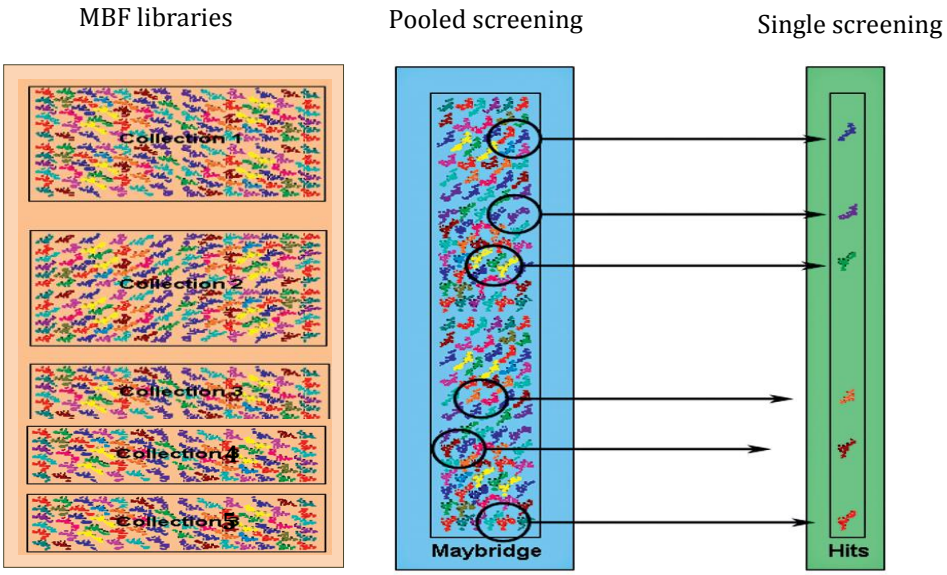

Figure 1.10 MBF screening

The importance of diversity; a highly diverse screening collection will provide a greater hit probability than larger (figure is modified from Major, et al 2011) (80). The current figure shows a schematic illustration of the five MBF libraries (consist of 2500 fragments), so through pooled screenings some fragments were selected and from those through single screening the active hits were selected.

1.7 STUDY DESIGN

1.7.1 IN-VITRO STUDIES PERFORMED IN THIS PROJECT

Studies in this project are carried out *in-vitro*, by means of two cell lines: human chronic myelogenous leukaemia blast crisis (K562) cell line and human neuroblastoma (SH-SY5Y) cell line. Mammalian cells are classified as either adherent or suspension cells. Adherent cells, such as the SH-SY5Y cells, need to attach to a surface to grow, whereas suspension cells grow in the culture media without the need to attach to a surface. K562 cell line used in this project consists of two populations: a sub-population of surface-adherent cells and a sub-population of non-surface adherent (suspension) cells.

In fact, SH-SY5Y cells and cisplatin were selected as a control in the current study to investigate if the selected hits would be drug/cell dependent or disease related. Moreover, SH-SY5Y is a sensitive cell line making it a good choice to compare against K562. In this regards, cisplatin is an anti-cancer drug used to treat different types of cancer. In this project cisplatin was used as a control drug to test if the effect of candidate MBFs are related to drug/cell combinations. (Figure 1.11).

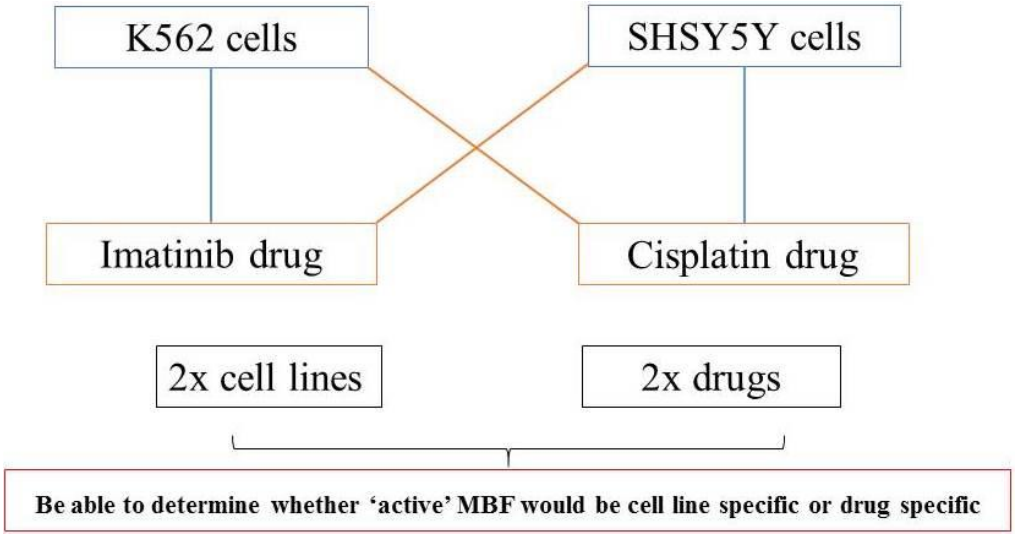

Figure 1.11 Experiment design; 2X cell lines and 2X drugs.

For investigating of MBFs effect with imatinib on K562 cell line as an in-vitro model of CML disease, cisplatin and SH-SY5Y cells were selected as a control model (a neuroblastoma model) to check the selected active MBFs would be cell line specific or drug specific.

1.7.2 CYTOTOXIC ASSAYS DEVELOPMENT

MTT assay is the viability assay studied and optimised in this project to assess cell viability/toxicity following drug and MBFs treatment.

In cytotoxicity assessments, imatinib considered as the main drug since it is the first option among TKIs in CML treatment but still it has drug resistance problem for patients. However, cisplatin was chosen as a control drug since it is an effective drug in the *in vivo* treatment of

neuroblastoma. It also can inhibit the growth of neuroblastoma cells and reduce cell viability (82).

MTT [(3-(4, 5-dimethylthiazol-2-yl)-2, 5-diphenyltetrazolium bromide)] cell viability assay measures the cell's viability through its mitochondrial dehydrogenase activity. Loss of mitochondrial membrane potential is measured by analysing the oxidoreductase enzyme activity, through the creation of the purple-coloured formazan crystals. A colour alteration, from yellow to purple, is observed in healthy cells with intact mitochondria as a result of MTT reduction to soluble formazan, by NADH. Measurement in this assay is carried out spectrophotometrically through taking absorbance measurements at 570 nm, with the absorbance values being a direct measurement of the number of functional and viable cells.

1.7.3 RT-QPCR ANALYSIS

Real-time quantitative polymerase chain reaction (RT-qPCR) method is broadly used for quantitative high-throughput and reproducible measurements. Furthermore, this measurement is highly sensitive has the ability to detect and measure very small amounts of nucleic acids. In RT-qPCR, the rise in fluorescence is directly related to the number of copies of amplicon, the synthesised gene fragment. Additionally, the quantity of synthesised amplicon in this method is measured either by using a fluorescent dye, such as SYBR green, or a modified DNA oligonucleotide probe. Therefore, the RT-qPCR method is optimised in this study, to provide a quantitative means to study transporter genes expression alteration by using SYBR green.

1.7.4 BINARY WEAPON APPROACH USING MAYBRIDGE FRAGMENTS

The fragment-based drug finding is a novel and generic methodology which uses the combination of chemotherapeutic drugs with fragments from the MBF so as to further direct the analogue drugs towards their transporters. These ligand-efficient fragments investigate

the chemical space of the target transporter protein, covering a comparatively large area due to their small sizes. This leads to enhanced transporter binding, which in turn enhances the intracellular transportation of drug and consequently it is increasing its drug efficacy. The following is a representation of the proposed binary weapon mechanism.

1.8 STUDY AIMS

Previous studies showed that fragment-based screening has proved to be an effective strategy for the discovery and development of drug leads (80, 83, 84). Moreover, it was shown that increased expression of the ABC transporters plasma membrane drug efflux pumps or either decreased expression of SLC22A1 transporter drug influx pumps on the membranes of cancer cells in CML disease, are involved in imatinib therapy resistance (61, 63).

From the above it is clear that the independent mechanism of imatinib resistance, through transporters may be significant in terms of response to imatinib. Additionally, there may be a possibility of finding new ways to increase drug uptake through transporters via a fragment-based approach.

Specifically, this study aims to screen and find the non-toxic hits from the first 500 MBFs from the 2,500 MBF library. Furthermore, the expression patterns were characterized for a different sub-family of ABC and SLC transporters after treatment of those selected active MBFs (hits) from the first library with imatinib and cisplatin (as a control drug). Cisplatin was selected as a control drug as, it is a highly effective and potent cytostatic anti-cancer drug used in the treatment of a wide variety of malignancies, especially for neuroblastoma. The cell lines investigated in this project were K562 (derived from the blast crisis phase of CML) and SH-SY5Y (a neuroblastoma sub-clone derived from SK-N-SH cells) as a control cell line.

The aims of this study are threefold, namely (Figure 1.11):

1. To screen the first 500 compound library of MBFs with an MTT assay to find useful MBF hits for K562 cells treated with imatinib. (The search for bioactive molecules).
2. To visualise the best concentration for those selected MBF hits with MTT assays.
3. To measure mRNA expression of efflux and influx transporters genes after treatment with MBF and imatinib or cisplatin with qPCR.

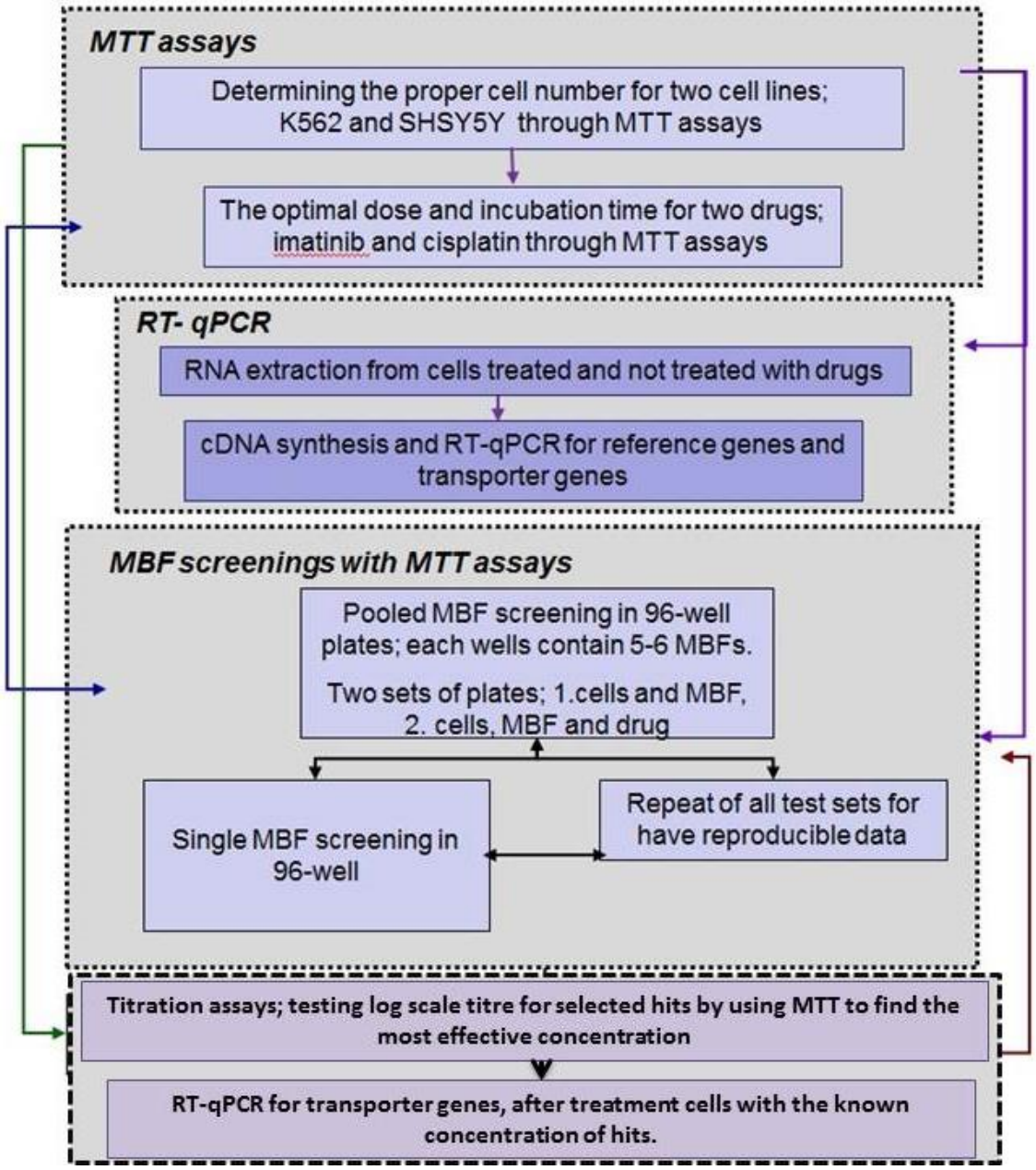

Figure 1.12 Overview of laboratory studies; MBF screenings and expression of transporters genes.

The enhancing effect of imatinib through MBFs was investigated on K562 cell line as an in-vitro model of CML disease, so cisplatin and SH-SY5Y cells was a control model but not in CML, for neuroblastoma.

CHAPTER 2

METHODS AND MATERIALS

2.1. CELL CULTURE

2.1.1. K562 CELL CULTURE

Human CML blast crisis cell line K562 (ATCC, Manassas, VA, USA) was grown in RPMI-1640 culture medium (Sigma, Poole, UK), supplemented with 10% heat-inactivated fetal bovine serum (FBS; Invitrogen, Paisley, United Kingdom), 2 mmol/L L-glutamine (SAFC Bioscience, Lenexa, KS, USA), 100U/mL penicillin and 100µg/mL streptomycin (Sigma-Aldrich, Poole, UK). This culture medium was used for all K562 cell manipulations. Cells were maintained at 37°C in 5% CO_2, every 3 or 4 days in T_{25} flask (BD Falcon™, Becton Dickinson, New Jersey, USA) to maintain a density between 1×10^5 and 1×10^6 cells per millilitre (mL). In addition, cell counting and viability were performed with a haemocytometer using the 0.1% trypan blue exclusion technique(85). Cell line authentication was confirmed through karyotyping testing (University of Manchester, UK).

2.1.2. SH-SY5Y CELL CULTURE

Human neuroblastoma cell line SH-SY5Y (ATCC® CRL- 2266™) was grown in mixture (1:1 ratio) of ATCC-formulated MEM (Minimum Essential Media) and Ham's F12 Nutrient Mixture culture medium (Gibco, UK), supplemented with 10% heat-inactivated fetal bovine serum (FBS; Invitrogen, Paisley, United Kingdom), 2 mmol/L L-glutamine (SAFC Bioscience, Lenexa, KS, USA), 100U/mL penicillin and 100µg/mL streptomycin. This culture medium was used for all SH-SY5Y cell manipulations. Cells were maintained at 37°C in 5% CO_2, every 3 or 4 days in T_{25} flask (BD Falcon™, Becton Dickinson, New Jersey, USA) to maintain a density between $1x10^5$ and $1x10^6$ cells per mL. In addition, cell counting and viability, and karyotyping was performed as described above (Section 2.1.1)

2.2. MTT ASSAY

Cell viability was measured by quantitative colorimetric assay with MTT (3-(4, 5-dimethylthiazol-2-yl)-2, 5-diphenyltetrazolium bromide) (Sigma), showing the MTT reduction by viable cells as described in the published literatures (86, 87). MTT stock solution (5 mg/mL) was prepared by dissolving MTT into phosphate buffered saline (PBS). The solution was filtered, aliquoted and stored at -20°C in amber micro centrifuge tubes. Each experimental condition was performed as triplicates in 96-well plates. After treatment, MTT (stock solution) was added to each well (10% vol/vol) and incubated for 3.5 h at 37°C in 5% CO_2. The resulting formazan crystals were dissolved by adding equal volume of MTT solubilisation solution (37% of 0.1 M HCL in anhydrous isopropanol), followed by trituration. Absorbance measurements were recorded at 570 nm wavelength using a plate reader (Tecan Infinite M200 PRO).

In the current study before commencing the main experiment procedure the MTT assay was first validated by investigating the effects of exposure to cytotoxic reagents; TritonX-100 (0.01%), NaCl (5M) and DMSO (2.5%, 100%) on viability of the cells.

Cell viability was calculated as described in the below formula;

Cell viability (%) = (Extract concentration reading - Blank reading / Control reading - Blank reading) × 100

In the current formula the blank is cell media only and control is cells without treatments.

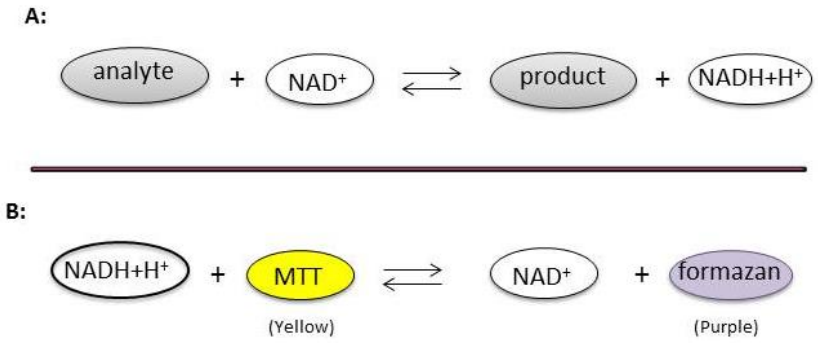

Figure 2.1 Mechanism of action in MTT assay (schematic representation)

Tetrazolium salts reduction is now widely accepted as a reliable way to study cell proliferation. The yellow tetrazolium MTT is metabolically reduced in viable cells, by the activity of dehydrogenase enzymes, to produce reducing compounds such as NADH and NADPH. The subsequent intracellular purple formazan can be dissolved and measured by spectrophotometric means.

2.2.1. EVALUATION OF OPTIMAL CELL NUMBER USING THE MTT ASSAY

Growth curves were determined to ensure that the cells were within the exponential growth phase. Cell proliferation was assessed by monitoring the conversion of MTT to formazan. The reduction of MTT is catalysed by mitochondrial dehydrogenase enzymes and is therefore a measure for cell viability.

Briefly, cells (100 µL/ well) were seeded at seeding densities of 1×10^3 to 2×10^4 cells / well, into 96-well plates and allowed to adhere overnight. The cell numbers were measured at three separate time courses; 24, 48 and 72 h. Cell viability was assessed on a daily basis by adding 10 µL of filter sterilised MTT (5 mg/mL in PBS) to each well. Following a 3.5 h incubation

period with MTT, the blue formazan crystals, trapped in cells, were dissolved in sterile solubilisation solution (37% of 0.1 M HCL in anhydrous isopropanol). The absorbance at 570 nm was measured to monitor the growth profile of the cells by plotting absorbance (blanked with media and HCL-IPI) against time. Separate experiments were conducted for K562 and SH-SY5Y cells.

2.2.2. EVALUATION OF OPTIMAL DRUG CONCENTRATION USING THE MTT ASSAY

The MTT assay (as described above) was also used to assess the *in-vitro* optimal concentration of drugs (imatinib and cisplatin) used in this study. In brief, K562 and SH-SY5Y cells (100 µL; 7×10^3 and 1.4×10^4 cells/well) were separately seeded into 96-well plates and left to adhere for 12 h. The next day, candidate drugs (imatinib or cisplatin) were added to these cell cultures to a log scale of final concentration of (0, 1, 3, 10, 30, 100 or 300 µM) followed by incubation at 37°C in 5% CO_2 for 24, 48 and 72 h. In the case of the 24 h incubation: MTT (10 µL of 5 mg/mL in PBS) was added to each well of the plates for each incubation times. Plates were incubated for a further 3.5 h. Then the solubilisation solution (37% of 0.1 M HCL in anhydrous isopropanol) (100 µL) was added.

Finally the absorbance at 570 nm was recorded using a Tecan plate reader (Tecan Infinite M200 PRO). Absorbance values were blanked against medium only wells with solubilisation solution and the absorbance of cells exposed to medium only (i.e. no drug added) were taken as 100% cell viability (i.e. control samples).

As a result, the percentage of cytotoxicity was calculated, after carrying out all blank subtractions from all readings, as described below:

Cell Viability (%) = (Sample-Background) / (control – Background) ×100

Cell Cytotoxicity (%) was expressed as (100 – cell viability).

2.3. MBF SCREENING EXPERIMENTS

2.3.1. MBF SCREENING EXPERIMENTS (IN POOLS)

Antiproliferative and cytotoxic effects of MBFs were measured *in-vitro* using the MTT assay, with the aim of enhancing the drug's efficacy. The first library of five libraries, containing two sets of 384-well plates (consisting 500 MBF) (Fisher Scientific) was screened. Echo® Liquid Handler for Screening (Labcyte, Sunnyvale, USA) was used to transfer 10 nL of 100 mM Maybridge fragments (in DMSO) from the 384-well plate to 96-well plates. Every 5-6 MBFs were combined in a single well of 96-well plates, followed by addition of K562 (50 µL: 7×10^3) and SH-SY5Y (50 µL; 1.4×10^4 cells/well) and incubation at 37°C in 5% CO_2 for 24 h. The following day based on the experiment design; 0.5 µM imatinib (for 24 h) or 1 µM cisplatin (for 48 h) were treated with cells. Cell viability was assessed by MTT assay. Additional 96-well plates were set up with MBFs only (without adding drugs) in the same condition. Experimental incubation conditions were performed in triplicate.

Finally, the absorbance at 570 nm was recoded with the Tecan plate reader following standard protocols as stated in Section 2.2.2

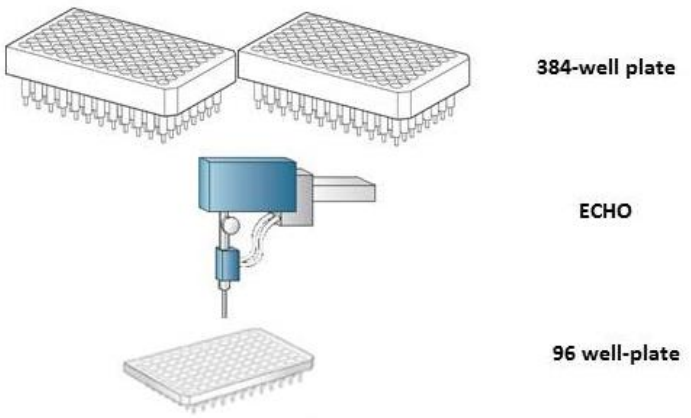

Figure 2.2 ECHO 550 liquid handler for screening (LABCYTE INC, SUNNYVALE, USA) was used to transfer 10 nl of 100 mm MBF.

The first library of MBFs contains 500 fragments (in two 384-well plates). For the initial screening as a pooled MBF screening, 5-6 MBFs (10 nL of 100 mM) from the 384-well plate were combined into one well of 96-well plate.

2.3.2. MBF SCREENING EXPERIMENTS (WITH SINGLE FRAGMENTS)

After identifying the most effective active pooled MBFs that supported cell viability, based on a defined cut off (cell viability between 50-70%) , the antiproliferative and cytotoxic effects of each the MBFs were assed separately. An Echo® Liquid Handler (Labcyte, Sunnyvale, USA) was used to transfer 10 nL of 100 mM Maybridge fragments (in DMSO) from the 384-well plate to 96-well plates, where each of the MBFs were transferred into a single well. The MTT assays were repeated following the same methodology as described in Section 2.3.1 with pooled assays for three time points in triplicate to check the reproducibility of our results.

2.3.3. TITRATION SCREENING ASSAY FOR THE SELECTED ACTIVE HIT MBFS

After performing the single fragment screening, and defining those active MBF hits in single, the titration experiment was designed to find the effective concentration of those selected active fragments. Therefore, a titration experiment was carried out with log scale concentration of each hit (active MBF) (0, 1, 3, 10, 30, 100 or 300 µM).

Additionally, the MTT assays were repeated with the same methodology of single assays for two time points in triplicate to check the reproducibility of the results.

2.4. RNA EXTRACTION

K562 and SH-SY5Y cells (5-10×10^6) were transferred to sterile 15 mL Falcon tubes (BD Biosciences, USA) and centrifuged at 1100 *g* for 5 min. The supernatant was aspirated and replaced with 10 mL of growth medium, and then the cells were counted using a haemocytometer (Scientific Laboratory Supplies Ltd, Nottingham, UK). Cells treated and not

treated with drug or MBF, in different design sets, and RNA was extracted by using Qiagen RNeasy Mini Kit (Qiagen, Manchester, UK) as described in the manufacturer's protocol. In an overview, this involved pipetting up to 1×10^7 cells and centrifuging at 100 *g*. RLT buffer (600 µL) was added to the cell pellet followed by pipetting up and down to disrupt the cell walls and plasma membranes and organelles, releasing all the RNA contained in the sample. Addition of 1 volume (600 µL) of 70% ethanol (Fisher Scientific) to the homogenised lysate then followed. Up to 700 µL of the sample were then transferred to an RNeasy mini spin column, centrifuged for 15 s at ~8,000 *g*. The flow-through was discarded, followed by the addition of 700 µL of Buffer RW1. Buffer RPE (500 µL) was pipetted into the column, centrifuged at ~ 8,000 *g* for 15 s. An additional 500 µL of Buffer RPE were added to the RNeasy column, with subsequent centrifugation for 2 min at ~ 8,000 *g* so as to dry the silica-gel RNeasy membrane. The final step involved discarding the collection tubes, and placing the RNeasy spin column into a new 1.5 mL collection tube. The extracted RNA was eluted from the RNeasy gel membranes by adding 30-50 µL RNase-free water directly onto the silica–gel RNeasy membrane, followed by 1 min centrifugation at ~ 8,000 *g*.

DNAse digest was carried out by adding 3 µL of the 10× DNase buffer and 1 µL of DNase enzyme (2U/µL) to the RNA sample. The mixture was gently vortexed and then incubated at 37°C for 30 min. Following the incubation period, 3.4 µL of DNase inactivation reagent was added, leaving the mixture to incubate at room temperature for 2 min. This was then centrifuged at 10,000 *g* for 1.5 min, and the RNA solution was transferred to a clean Eppendorf tube.

2.4.1. RNA ANALYSIS

2.4.1.1. RNA QUANTIFICATION

RNA was quantified using a NanoDrop ND-1000-Spectrophotometer (NanoDrop Technologies, Wilmington, USA). RNA concentration was quantified by placing 1.2 µL of the RNA solution onto the lower measurement pedestal while the sampling arm was open. To calculate the RNA concentration, samples were exposed to ultraviolet light at 280 and 260 nm and then spectrophotometric readings were automatically converted into ng/µL by the Nanodrop 1000 software. In addition, the ratio of the absorbance at 260nm and 280nm (260/280) was used to analyse the RNA purity, with 260/ 280 ratios of 1.8 - 2.0 signified as high purity RNA extract.

2.4.1.2. RNA QUALITY

RNA quality was assessed using an Agilent 2100 Bioanalyser prior to reverse transcribing it into cDNA. The virtual gels and electropherograms (Figures 3.21 and table3.1) were used to determine the rRNA 28S/18S ratio and RNA integrity number (RIN). A RIN number of 9.0 or above, and an rRNA ratio with a value close to 2, indicate high quality RNA.

RNA integrity of each extracted RNA sample was determined using the Agilent RNA 6000 Nano assay kit (Agilent Technologies, Cheadle, UK), following manufacturers protocol. Briefly, preparation of Gel-Dye matrix is made by addition of 2 µL of the concentrated RNA dye into a 130 µL aliquot of filtered gel. The loading process of the Agilent assay first requires loading the Gel-Dye Mix, followed by loading of the Agilant RNA 6000 Nano Marker. The Gel-Dye Mix (9 µL) was pipetted into the well-marked as G on the chip. The plunger was positioned at 1 mL, pressed and then held for 30 sec before it was pulled slowly back to its initial position. The chip was checked for any bubbles before loading 5 µL of Agilent RNA Nano Marker in all 12 sample wells. Finally, 1 µL of the RNA samples and

RNA 6000 ladder were pipetted into the allocated wells. The chip was vortexed for 1 min at 2400 *g* in the adapter of the IKA vortexer (Staufen, Germany) before running the chip on the Agilent 2100 Bioanalyzer within 5 min. Analysis was carried out using the Agilent 2100 Bioanalyzer Software.

Samples having an RNA Integrity Number (RIN) higher than 9.0 were considered to be of good quality. Furthermore, the quality of the extracted RNA was determined by the ratio of the 28S: 18S ribosomal RNA, with a value close to two giving a further indication that the extracted RNA is of good quality.

2.5. COMPLEMENTARY DNA (CDNA) SYNTHESIS

Extracted RNAs were reverse transcribed into cDNA by SuperScript™ II Reverse Transcriptase, RNAse Reverse Transcriptase kit (Life Technologies, Paisley, U.K.), and Rnaseout™ (Invitrogen, Carlsbad, CA, USA) following manufacturer's recommended protocol. A final reaction volume of 20 µL was used for 2 µg of total RNA. This reaction volume was prepared as follows: firstly a mixture was prepared using 1 µL of Oligo (dT)12-18 (500 µg/mL), 1 µg of total RNA, 1 µL dNTP Mix (10 mM each dATP, dGTP, dCTP and dTTP at neutral pH), together with 1 µg of RNA in 10 µL of sterile and DEPC treated water. This mixture was then heated to 65°C for 5 min before quick chilling on ice followed by cDNA synthesis mix was then prepared by adding 4 µL of 5× First-Strand Buffer, 1 µL of 0.1 M DTT, 1 µL Rnaseout™ Recombinant RNase Inhibitor (40 units/µL) and 1 µL SuperscriptTM III RT (200 units/µL) to the Eppendorf tube containing the RNA. The contents were gently mixed and incubated at 50°C for 1 h, followed by inactivation of the reaction by heating at 70°C for another 15 min. For gene expression profiling experiments 1 µg of RNA was reverse transcribed to cDNA.

2.6. DESIGN OF PRIMERS FOR RT-QPCR

Transcript sequences were obtained from the NCBI and tested for the available primer sets by searching the human universal gene library, available from Roche Diagnostics website: https://www.roche-applied-science.com/sis/rtpcr/upl/ezhome.html .

Primer pairs should preferably be located in particular regions on the mRNA sequence, with forward primer on one exon, and the reverse primer on the adjacent exon. This is a typical approach to avoid co-amplification of genomic DNA which may interfere with the RT-qPCR results.

Primer stock solutions were prepared (100 µM), and used for preparing a diluted working solution with a final concentration of 20 µM. In order to homogenise the primers, diluted solutions were vortexed for 30 s followed by centrifugation at 12,000 *g* for one minute before and after dilution. The probes were stored at 4 ºC, and primers at -21 ºC.

2.7. RT-QPCR ANALYSIS

RT-qPCRs were performed using 384-well plates, with a final volume of 10 µL in each well, consisting of 4 µL of cDNA, 5 µL of 2x SYBR Green LightCycler 480TM PCR master mix (Roche Life Sciences), 0.6 µL of sterile distilled water, 0.1 µL of 20 µM reverse primer and 0.1 µL of 20 µM forward primer. All reactions were performed in triplicates. A negative control sample was prepared by adding 4 µL of H2O instead of cDNA. Following pipetting, the 384-well plate was thoroughly sealed using an optically clear adhesive strip, and centrifuged for approximately 30 s at 4,000g. RT-qPCR reaction was carried out using the Roche LightCycler LC480-qPCR platform, where fluorescence signals were measured at real-time. The protocol was set up with thermal cycling conditions consisting of one cycle at 95°C for 10 min, followed by 45 cycles of amplification at 95°C for 10 s and 60°C for 30 s.

Roche LightCycler Data Analysis Software was used to determine the melt curve data as well as the quantification cycle values.

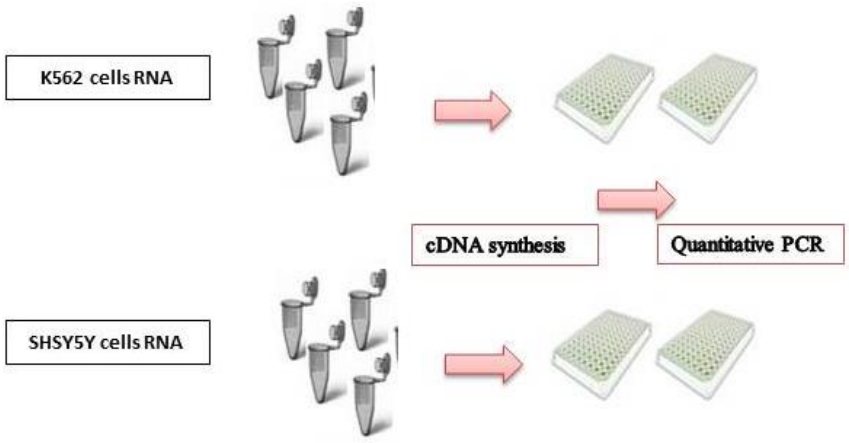

Figure 2.3 Flowchart showing first strand cDNA synthesis

cDNA synthesis and qPCR in K562 and SH-SY5Y cells. Reverse transcriptase (RT) enzyme was applied to RNA samples for each cell line. RNA was extracted in different time courses of drug treatments (1-4 h). After that the cDNAs were used as templates for qPCR assay to detect the quantity of related gene expression.

2.7.1. IDENTIFICATION OF IDEAL REFERENCE GENES

To exclude dissimilarities in cell number, RNA extraction, reverse transcription and PCR amplification efficiency, endogenous 'house-keeping' reference genes were chosen using the geNorm algorithm (The accurate normalization of real-time quantitative RT-PCR data by geometric averaging of multiple internal control genes). According to the original research by Vandesompele et al (2002) entitled, "Accurate normalization of real-time quantitative RT-PCR data by geometric averaging of multiple internal control genes", the geNorm algorithm is described as a means for finding internal control for performing qPCR. The method is highly utilized to normalize transcriptome data from qPCR, consisting of 8 stably expressed housekeeping genes which are not from the same pathways and express independently (88).

Prior to RT-qPCR analysis of mRNA expression in K562 and SH-SY5Y cells, triplicate cDNA samples were analysed for each of the nine candidate reference genes. Accordingly, two cell types were screened for the nine following reference genes: ACTB (Beta-Actin), B2M (βeta-2 microglobulin), GAPDH (glyceraldehyde 3 phosphate dehydrogenase), HMBS (hydroxymethyl-bilane synthase), HPRT1 (hypoxanthine phosphoribosyl transferase 1), RPL13A (ribosomal protein L13a), RPL32 (ribosomal protein L32) and SDHA (Succinate dehydrogenase complex, subunit A) for both cell lines and BCR-ABL (Abelson) for K562 only (see Figure 2.8).

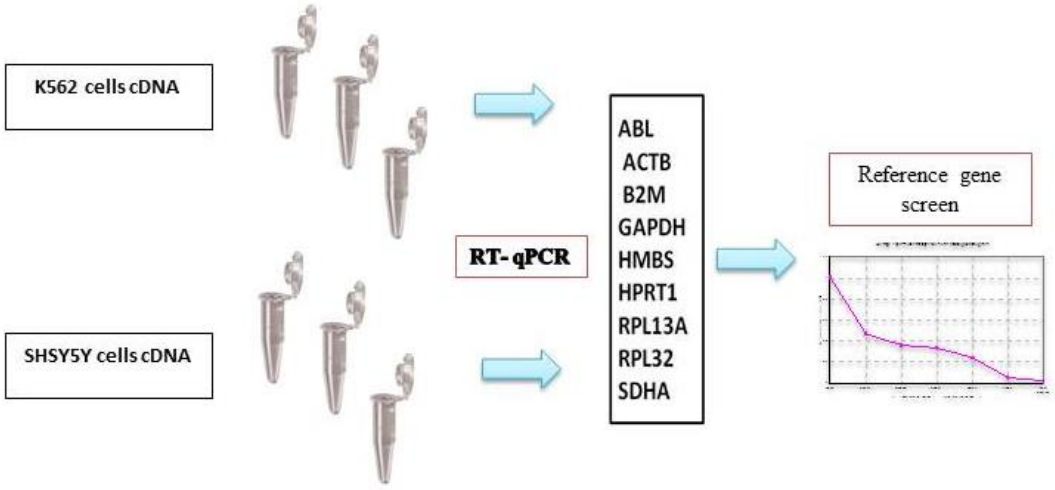

Figure 2.4 Identification of ideal reference genes in K562 and SH-SY5Y cells

Flowchart shows the analysis of K562 and SH-SY5Y optimal reference gene with RT-qPCR. Nine pairs of reference genes primers where investigated in qPCR assay and the amplification were assessed by gNorm algoritm in order to identify the most steady expressed genes.

The real-time PCR assays were performed on a Roche LC480 platform (Roche Diagnostics, Switzerland) as described in section 2.7. Following PCR amplification, the Cq values were analysed accordingly, by utilisation of the geNorm algorithm software package. This algorithm analyses the stability of each transcript, and thereafter eliminates the least stable mRNAs until most stable genes remain. Essentially, the software compares the stability of each gene tested within the samples sequentially until reaching a stability value M of 0.4

or less (Average expression stability values (M)). Any value below 0.4 is considered as stable (having minimal variation in expression). Although this is an arbitrary cut off value, demonstrated by Vandesompele's group, it is widely accepted as a reliable threshold.

M value is known as an average expression stability value. Considering the original research by Vandesompele et al (2002), this measure relies on the principle that the expression ratio of two ideal internal control genes is identical in all samples, regardless of the experimental condition or cell type.

Moreover, through that research they identified 8 most prevalent reference genes, which are independent in terms of pathways housekeeping genes. Then they measured those 8 reference genes across all samples and then the software eliminates the reference gene which is considered to be least stably expressed across all the tested samples to leave 7 candidates reference genes. The process is continued until the most stable pair of reference gene is that identified. So the M-value is the assessment of stability and the number of below 0.4 is considered by authors to signify adequacy for use as a reference gene in qPCR assays. Therefore, it is a term for showing the extent of reference gene stability. Through pair-wise algorithm analysis and by eliminating transcripts which are not equally expressed, GeNorm demonstrates the most stable reference gene expression in samples (88).

Official symbol	Forward Primer	Reverse Primer
GAPDH	AGCCACATCGCTCAGACAC	GCCCAATACGACCAAATCC
ACTB	ATTGGCAATGAGCGGTTC	GGATGCCACAGGACTCCAT
B2M	TTCTGGCCTGGAGGCTATC	TCAGGAAATTTGACTTTCCATTC
HPRT1	TGACCTTGATTTATTTTGCATACC	CGAGCAAGACGTTCAGTCCT
RPL32	GAAGTTCCTGGTCCACAACG	GCGATCTCGGCACAGTAAG
SDHA	AGAAGCCCTTTGAGGAGCA	CGATTACGGGTCTATATTCCAGA
HMBS	AGCTATGAAGGATGGGCAAC	TTGTATGCTATCTGAGCCGTCTA
RPL13A	GAGGCCCCTACCACTTCC	TGTGGGGCAGCATACCTC
BCR-ABL1	ATGCTACTGGCCGCTGAA	GGGTTTCTGAATGTCATCGTC

Table 2.1Showing the primers designed for the reference genes and BCR-ABL as a control gene.

2.7.2. IDENTIFICATION OF EXPRESSED IMATINIB OR CISPLATIN INFLUX AND EFFLUX TRANSPORTER GENES IN K562 CELLS AND SH-SY5Y CELLS

RT-qPCR analyses were performed to study which of the seven influx and efflux transporters, namely ABC (B1, B10, C1, and G2), SLC22A1 (OATP1A2) and SLCO1A2 (OCT-1), are expressed in K562 and SH-SY5Y cells. RT-qPCR reaction was performed as described in Section 2.7, using the primers specific for each candidate transporter gene as shown in Table 2.2. Roche LightCycler Data Analysis Software was used to obtain amplification curves.

Official symbol	Forward Primer	Reverse Primer
SLCO1A2	TGGAACAAAGCTTGATCCTCTT	GGGGCATGCAGGATATATGA
ABCC1	AATTAAAAAGGTAGCAAGCAGCAT	GGAAAGAAGTCGGGGCATA
ABCB1	ACTGTAATAATAGGCATACCTGGTCA	GAAATTTAGAAGATCTGATGTCAAACA
SLC22A1	TGGTCCATTATCTTTATTGCTTCA	TCCTCTTCCTGCTCTACTACTGG
ABCG2	TCGTCCCTGCTTAGACATCC	TGGCTTAGACTCAAGCACAGC
ABCB10	TTCCCAAAAGCTCGAACAGT	CAGGATTCCCTGGCACAA

Table 2.2 Showing the primers designed for the transporter genes. All the primer sequences 5' to 3' orientation.

2.7.3. IMATINIB AND CISPLATIN TREATMENT EFFECTS ON TRANSPORTER GENE EXPRESSION

K562 and SH-SY5Y cells were seeded in a 6-well plate at a density of 1 × 105 cells per well, and incubated with 0.5 μM imatinib, for 1-5 h. Following treatment, RNA was extracted as described in section 2.4, and reverse transcribed to cDNA. RT-qPCR was performed as described in Section 2.3.6, using primers specific for K562 and SH-SY5Y housekeeping genes beside the transporter genes as shown in Tables 2.1 and 2.2 for 7 relative amounts of the target transporter genes mRNA expression were normalised to the mRNA expression of reference genes. The ΔΔCq method was used to calculate any up-regulations or down-regulations in the target transporter genes following imatinib treatment, when compared to gene expression in control (untreated) cells. The same procedures were performed for K562 and SH-SY5Y cells and 1 μM cisplatin (for 1-4 h of drug treatment).

2.7.4. STATISTICAL ANALYSIS FOR RT-QPCR

Generally, in a RT-PCR assay a positive reaction is detected by accumulation of a fluorescent signal and the Cq value (quantification cycle value) is the point within the PCR process at which the fluorescence is statistically defined to be above the background. Ct (using ABI), Cp (using Roche) and Cq (the academic term that does not have connections to companies) are all the same term describing the number of cycles required for the fluorescent signal to cross the threshold (ie exceeds background level, often by a value of 10 x). In RT-qPCR for a specific sample, the amount of the gene of interest is quantified in comparison to the amount of a reference gene. Therefore, the ΔCq was resulted from the subtraction of the reference gene Cq value from the Cq value of target gene (ΔCq = Cq target - Cq reference). Consequently, ΔΔCq method was used for estimating the copy number (Relative Normalised Ratio), of 6 transporter target genes and the reference genes. The ΔΔCq was calculated by subtracting the ΔCq of control samples from the ΔCq of the test samples (ΔΔCq = ΔCq test (Treated) - ΔCq control (Non-treated))

So the ΔΔCq method is used to calculate the fold change in gene expression between two samples. Using housekeeping genes for normalization and calculating the fold change relative to the normalized gene against the control group (Non-treated). As a result, by utilizing the comparative ΔΔCq method, the relative expression of genes was produced and the logarithmic numbers were changed to the actual numbers by applying the formula $2^{-\Delta\Delta Cq}$.

2.7.5. STATISTICAL ANALYSIS

Normal distribution of the data was confirmed by Shaphiro-Wilks test. Statistical analysis was performed first by Levene's test to assess homogeneity of variance. When no significant differences were found in the variances of the different groups, statistical analysis was continued by one-way ANOVA and Tukey's post-hoc test. When variances were unequal, the

analysis was followed with Welch ANOVA and Games-Howell's post-hoc test. Probability values <0.05 were regarded as significant. SPSS software version 20.0 was used to perform this analysis (The name of test which was used for each gene was presented in 3 table, in appendix 4).

CHAPTER 3

RESULTS

3.1. MTT ASSAY OPTIMISATION

The MTT assay of cell proliferation was used to measure the effect of cell toxicity and cell viability when treated with imatinib or cisplatin with MBFs to find hits. Thus, MTT assay was optimised for cell number and drug concentrations to utilize in identification of the most effective active fragments.

3.1.1. EVALUATION OF OPTIMAL CELL NUMBER USING THE MTT ASSAY

The assay was first validated by investigating the effects of exposure to cytotoxic reagents (TritonX-100, NaCl and DMSO) on viability of the cells using a range of concentrations. The results of these experiments are shown in Figures 3.1 and 3.2 for K562 and SH-SY5Y cells respectively. In all experiments, the cells were also exposed to 0.01% TritonX-100 for 30 min

to achieve approximately 100% cell lysis. Therefore a positive result was considered when a reagent killed the cells, for instance Triton X-100 and DMSO. Negative control samples (such as PBS) were viability test samples and did not kill cells. Moreover, 0% means all cells were dead, and 100% means all cells were alive and no dead cells were seen.

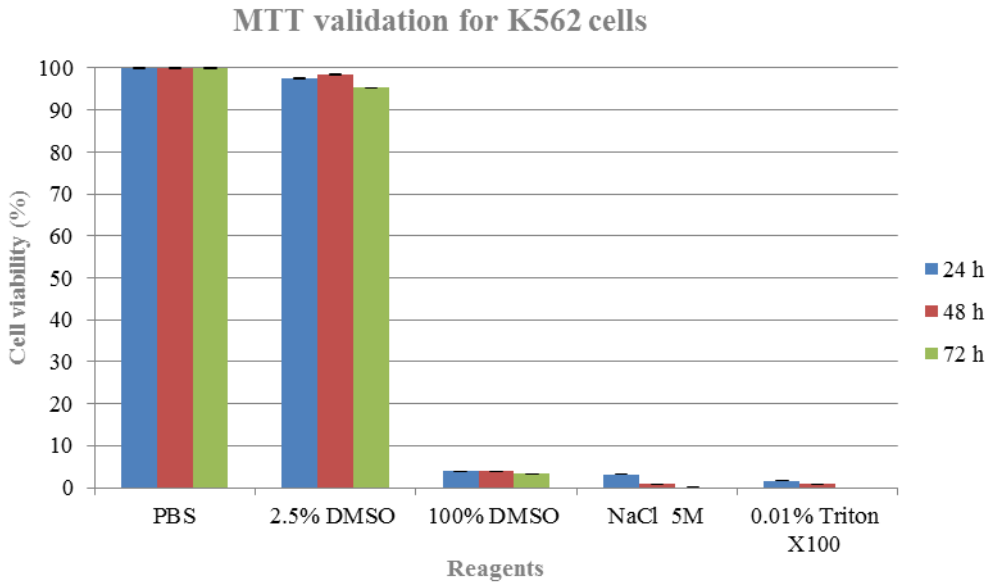

Figure3.1 MTT validation through absorbance measurements as a function of the different cytotoxic reagents.

Showing K562 cell's viability after different incubation times with cytotoxic reagents. cell viability was decreased to about 10% or less for all reagents. TritonX-100 was selected as a positive control and PBS as a negative control of following experiments. All experimental incubation conditions were performed in triplicate samples. Error bars display the STDEV (standard deviation- which illustrates the difference of each technical replicates from the mean value of all replicates).

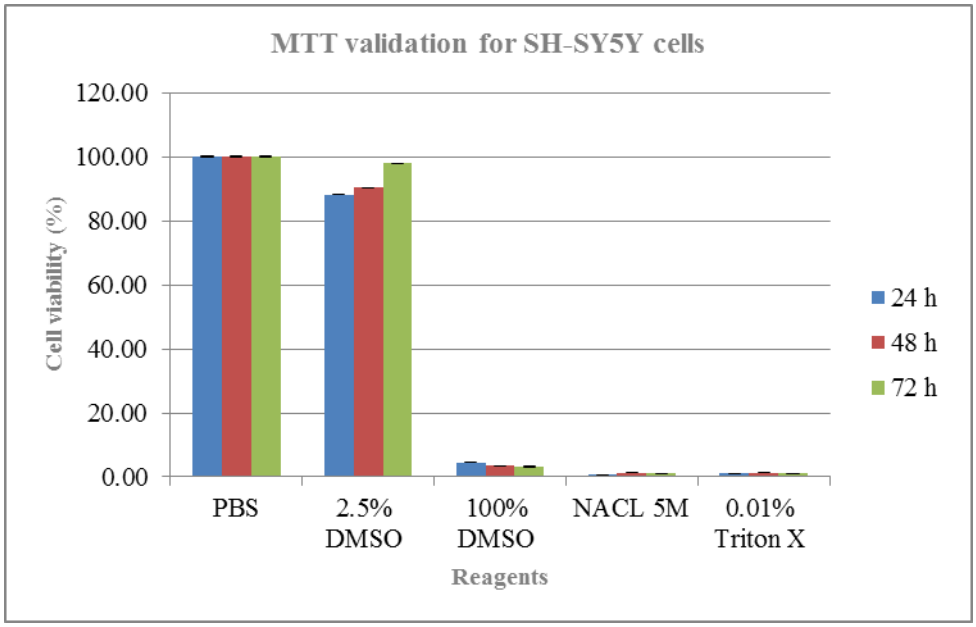

Figure 3.2 MTT validation through absorbance measurements as a function of the different cytotoxic reagents (DMSO, NaCl and Triton X-100).

Showing SH-SY5Y cell's viability after different incubation times with cytotoxic reagents. Cell viability was decreased to lower than 10% for all reagents. TritonX-100 was selected as a positive control and PBS as a negative control of the following experiments. All experimental incubation conditions were performed in triplicate samples. Error bars display the STDEV (standard deviation- which illustrates the difference of each technical replicates from the mean value of all replicates).

The comparison of figure 3.1 and 3.2 shows that SH-SY5Y cells are more sensitive than K562, since they had less cell viability after treatment with identical cytotoxic reagents.

Moreover, to determine the sensitivity and dynamic range of the MTT assay for SH-SY5Y and K562 cells, serial dilutions (5×10^3 to 2×10^4 cells per well) of neuroblastoma and leukaemia cells were seeded in 96-well plates. Figurer 3.3 shows the difference in absorbance for K562 cell numbers which by increasing the number of cells per well, the absorbance was increased, but after 48 h from 1.2×10^4 cells per well the trend shows fluctuations; although the cell number had an increasing trend, the absorbance showed the decreasing ones only for 2×10^3. As a result the 7×10^3 cells per well was selected since not only it had an upward trend in absorbance through all time points but also it had smaller error bars compared to other cell ranges (figure 3.3).

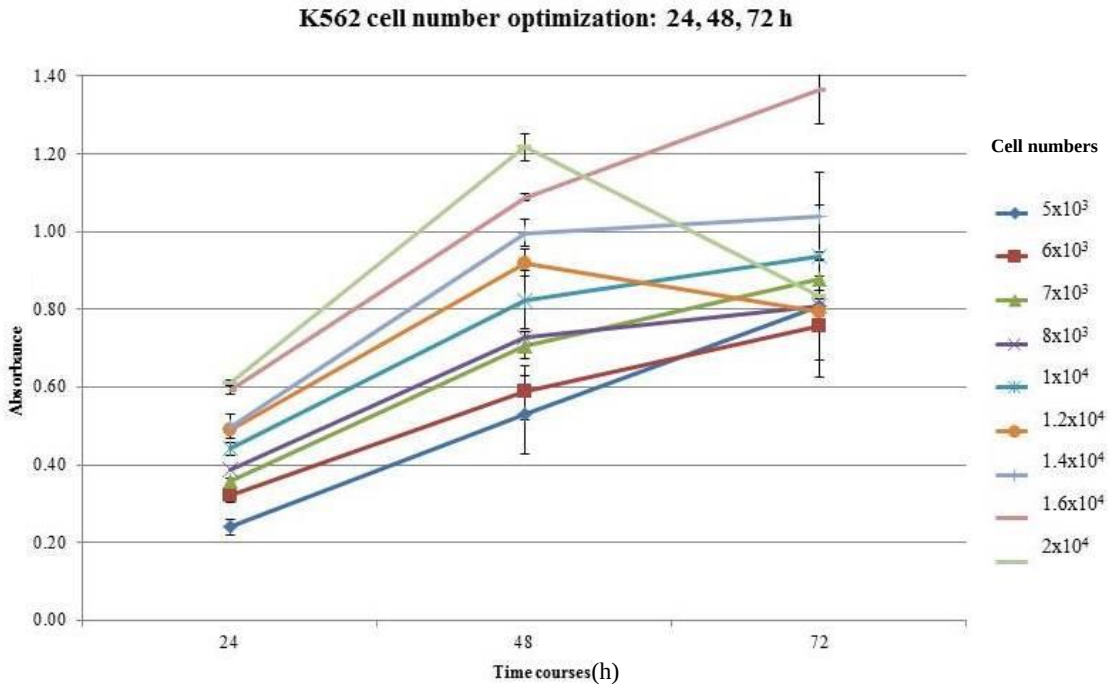

Figure 3.3 Serial dilution of viable K562 cells ranged from 5×10^3 to 2×10^4 for 24, 48 and 72 h.

The line graph shows by increasing cell numbers the absorbance is increased. However, this uprising trend continued up to 1×104 cells per well for 72 h. After that they had fluctuations in the absorbance which is the indication of reaching saturation point in cell growth. Error bars display the STDEV (standard deviation- which illustrates the difference of each technical replicates from the mean value of all replicates). (Absorbance was read at 570 nm).

Similar to K562, figure 3.4 shows the optimal cells for SH-SY5Y, which indicates the cell number between 1.2×10^4 and 1.5×10^4 which will have expected differences in absorbance for all 3 time courses and also their error bars are smaller than other cell numbers. As a result, 1.4×10^4 cells per well was selected.

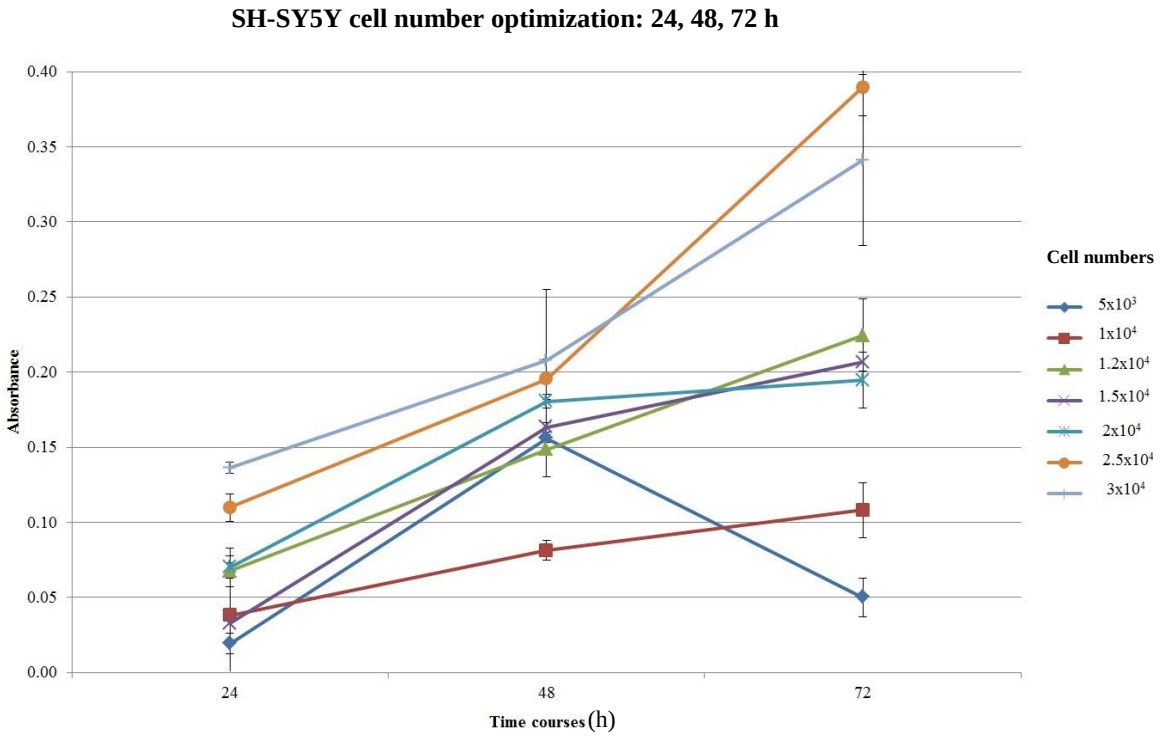

Figure 3.4 Serial dilution of SH-SY5Y cells ranged from 5×10^3 to 3×10^4 for 24, 48 and 72 h.

The line graph shows by increasing cell numbers the absorbance is increased. However, this uprising trend continued up to 1.5×104 cells per well for 72 h. After that they had fluctuations in the absorbance which is the indication of reaching saturation point in cell growth. Error bars display the STDEV(standard deviation- which illustrates the difference of each technical replicates from the mean value of all replicates). (Absorbance was read at 570 nm).

The assay was validated by seeding different range of cell numbers (per well), which comparing the cell number serial dilutions for K562 and SH-SY5Y and based on the fact that K562 cells have a lower doubling time (21 h) compared to SH-SY5Y cells which have a doubling time of 48 h, so K562 can reach the cell growth saturation point much sooner than SH-SY5Y cells and they have higher absorbance rates. Therefore, 7×10^3 and 1.4×10^4 cells per well were selected for K562 and SH-SHY5Y, respectively.

3.1.2. EVALUATION OF OPTIMAL DRUG CONCENTRATION USING THE MTT ASSAY

Imatinib activity against the K562 and SH-SY5Y cell lines following three times of incubations (24, 48, 72 h) was assessed by using the MTT assay in which cells were exposed

to a log scale of drug concentrations (0, 0.001, 0.003, 0.01, 0.03, 0.1, 0.3, 1, 3, 10, 30 μM). The same experiments were performed with cisplatin log scale concentrations (0, 0.001, 0.003, 0.01, 0.03, 0.1, 0.3, 1, 3, 10, 30, 100, 300 μM).

Dose-response curves show there was a concentration-dependent decrease in cell viability. Figure 3.5–3.8 depicts average results of minimum three repeats of experiments in which there were actual decreases in viable cell numbers compared to control.

Percentage viability at each extract concentration was calculated as following:

Cell viability (%) = (Extract concentration reading – Blank reading / Positive control reading (cells with PBS treatment (0 μM)) – Blank reading) × 100

Cell Cytotoxicity (%) was expressed as (100 – cell cytotoxicity)

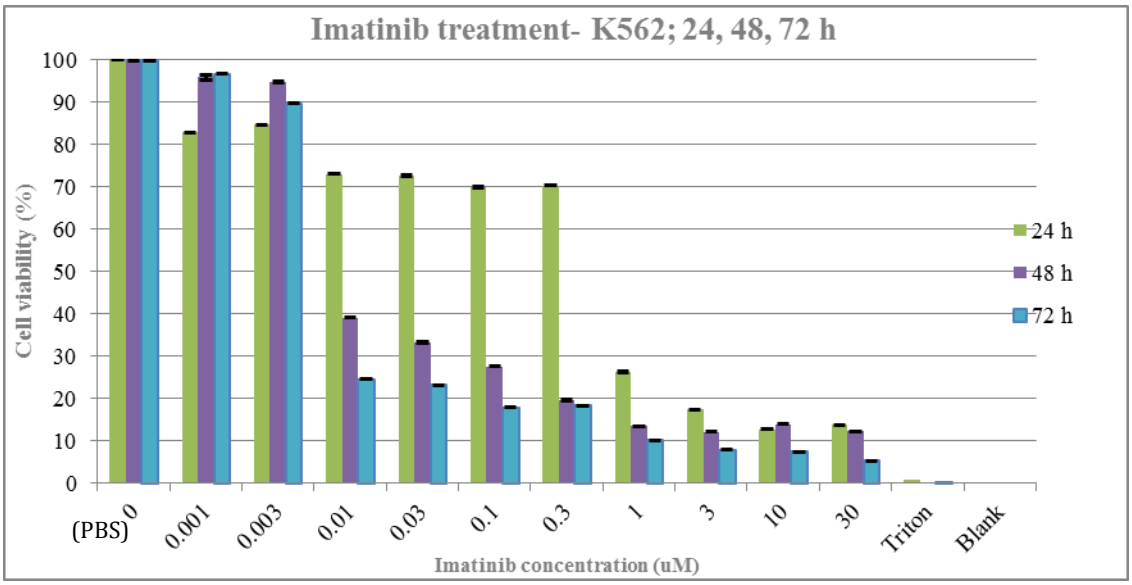

Figure 3.5 Dose-response for imatinib-treated K562 cell incubated in different time courses for 24, 48 or 72 h followed by 3.5 h incubation with MTT salt.

All experiment incubation conditions were performed in triplicate samples. Error bars display the STDEV (standard deviation- which illustrates the difference of each technical replicates from the mean value of all replicates).

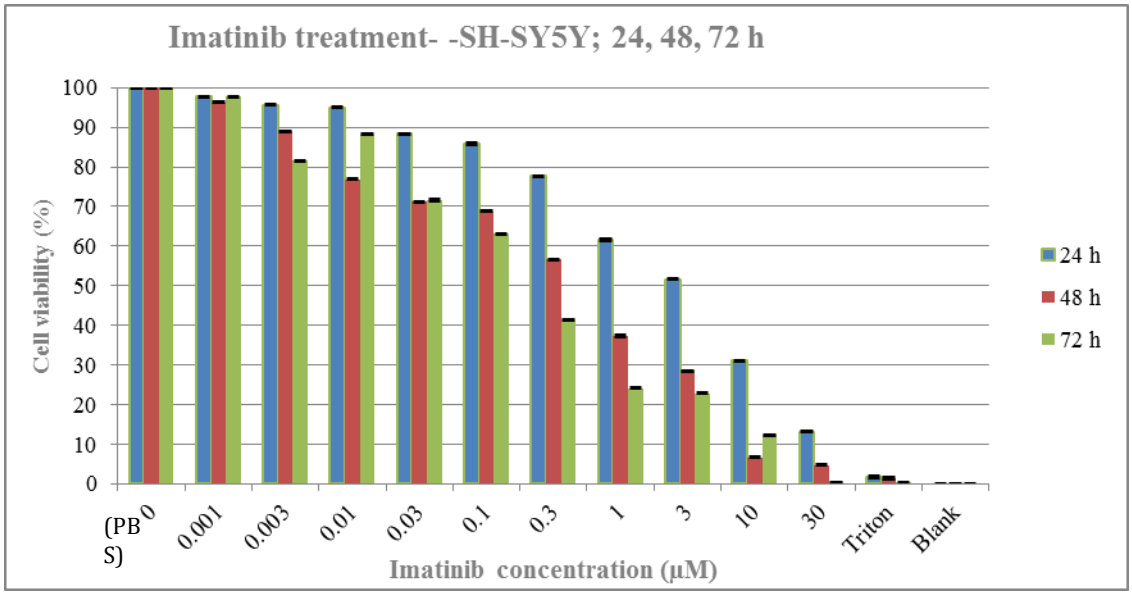

Figure3.6 Dose-response for imatinib-treated SH-SY5Y cell incubated in different time courses for 24, 48 or 72 h followed by 3.5 h incubation with MTT salt.

All experiment incubation conditions were performed in triplicate samples. Error bars display the STDEV (standard deviation- which illustrates the difference of each technical replicates from the mean value of all replicates).

Figure 3.5 and 3.6 depicts average results of minimum three repeats of experiments in which there were actual decreases in viable cell numbers compared to control. Dose-response curves for the effect of different imatinib concentrations on K562 and SH-SY5Y cells show decreasing trends for cell viability by increasing the imatinib concentrations. However, the pattern of this trend was not the same for the two cell lines. Although SH-SY5Y had higher cell viability for the majority of imatinib doses, the cell viability decreased suddenly for doses higher than 0.3 µM after 48 h. Conversely, K562 showed more cell deaths from 0.01 µM.

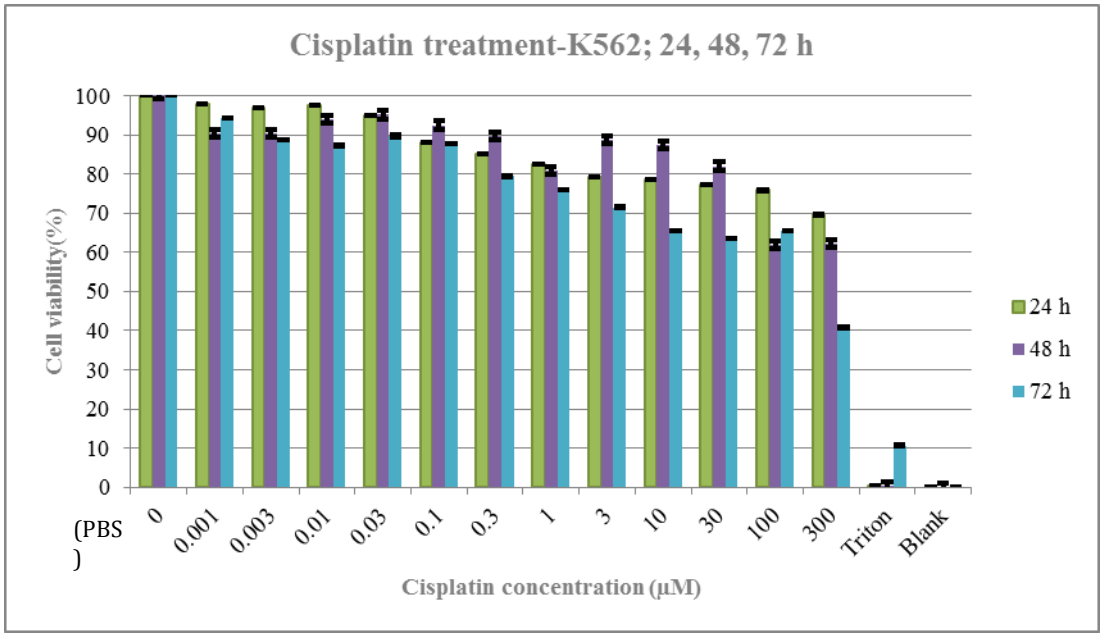

Figure3.7 dose-response for cisplatin-treated K562 cell incubated in different time courses for either 24, 48 or 72 h followed by 3.5 h incubation with MTT salt.

All experiment incubation conditions were performed in triplicate samples. Error bars display the STDEV (standard deviation- which means the difference of each technical replicates from the mean value of all replicates).

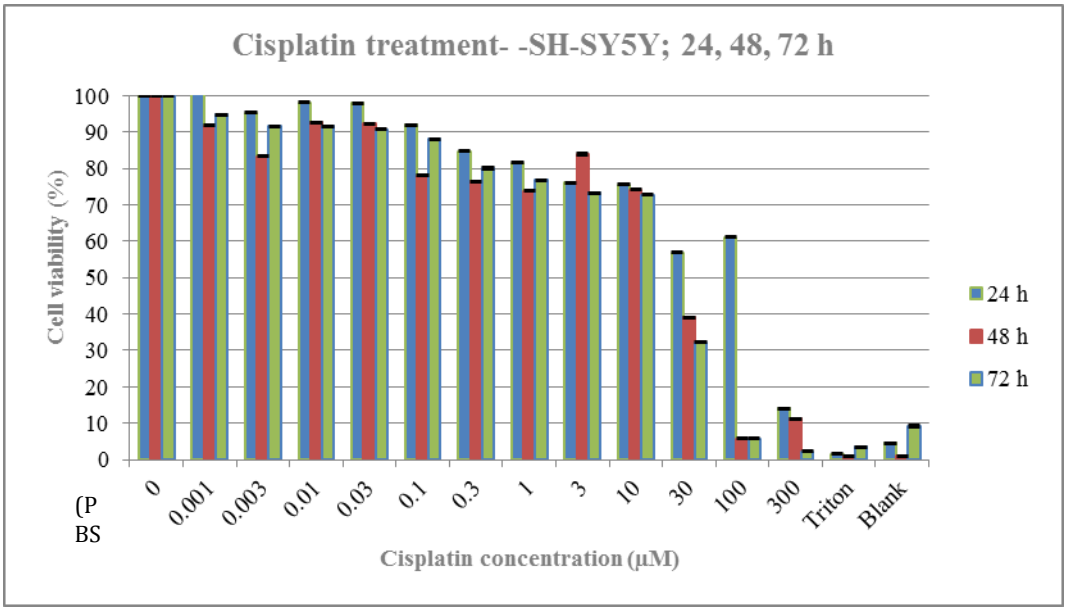

Figure3.8 Dose-response for cisplatin-treated SH-SY5Y cell incubated in different time courses for 24, 48 or 72 h followed by 3.5 h incubation with MTT salt.

All experiment incubation conditions were performed in triplicate samples. Error bars display the STDEV (standard deviation- which illustrates the difference of each technical replicates from the mean value of all replicates).

Figure 3.7 and 3.8 showed the results for cisplatin concentration for each cell line. In which both cell lines viability for lower doses remain constant, around 90% of viability, then in SH-SY5Y cells it decreases from 30 µM concentration after 24 h. However the viability for K562 at the highest concentration (300 µM) remained around 60% of cell viability after 48 h.

Since the following experiments for MBF screenings of the 70-80% of cell viability is needed for both cell lines (based the experiment design); the concentration was selected that caused around 80% of cell death. Therefore, the concentration value for imatinib was 0.3 µM after 24 h of incubation and for cisplatin was 1 µM after 48 h incubation.

3.2. MBF SCREENING EXPERIMENTS

3.2.1. MBF SCREENING EXPERIMENTS (IN POOLS)

The cytotoxic effects of MBFs were assessed through using the MTT assay, with the aim of enhancing the drug's efficacy. Different experiment designs were performed for each drug and cell line separately. Since the first library of MBFs consist of 500 MBFs for saving time and materials first experiments was started with pooled screening which is referring to every 5-6 MBFs were combined in a single well of 96-well plates and checking the cell viability

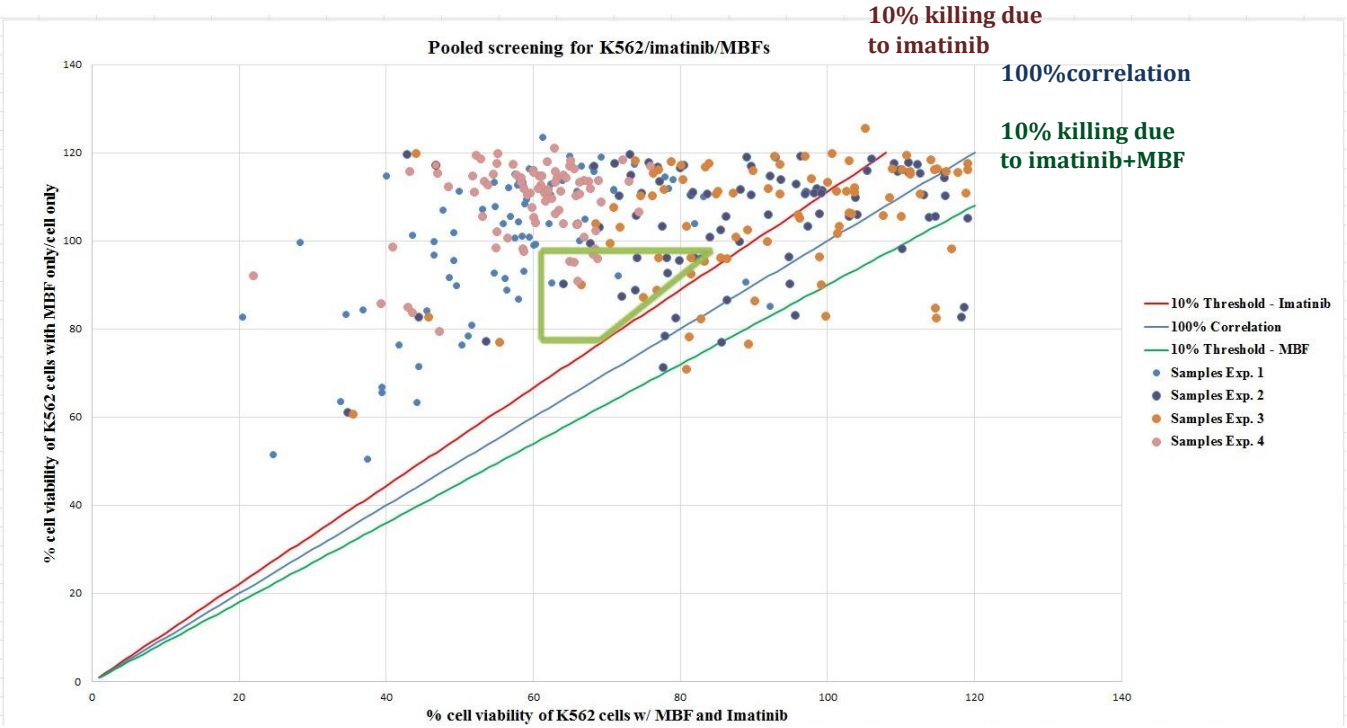

Figure 3.9 Four replication of MTT assays for K562- imatinib/MBFs screening (pooled).

Cell viability of K562 after treatment with MBFs only versus cell viability of them after treatment with both MBFs and imatinib. Each colour representative of one set of experiments consisted of two 96 well plates; one contained K562 and MBFs only and the other one contained MBFs and Imatinib with K562 cells. Therefore the current graph shows 4 replications of the same experiment. The defined cut off for the selecting of those active MBFs (hits) for all experiments for MBF screenings is a 10% threshold including cells with MBFs only or cells with MBFs and drugs. Therefore, those for 3 biological repeats have viability between 60-80% with imatinib and MBFs besides have viability between 80-100% with MBFs only will be considered and those shown in the green trapezoid were selected for single screenings.

In figure 3.9, 3.10, 3.11 and 3.12 the green trapezoid on all the graphs were added to represent the area of selected MBFs. In all graphs related to MBF screenings, the defined cut-off for the selecting of those active MBFs (hits) for all experiments is a 10% threshold for cells with MBFs only or cells with MBFs plus drugs. Therefore, those results located above the red line for the +10% threshold for imatinib or cisplatin were considered. For instance, Figure 3.9 showing the percentage of cell viability of K562 cells incubated with MBF only on the y-axis and percentage of cell viability of K562 cells with MBF and 0.3 µm imatinib on the x-axis. The threshold

determining which MBFs had an effect on the drug/cell's viability was taken to be 10%. The "100% correlation" data series indicated there was no significant difference between the cells treated with fragments only and the cells treated with the fragments and imatinib.

The results which fall in the band between the "10% killing due to imatinib" and the "10% killing due to MBF" data series were not considered as MBF hits because the difference in percentage of cell death between cells treated with MBF only and cells treated cells treated with MBF plus imatinib was considered to be insignificant, since was lower than the threshold set. The results which fell beneath the -10% imatinib green data series "10% killing due to MBF" were also not considered as hits because here cell death was being caused by MBF rather than the drug. The MBFs considered as hits were those above the red data series "10% killing due to imatinib". Here the difference in percentage of cell viability between cells treated with MBF only and cells treated with MBF+imatinib was significant, since it was greater than the set threshold, showing that when the cells were treated with imatinib in the presence of MBF, the percentage cell death was significantly higher than when the cells were incubated with just the fragments. Only those with viability between 60-80% with imatinib and MBFs were considered and among were selected for single screenings. Therefore, from pooled screening results for K562 and imatinib, 7 wells (40 MBFs) and a minimum of 3 replicates experiments showed results in the cut-off area were selected as suitable candidates for single screenings. After 3 or 4 biological repeats of the experiment, replicates showing approximately similar result, were selected for subsequent screening either within pools or singularly.

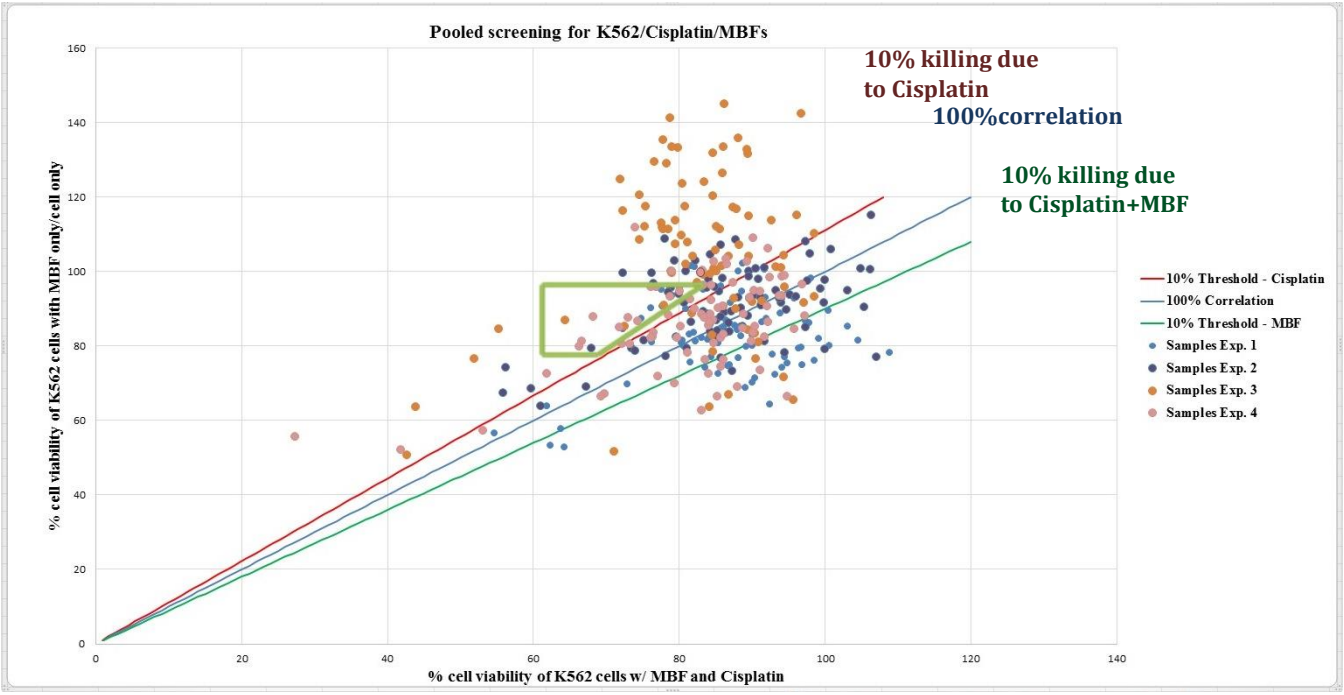

Figure 3.10 Four replication of MTT assays for K562-cispaltin MBFs screening (pooled).

Cell viability of K562 after treatment with MBFs only versus cell viability of them after treatment with both MBFs and cispaltin. Each colour representative of one set of experiments consisted of two 96 well plates; one contained k562 and MBFs only and the other one contained MBFs and cisplatin with K562 cells. Therefore the current graph shows 4 replications of the same experiment. The defined cut off for the selecting of those active MBFs (hits) for all experiments for MBF screenings is a 10% threshold including cells with MBFs only or cells with MBFs and drugs. Therefore, those for 3 biological repeats have viability between 80-100% with MBFs only will be considered and those shown in the green trapezoid were selected for single screenings.

The same methodology for pooled screening with K562 and imatinib (figure 3.9) was performed for K562 and cisplatin MBF screening (pooled). In figure 3.10, showing the percentage of cell viability of k562 cells incubated with MBF only on the y-axis and percentage of cell viability of K562 cells with MBF and 0.3µm CISPLATIN on the x-axis. Those have viability between 60-80% with cisplatin and MBFs besides has viability between 80-100% with MBFs only will be considered and among were selected for single screenings. Therefore, from pooled screening results for K562 and cisplatin 5 wells (30 MBFs) after minimum 3 times repeating of the experiments showed results in the cut off area were selected as suitable candidates for single screenings. So after 3 or 4 biological repeats of the

experiment, those showing approximately similar result, were selected for subsequent screening either within pools or singularly.

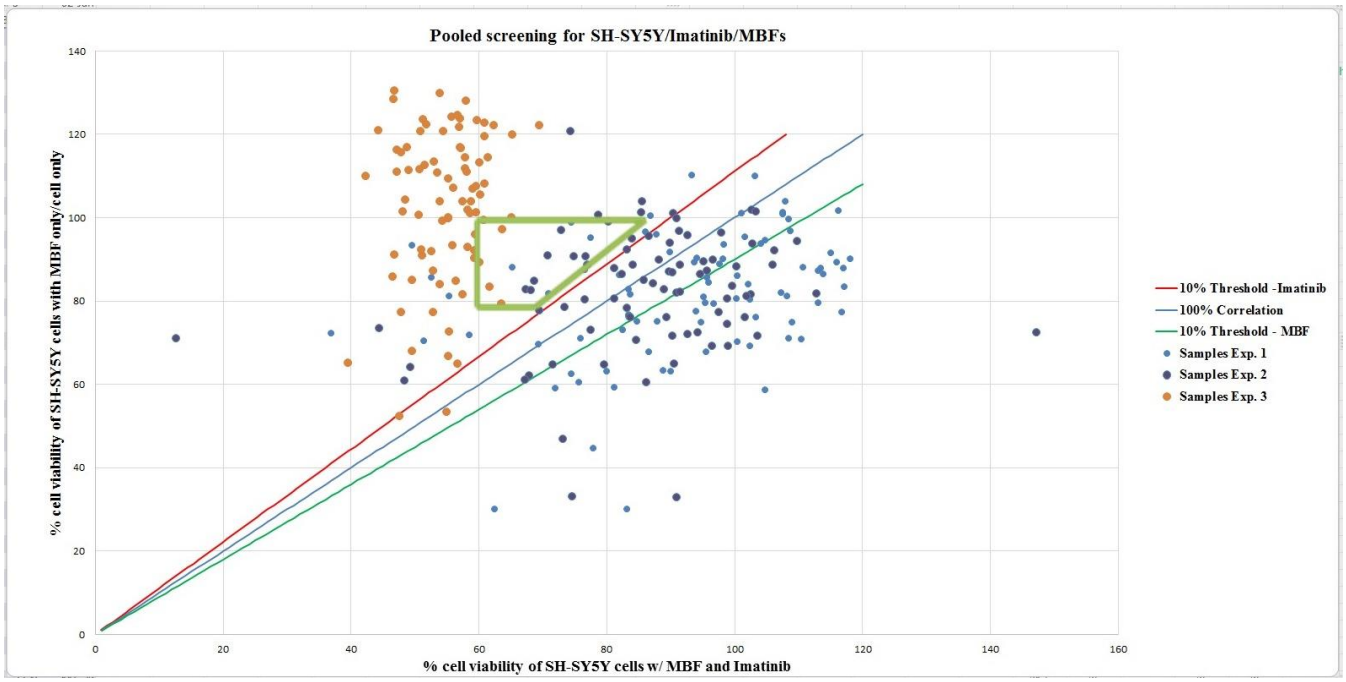

Figure 3.11 Three replication of MTT assays for SH-SY5Y -imatinib MBFs screening (pooled).

Cell viability of SH-SY5Y after treatment with MBFs only versus cell viability of them after treatment with both MBFs and imatinib. Each colour representative of one set of experiments consisted of two 96 well plates; one contained SH-SY5Y and MBFs only and the other one contained MBFs and imatinib with SH-SY5Y cells. Therefore the current graph shows 3 replications of the same experiment. The defined cut off for the selecting of those active MBFs (hits) for all experiments for MBF screenings is a 10% threshold including cells with MBFs only or cells with MBFs and drugs. Therefore, those for 3 biological repeats have viability between 80-100% with MBFs only will be considered and those shown in the green trapezoid were selected for single screenings.

For pooled screenings, the same methodology for pooled screening with K562 was performed for SH-SY5Y cells either with imatinib or cisplatin. Therefore, from pooled screening results for SH-SY5Y and each drug 3 wells (18 MBFs) after minimum 3 times repeating of the experiments was selected as suitable candidates for single screenings (figure 3.11 and 3.12). All related tables for pooled screening cell viabilities were presented in appendix1.

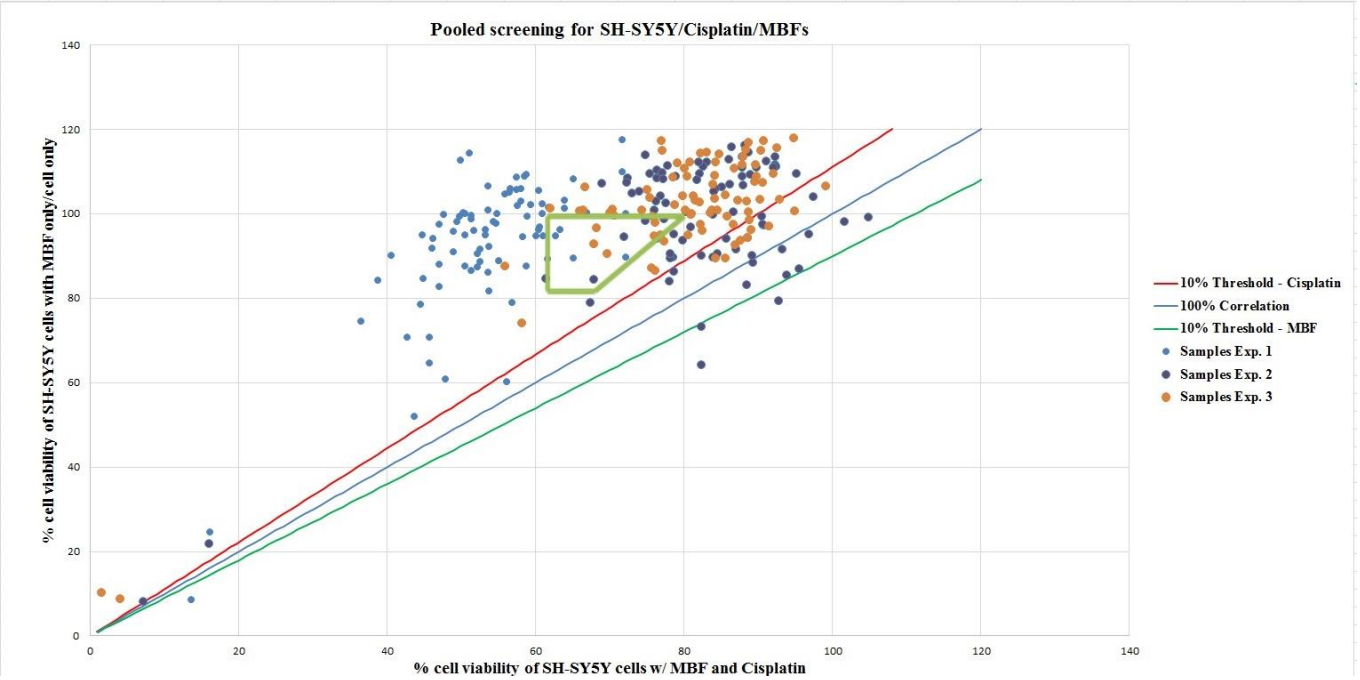

Figure 3.12 Three replication of MTT assays for SH-SY5Y -cisplatin MBFs screening (pooled).

Cell viability of SH-SY5Y after treatment with MBFs only versus cell viability of them after treatment with both MBFs and cisplatin. Each colour representative of one set of experiments consisted of two 96 well plates; one contained SH-SY5Y and MBFs only and the other one contained MBFs and cisplatin with SH-SY5Y cells. Therefore the current graph shows 3 replications of the same experiment. The defined cut off for the selecting of those active MBFs (hits) for all experiments for MBF screenings is a 10% threshold including cells with MBFs only or cells with MBFs and drugs. Therefore, those for 3 biological repeats have viability between 80-100% with MBFs only will be considered and those shown in the green trapezoid were selected for single screenings.

3.2.2. MBF SCREENING EXPERIMENTS (IN SINGLE MBFS)

By finishing pooled screenings and identifying the active MBFs that supported cell viability, based on a defined cut off (cell viability between 50-70%), the cytotoxic effects of each the MBFs were assed separately, it means that each selected hit from pooled screening placed in one well of 96-well plate.

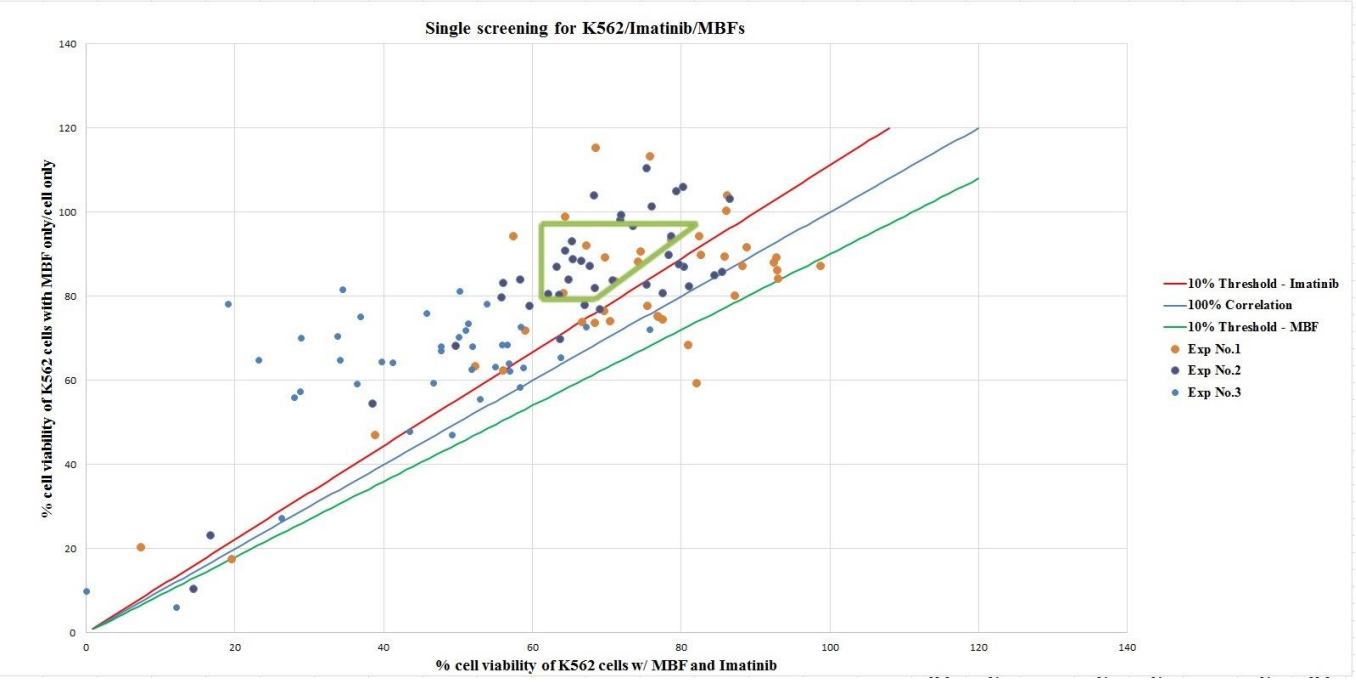

Figure 3.13 Three replication of MTT assays for K562-imatinib MBFs screening (single MBFs).

Cell viability of K562 after treatment with MBFs only versus cell viability of them after treatment with both MBFs and imatinib. Each colour representative of one set of experiments consisted of two 96 well plates; one contained K562 and MBFs only and the other one contained MBFs and imatinib with K562 cells. The green trapezoid on the graph represents the area of selected MBFs.

For single screenings also, the same methodology for pooled screening with K562 and SH-SY5Y was performed for both cells either with imatinib or cisplatin. The defined cut off for the selecting of active MBFs (hits) for single screening was the same with pooled ones. Therefore, from 40 candidates that resulted from pooled screening assays, six MBFs were recognized (after three replication assays in which assay also we had triplicates) as active molecules that showed cell viability in the cut off.

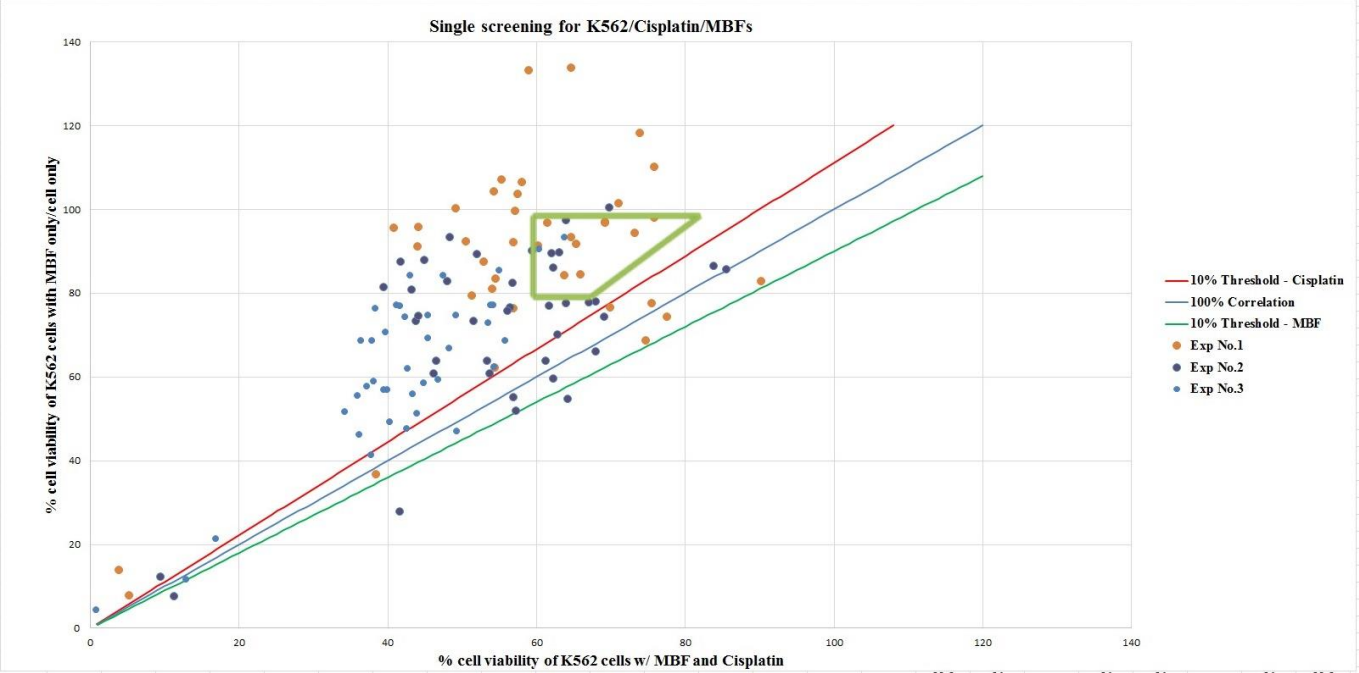

Figure 3.14 Three replication of MTT assays for K562-cisplatin MBFs screening (single MBFs).

Cell viability of K562 after treatment with MBFs only versus cell viability of them after treatment with both MBFs and cisplatin. Each colour representative of one set of experiments consisted of two 96 well plates; one contained K562 and MBFs only and the other one contained MBFs and cisplatin with K562 cells. The green trapezoid on the graph represents the area of selected MBFs.

The defined cut off for the selecting of active MBFs (hits) for single screening was the same with pooled ones. Therefore, from 30 candidates that resulted from pooled screening assays, four MBFs were recognized (after three replication assays in which assay also we had triplicates) as active molecules that showed cell viability in the cut off.

The same experiment designs were performed for SH-SY5Y cell with cisplatin and imatinib and from each screening assay after two times of repeating two MBFs from total of 18 MBFs in each set were selected as active hits. Data were presented in figure 3.15 and 3.16.

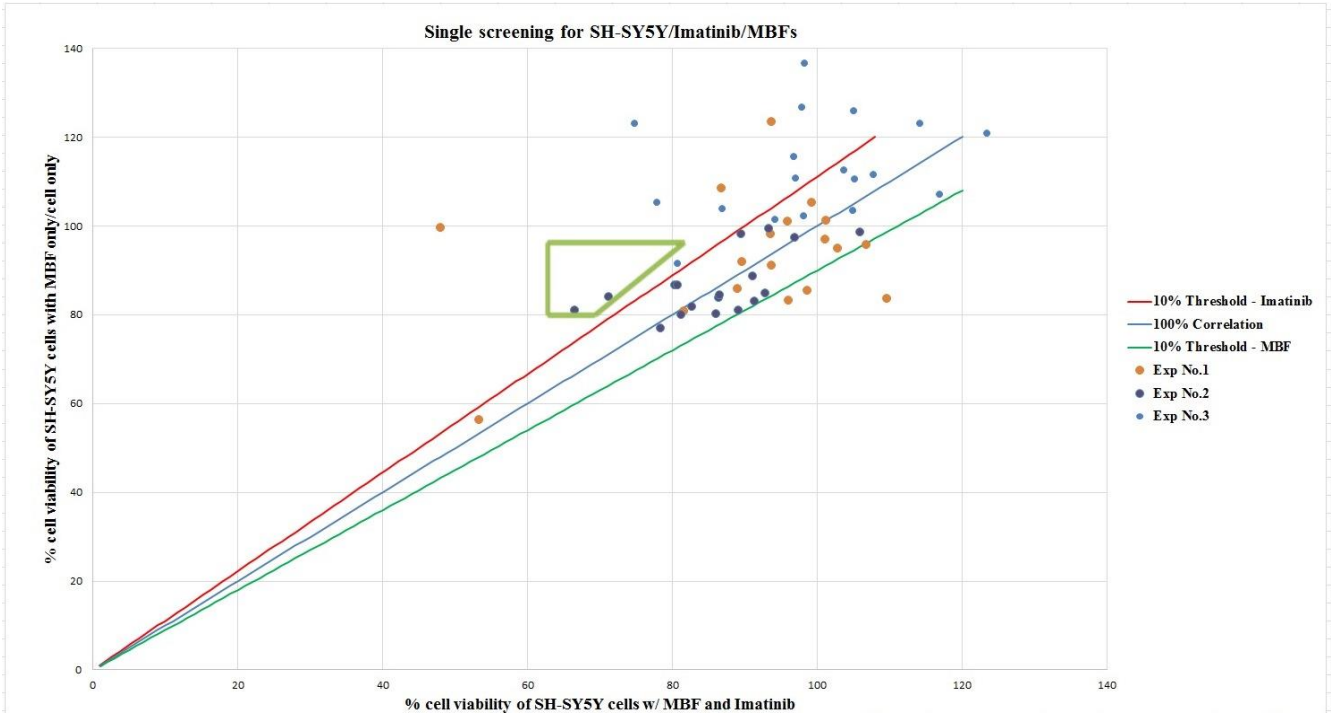

Figure 3.15 Three replication of MTT assays for SH-SY5Y-imatinib MBFs screening (single MBFs).

Cell viability of SH-SY5Y after treatment with MBFs only versus cell viability of them after treatment with both MBFs and imatinib. Each colour representative of one set of experiments consisted of two 96 well plates; one contained SH-SY5Y and MBFs only and the other one contained MBFs and imatinib with SH-SY5Y cells. The green trapezoid on the graph represents the area of selected MBFs.

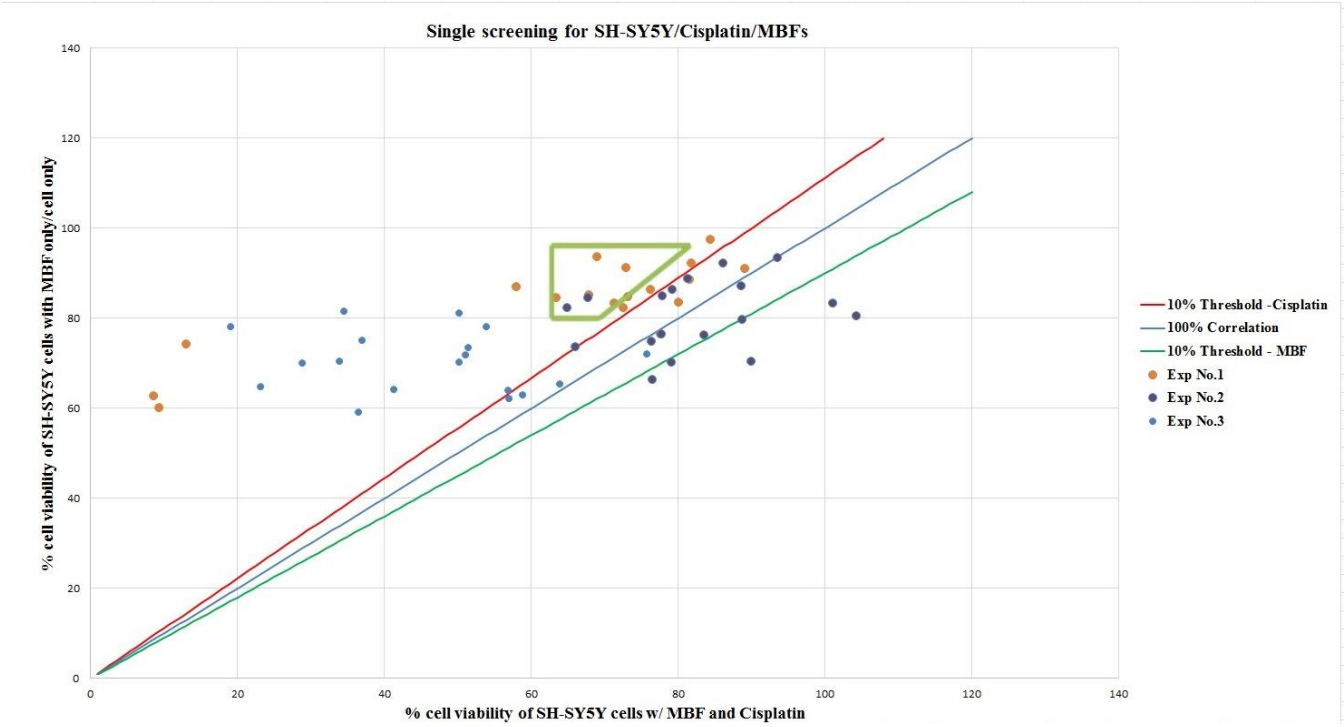

Figure3.16 Three replication of MTT assays for SH-SY5Y-cisplatin MBFs screening (single MBFs).

Cell viability of SH-SY5Y after treatment with MBFs only versus cell viability of them after treatment with both MBFs and cisplatin. Each colour representative of one set of experiments consisted of two 96 well plates; one contained SH-SY5Y and MBFs only and the other one contained MBFs and cisplatin with SH-SY5Y cells. The green trapezoid on the graph represents the area of selected MBFs.

All related tables for single screening cell viabilities were presented in appendix2.

3.2.3. TITRATION SCREENING ASSAY FOR SELECTED HITS

The selected active MBF hits from single screenings were used for the titration experiment to find the effective concentration of those selected active fragments as well as finding those active hits that have activity in all concentration. Moreover, their chemical structures were extracted from the first library information.

Results for titration experiment with log scale concentration of each hit (active MBF) (0, 1, 3, 10, 30, 100 or 300 µM) were presented in figure 3.17-20. The presented results are the average of minimum two times biological replications and each replication was performed in triplicates. Furthermore, the same 10% cut off with other screening experiments were applied for selecting the most active one.

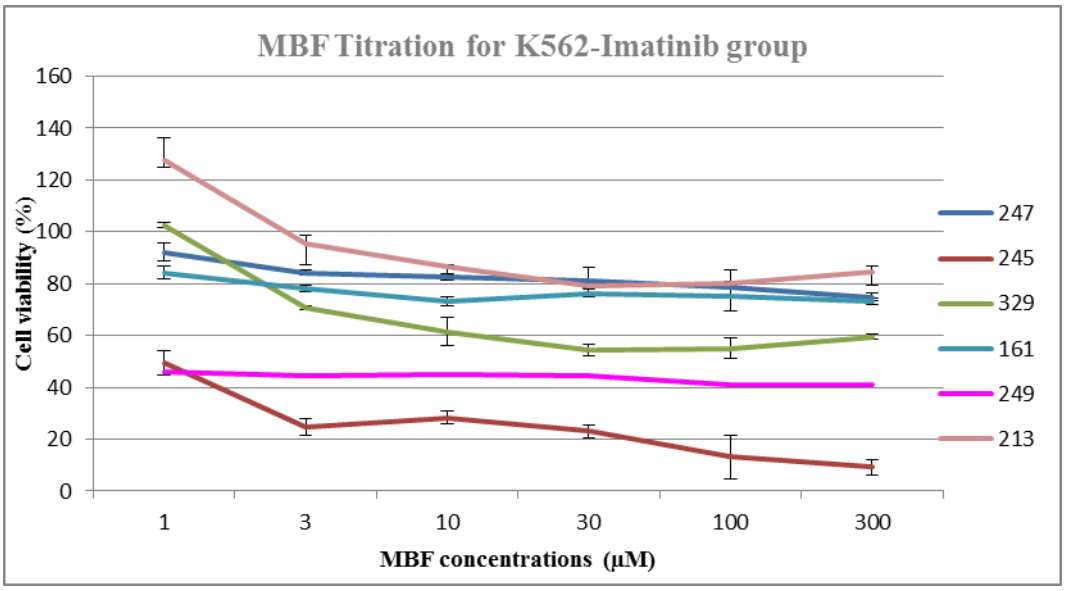

Figure 3.17 Titration assays for selected active hits. Minimum two replications of MTT assays for K562-imatinib MBFs screening.

Cell viability of K562 after treatment with log scale concentrations of MBFs (1, 3, 10, 30, 100 and 300).These experiments were performed with MBFs only without treatment of any drugs to see the effect of concentration. Each colour represents one the MBFs and their concentrations. Error bars are standard deviation – which means the difference of each technical replicates from the mean value of all replicates.

Figure 3.17 represents the effective concentrations for each active MBF with K562 cells, , these hits resulted from screening MBFs with imatinib (pooled and single screenings).. Among these six hits 2-(4-chlorophenyl)-2-morpholinoacetonitrile (247) and 2-(3-chlorophenoxy) ethanethioamide (161) were selected since they showed activity in the majority of their concentrations. MBFs 161 and 247 were selected among these six candidates since they showed similar cell viabilities across different concentrations which is indicative of less toxicity. Additionally, after treatment without imatinib these MBFs showed higher cell viabilities (80-90%) compared to other selected hits which showed wide range of viabilities from 10% to above 100%.

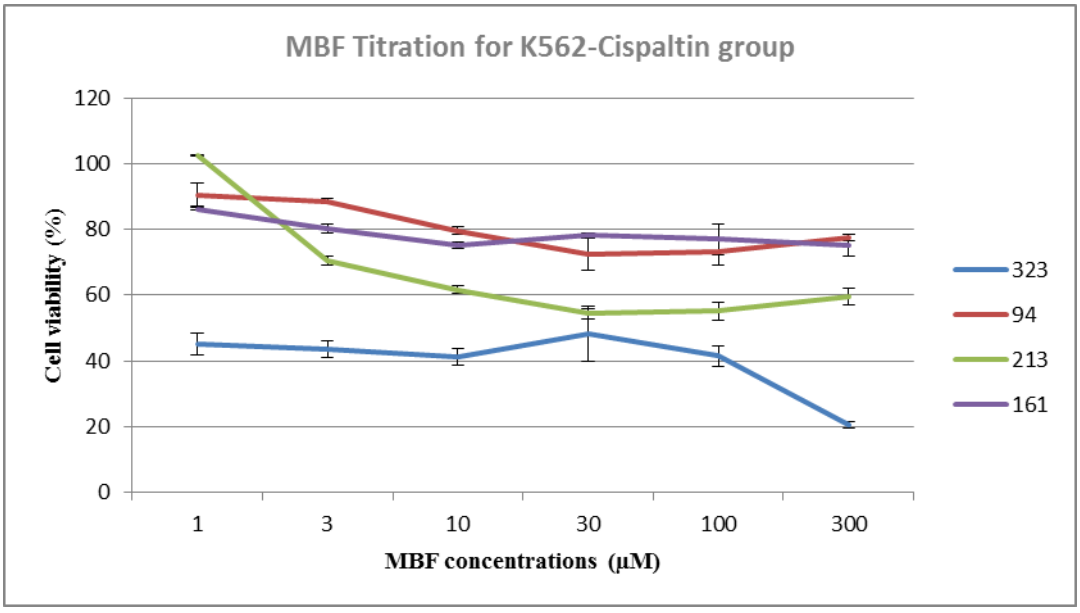

Figure 3.18 Titration assays for selected active hits. Minimum two replications of MTT assays for K562-cisplatin-MBFs screening.

Cell viability of K562 after treatment with log scale concentrations of MBFs (1, 3, 10, 30, 100 and 300). This experiments were performed with MBFs only without treatment of any drugs to see the effect of concentration. Each colour represents one the MBFs across the concentrations used. Error bars are standard deviation – which means the difference of each technical replicates from the mean value of all replicates.

Figure 3.18 represents the effective concentrations for each active MBS with K562 cells, these hits are resulted from screening of MBFs with cisplatin (pooled and single screenings), to check the toxicity of these hits in different concentrations. Among these four hits based on the cut off 2, 2-dimethyl-N-(pyridin-3-ylmethyl)-N-(2-thienylmethyl) propanamide (94) and 2-(3-chlorophenoxy) ethanethioamide (161) were selected since they showed activity in the majority of their concentrations. In fact, those MBFs (161, 94) were selected among these four, since they showed similar cell viabilities for different concentrations that is indicative of reduced toxicity. Additionally, after treatment they showed higher cell viabilities (70-90%) compared to other selected hits which showed wide range of viabilities from 20% to above 100%.

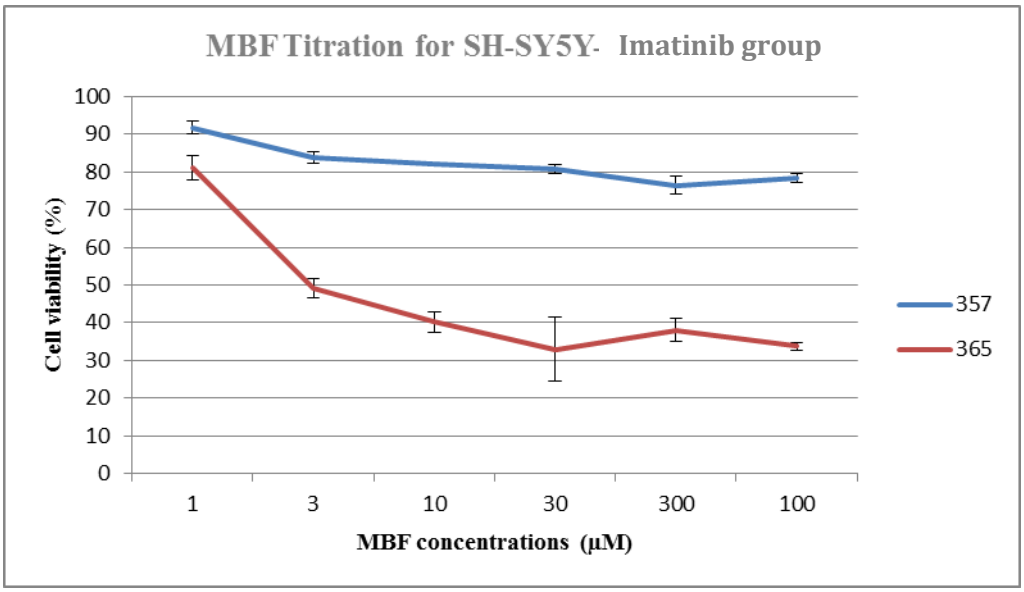

Figure 3.19 Titration assays for selected active hits. Minimum two replications of MTT assays for SH-SY5Y-cisplatin-MBFs screening

Cell viability of SH-SY5Y after treatment with log scale concentrations of MBFs (1, 3, 10, 30, 100 and 300).This experiments were performed with MBFs only without treatment of any drugs to see the effect of concentration. Each colour representative of one the MBFs and their concentrations versus the cell viabilities. Error bars are standard deviation – which is the difference of each technical replicate from the mean value of all replicates.

Figure 3.19 represents the effective concentrations for each active MBFs with SH-SY5Y cells where these hits resulted from screening of MBFs with imatinib (pooled and single screenings), to check the toxicity of these hits in different concentrations. Among these two hits based on the cut-off, 3-(tert-butyl)-1-methyl-4, 5-dihydro-1H-pyrazol-5-one (357) was selected. Furthermore, this MBF (357) were selected since it showed similar cell viabilities for different concentrations which is indicative of being less toxic. Additionally, after treatment it showed higher cell viabilities (70-90%) compared to the other selected hit which showed wide range of viabilities from 40% to above 80%..

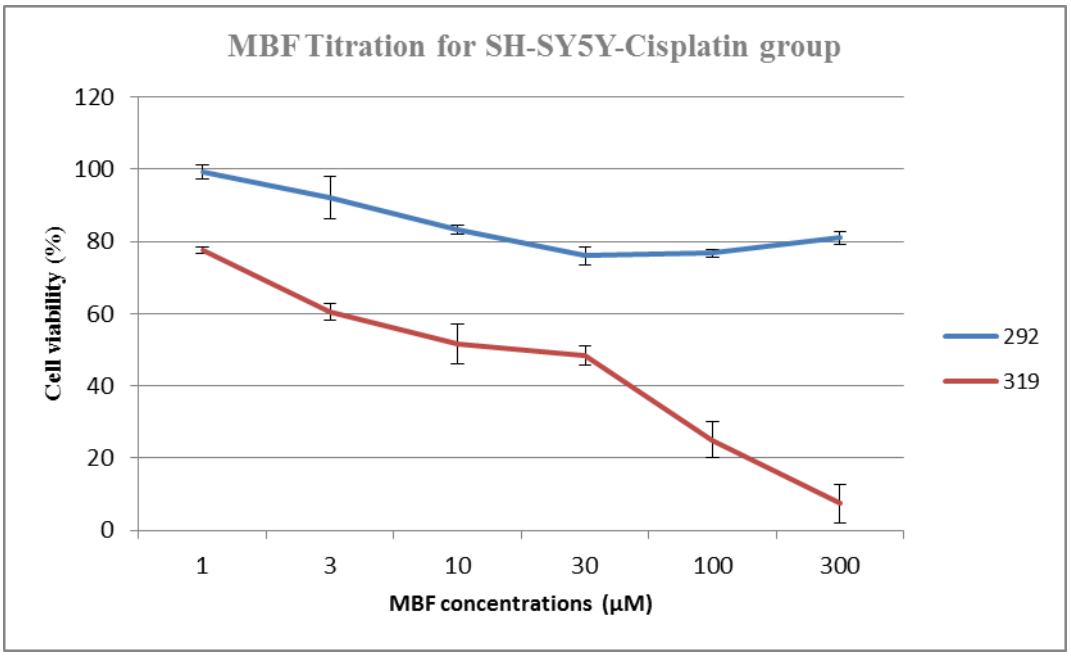

Figure 3.20 Titration assays for selected active hits. Minimum two replications of MTT assays for SH-SY5Y -imatinib-MBFs screening.

Cell viability of SH-SY5Y after treatment with log scale concentrations of MBFs (1, 3, 10, 30, 100 and 300).This experiments were performed with MBFs only without treatment of any drugs to see the effect of concentration. Each colour represents one of the MBFs and their concentrations. Error bars are standard deviation – which means the difference of each technical replicates from the mean value of all replicates.

Figure 3.20 represents the effective concentrations for each active MBFs with SH-SY5Y cells, these hits are resulted from screening of MBFs with cisplatin (pooled and single

screenings), to check the toxicity of these hits in different concentrations. Among these two hits based on the cut off 2-chloroanisole (292) was selected. In fact, this MBF (292) was selected among these two, since it showed similar cell viabilities for different concentrations which is indicative of being less toxicity. Additionally, after treatment it showed higher cell viabilities (80-100%) compared to the other selected hit which showed wide range of viabilities from 5% to 80%.

3.3. RNA EXTRACTION

3.3.1. RNA QUALITY

The RNA quality of each sample was assessed using an Agilent Bio-analyser as described in section 2.4.1.2. Electropherograms measured the ribosomal 18s and 28s peaks, which provided an indication of integrity (quality) of the RNAs extracted from cells. Distinct ribosomal peaks identified by the bio-analyser software without extra erroneous spikes indicate RNA free of degradation (Figure 3.22). If the rRNA ratio is close to 2.0, it will suggest that the extracted RNAs are of good quality. All the RNA samples extracted from K562 and SH-SY5Y cells in the present study had an acceptable rRNA ratio [28s/18s] of above 1.7. The overall composition of each sample was shown to be satisfactory before performing the BCR-ABL gene expression study with RT-qPCR, All RNA samples had a RIN number above 9.0.

3.4. IDENTIFICATION OF IDEAL REFERENCE GENES

3.4.1. GENORM ANALYSIS FOR REFERENCE GENES

To compensate for the non-biological variations in RNA extractions, reverse transcription and amplification qPCR efficiency value (Ev), a stable endogenous reference gene was required. This gene was selected from 9 commonly tested reference genes through geNorm algorithm analysis; as described in section 2.7.1, the threshold for the stability value M is 0.4.

A reference gene with the lowest M value was considered to be the most stable reference gene across the sample cohort. After one round of geNorm analysis, the most stable reference genes were found to be GAPDH and ACTB for K562 treated with imatinib (figure 3.23).

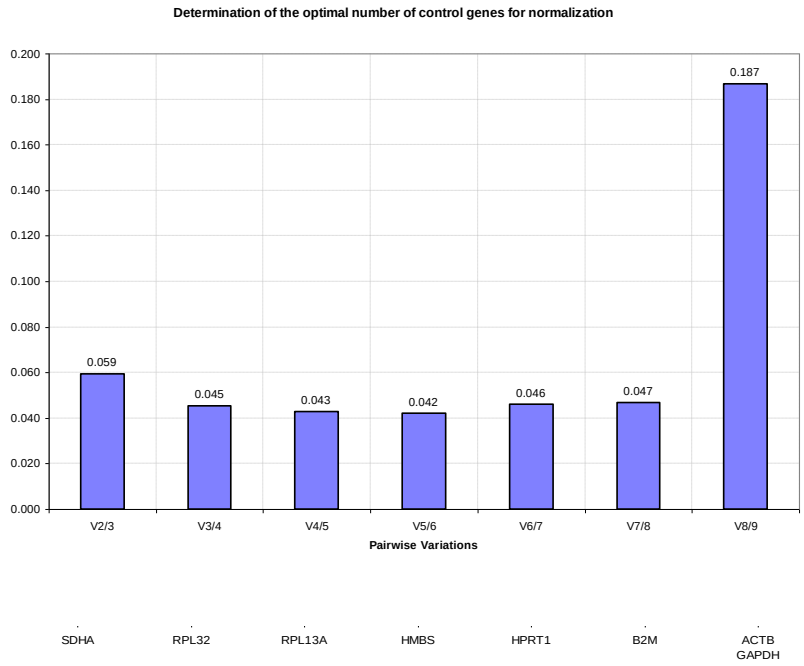

Figure 3.21 Average expression stability values of reference gene for K562 cells and imatinib treatment (different time points).

The figure illustrates the average expression stability values M of the genes analysed by geNorm. The reference genes of GAPDH and ACTB had the M value (0.1); however the stability values other six genes were still below 0.4. It is hence considered to be stably expressed and usable as a control.

The most stable reference genes were found to be HPRT1 and RPL13 for K562 treated with cisplatin (figure 3.24).

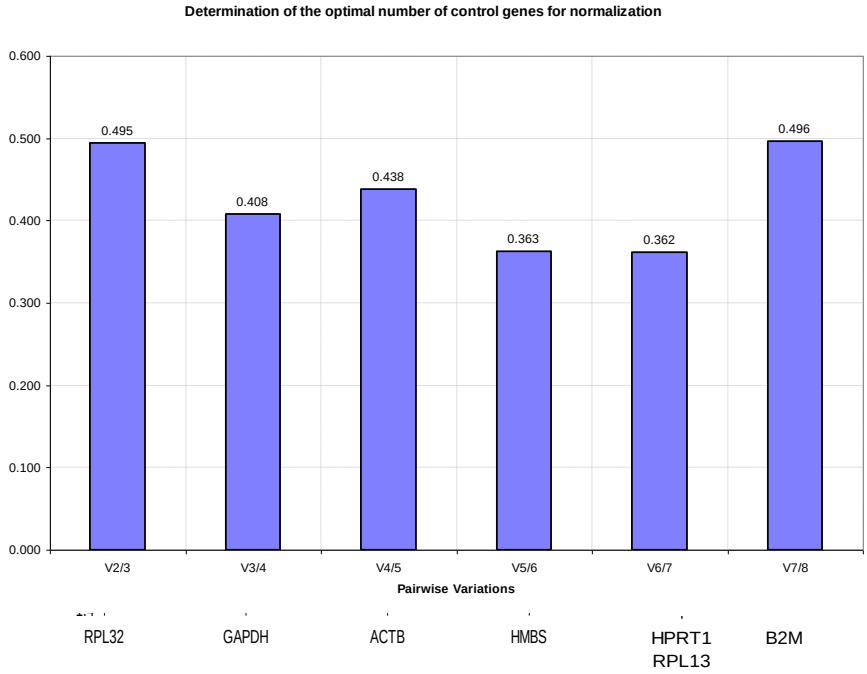

Figure 3.22 Average expression stability values of reference gene for K562 cells and cisplatin and MBFs treatments (different time points).

The figure illustrates the average expression stability values M of the genes analysed by geNorm. The reference genes of HPRT1 and RPL13 had the lowest M value; and the stability values other six genes were high hence, they cannot is considered to be stably expressed and usable as a control.

The most stable reference genes were found to be GAPDH and ACTB for SH-SY5Y treated with either imatinib or cisplatin (figure 3.25).

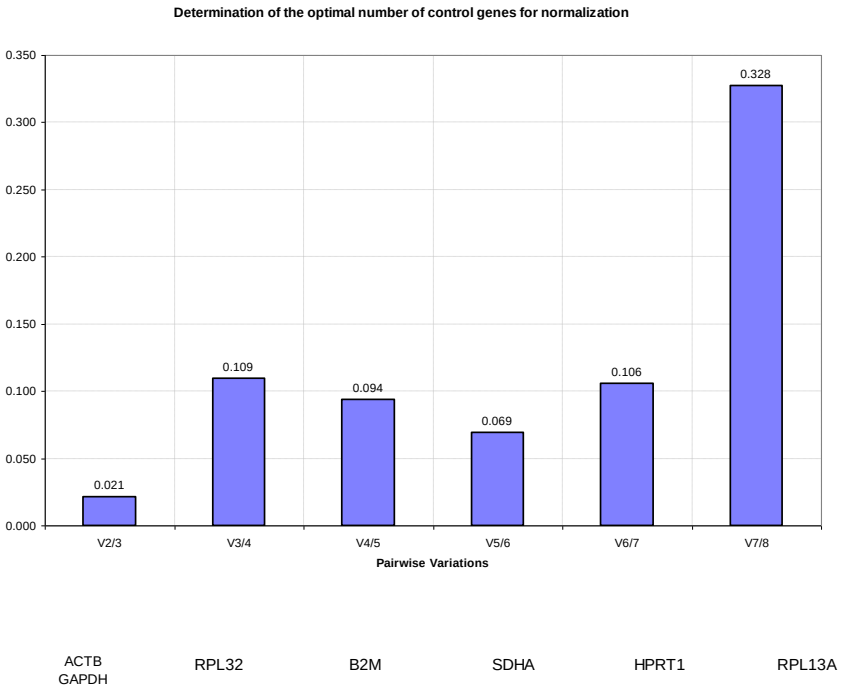

Figure 3.23 Average expression stability values of reference gene for SH-SY5Ycells and cisplatin and imatinib treatments separately (1h)

The figure illustrates the average expression stability values M of the genes analysed by geNorm. The reference genes of GAPDH and ACTB had the lowest M value (0.50).

3.5. RT-QPCR ANALYSIS

3.5.1. QPCR ASSAYS FOR K562 AND SH-SY5Y CELLS BEFORE AND AFTER DRUGS TREATMENT

Prior to performing any experimental analysis to determine significant changes in transporter genes expression following drug treatment, the expressed influx transporters in the two cell lines under study were first determined.

3.5.3. IDENTIFICATION OF EXPRESSION FOR CELL TRANSPORTERS BY WITH IMATINIB AND CANDIDATE MBFS IN K562 CELLS

K562 cells were incubated with a final concentration of 0.3 µM imatinib either for 1, 2, 3, 4 or 5 h in order to study imatinib treatment effects on transporter gene expression. Following treatment, RNA was extracted and reverse transcribed and results for gene expression compare to untreated cells, as can be observed in Figure 3.24.

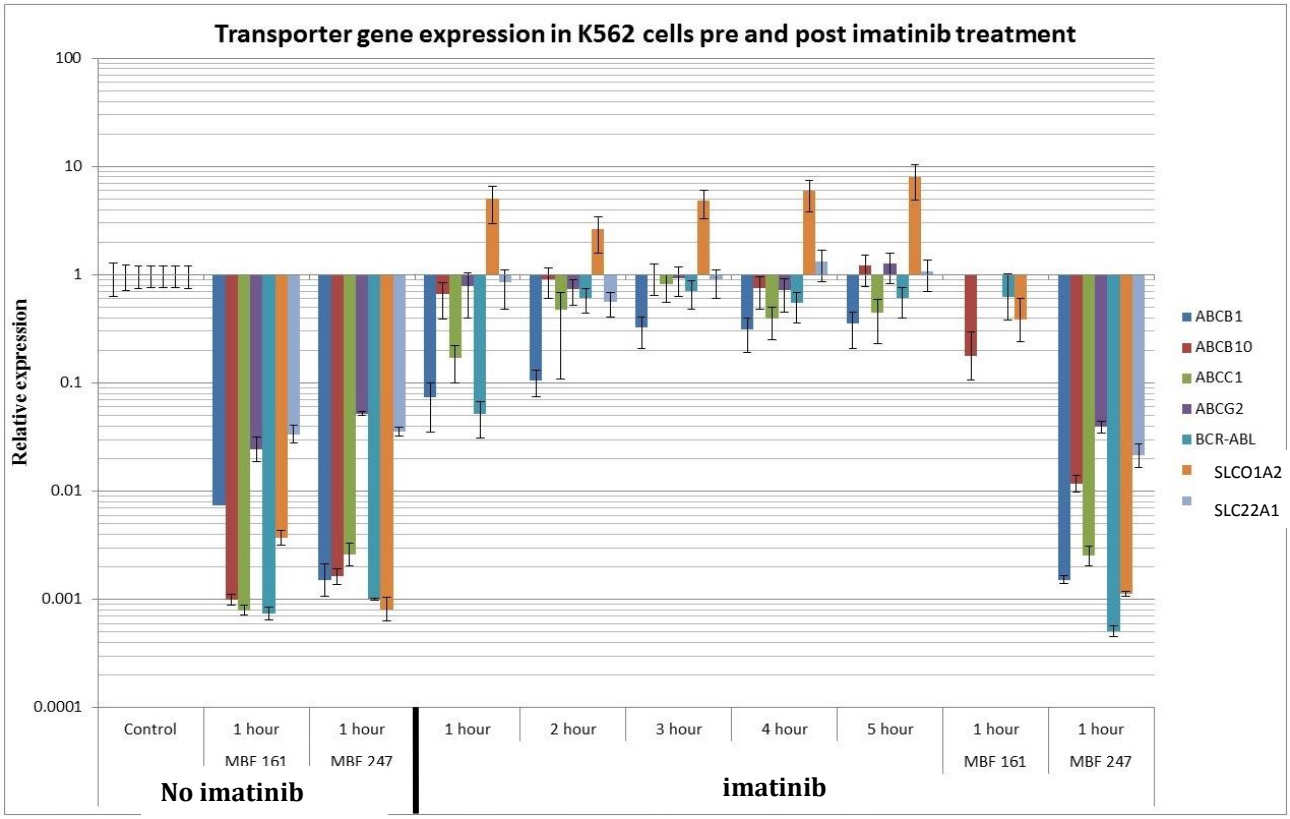

Figure 3.24 Expression values for transporter genes and BCR-ABL for k562 cells treated and untreated with imatinib (different time points) and selected candidate MBFs (247, 161)

The figure illustrates the different expression values of the cell surface transporter genes. Error bars are standard deviation – which means the difference of each technical replicates from the mean value of all replicates.

Figure 3.24 demonstrates the results for transporter gene expression after exposure of K562 cells to 3 different treatment conditions: imatinib (1-5h), hits (161 and 247) and imatinib with each hit (1h). Moreover the control group is representative of no treatment, that is to say gene expression of K562 cells without treatment. Compared to the control group, when K562 cells

were treated with MBFs (161, 247), all transporters, efflux and influx, showed downregulation (P-value =0.05 and P-value =0.001 respectively). Treatment with imatinib for 1, 2 and 3 hours all transporters showed downregulation, except for SLCO1A2SLCO1A2that showed significant upregulation after 1 and 3 hours (P-value =0.001 and P-value = 0.006 respectively). The upregulation continued during 4 and 5 hours of treatment (P-value = 0.001). Nonetheless, the expression pattern for SLC22A1 was changed insignificantly from downregulation to upregulation, after 4 hour of imatinib treatment.

Similarly, the pattern of ABCB10 and ABCG2 were changed to insignificant upregulation. Treatment with imatinib and MBF No. 161 for 1 hour showed downregulation for ABCB10, BCR-ABL and SLCO1A2SLCO1A2(P-value = 0.001). However, the expression for other transporters were not dysregulated (no upregulation no downregulation) (P-value =0.001), they showed the same expression with the control group. Moreover, treatment of K562 cells with imatinib and MBF hit No. 247, all influx and efflux transporters were downregulated significantly. Lastly, the BCR-ABL expression in all different conditions showed downregulation.

3.5.4. IDENTIFICATION OF EXPRESSION FOR CELL TRANSPORTERS BY WITH CISPLATIN AND CANDIDATE MBFS IN K562 CELLS

K562 cells were incubated with a final concentration of 1 µM cisplatin either for 1, 2, 3 or 4 h in order to study cisplatin treatment effects on transporter gene expression. Following treatment, RNA was extracted and reverse transcribed.

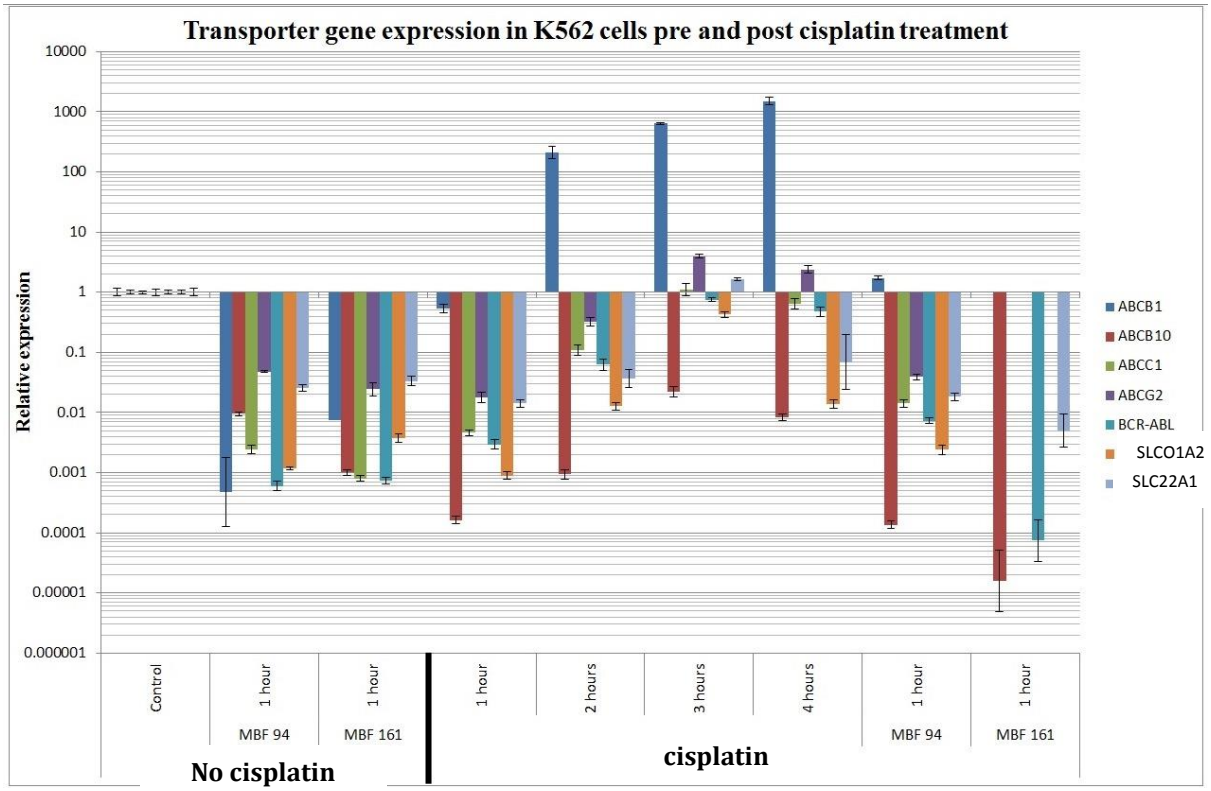

Figure 3.25 Expression values of transporter genes and BCR-ABL and for k562 cells treated and untreated with cisplatin (different time points) and selected candidate MBFs (94, 161)

The figure illustrates the different expression values of the cell surface transporter genes. Error bars are standard deviation – which means the difference of each technical replicates from the mean value of all replicates.

Figure 3.25 demonstrates the results for transporter gene expression after exposure of K562 cells to 3 different treatment conditions: cisplatin (1-4h), hits (161 and 94) and cisplatin with each hit (1h). Moreover, the control group represents no treatment with gene expression of K562 cells in a normal situation.

Compared to the control group, when K562 cells were treated with MBFs 161 or 94, all transporters showed downregulation, which were significant for SLCO1A2 (P-value = 0.04 for hit No.94) and ABCG2 (P-value = 0.03 for hit No.94). Through the first hour of cisplatin treatment, all genes showed significant downregulations (P-value =0.005). But after that through 2, 3 and 4 hours ABCB1 showed significant upregulation (P-value = 0.01). Similarly, ABCG2 for 3 and 4 hours of cisplatin treatment showed significant upregulated pattern (P-value = 0.04, 0.004 and 0.003 respectively).

During the 3 hours of cisplatin treatment SLC22A1 showed a significant upregulation (P-value = 0.04), however after 4 hours of treatment it was downregulated insignificantly.

In the last condition, cells were exposure to cisplatin and MBF hits 94 and 161 separately for 1 hour. For MBF 94 after 1 hour plus cisplatin, all genes displayed a downregulated patterns except for ABCB1 which was upregulated but not significantly.

For MBF 161 plus cisplatin all the gene expression was not dysregulated (no up-regulation no down-regulation) (P-value =0.001), showed the same expression with the control group, except for ABCB10, BCR-ABL and SLC22A1 which were down-regulation. However, the down-regulation was significant just for ABCB10 (P-value = 0.007). Furthermore BCR-ABL in all 3 conditions showed significant down-regulation, except in 3 conditions (MBF treatments alone and 161 with cisplatin).

3.5.5. IDENTIFICATION OF EXPRESSION FOR CELL TRANSPORTERS BY WITH CISPLATIN AND IMATINIB IN SH-SY5Y CELLS

SH-SY5Y cells were incubated with a final concentration of 1 µM of cisplatin either 0.3 µM of imatinib for 1h in order to study treatment effects on transporter gene expression. Following treatment, RNA was extracted and reverse transcribed.

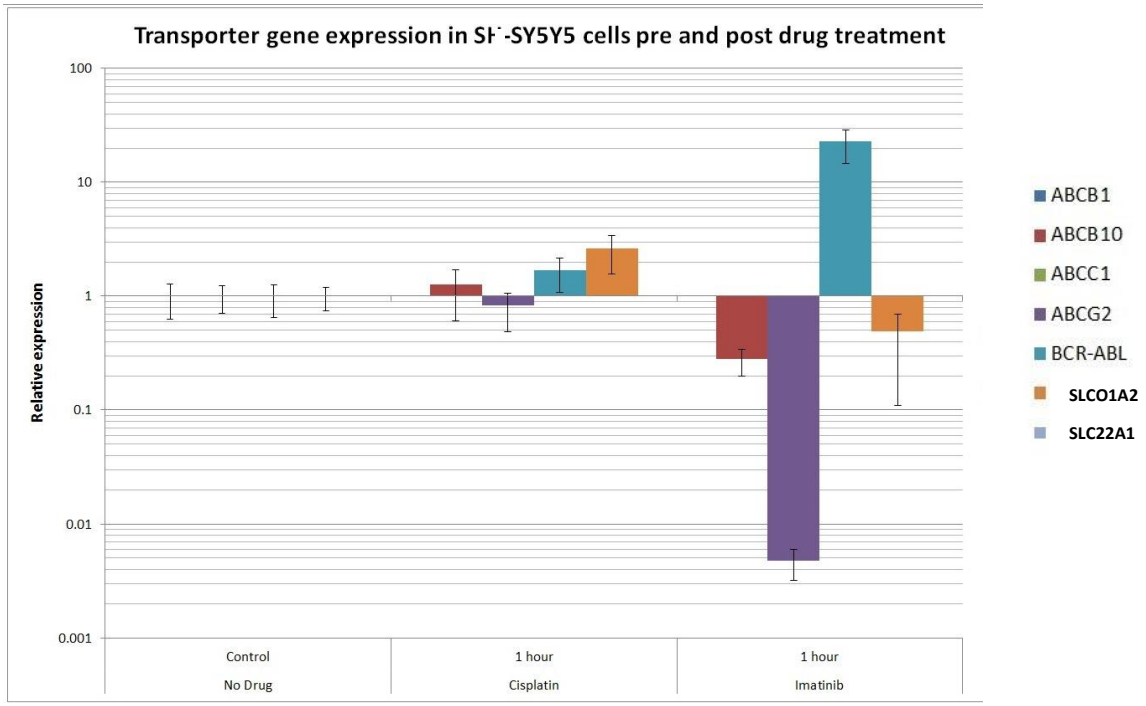

Figure 3.26 Expression values of transporter genes and BCR-ABL and for SH-SY5Y cells treated and untreated with cisplatin or imatinib.

The figure illustrates the different expression values of the cell surface transporter genes. Error bars are standard deviation – which means the difference of each technical replicates from the mean value of all replicates.

Figure 3.26 demonstrates the results for transporters gene expression after exposure of SH-SY5Y cells to 3 different treatment conditions: cisplatin, imatinib and no drug treatment). Exposure of SH-SY5Y cells either to cisplatin or imatinib for 1 h for ABCB1,ABCC1 and SLC22A1 showed no dysregulation in gene expression (no upregulation no downregulation) (P-value =0.001), they showed the same expression with the control group (for cisplatin P-value = 0.02 and for imatinib P-value = 0.01). ABCG2 which showed a non-significant down-regulation with administration of cisplatin. ABCB10, BCR-ABL and SLCO1A2SLCO1A2showed up-regulation after treatment with cisplatin however, SLCO1A2SLCO1A2has the highest up-regulation (P-value = 0.001). ABCG2 and ABCB10 showed down-regulation with imatinib treatment (P-value = 0.002). But BCR-ABL after imatinib treatment had a significant up-regulation (P-value = 0.001).

CHAPTER 4

DISCUSSION

This project proposed to test if imatinib efficacy will be enhanced using MBFs as binary weapons for the efficient transportation of imatinib.Prior to the actual screening of the 500 MBFs, a number of optimisation experiments were performed for cytotoxic assays to assess cell viability and cell toxicity following treatment with the fragments and drugs; this research project has been divided into three chapters; (1) Screening the first 500 compound library of MBFs to find useful hits for K562; (2)Screening the first 500 compound library of MBFs to find useful hits for K562 cells treated with imatinib. (The search for bioactive molecules) 3) Transporter gene-expression profiling studies using RT-qPCR analysis to assess imatinib and MBFs treatment on cell surface transporter gene expression. In all experiment procedures SH-SY5Y was utilized as a control cell line in conjunction with cisplatin as a control drug since cisplatin is a chemotherapy agent and anti-cancer drug which is used to treat neuroblastoma.

CML is a clonal myeloproliferative disease, which is a type of cancer that begins in the bone marrow (89). It develops slowly in the blood-forming cells inside the marrow, and eventually

spreads through the blood. It caused by Philadelphia chromosome which produces too much of a protein called tyrosine kinase. And this chimeric BCR-ABL protein affects cellular differentiation, growth, apoptosis and adhesion (90, 91).

CML is commonly taken as a model of cancer for many reasons. It is a hematopoietic stem cell disease characterized by the clonal expansion of terminally differentiated myeloid cells. However, the main reason for choosing CML as a model relates to the discovery of a constitutively active BCR-ABL tyrosine kinase, the functional result of a reciprocal translocation between chromosomes 9 and 22 that generates the famous Philadelphia chromosome (22, 32). Not only is BCR-ABL a cancer marker, it is also the causative lesion in CML, leading to the development of the first tyrosine kinase inhibitor (TKI), imatinib (92, 93). As a result, CML is also a model of targeted therapy for human malignancies. Therefore, in the current project the CML was selected as the model of study for MBFs for inducing imatinib therapeutic effect.

The use of MBFs with cancerous cells to change cell membrane transporter gene expression, is new and there has not been previously reported. Therefore, we are not able to compare the current results with other studies. However, currently, fragment-based screening is a useful and practical approach for drug discovery. Although some of these fragments are toxic against mammalian cells, some of them revealed acceptable potential through the success of drug discovery. The fundament is to identify active fragments with less toxicity by screening a library of compounds, with resulting hits serving as starting points for chemical elaboration to achieve potency (83, 84). In this regard, Rees et al (2016) hypothesized that differential basal gene expression could be correlated with patterns of small-molecule sensitivity across many cell lines to illustrate the actions of compounds. So, to test this idea, they correlated the sensitivity patterns of 481 compounds with ~19,000 basal transcript levels across 823 different human cancer cell lines and identified selective outlier transcripts. As a result, they

concluded that through unknown mechanisms, gene expression changed in response to small-molecules (94).

In this research, we have investigated the concept of producing next generation high therapeutic index polypharmacy drugs through employing a low molecular weight chemical library, or binary weapon approach to demonstrate the probability and likelihood of increasing intracellular uptake of imatinib in chronic myeloid leukaemia K562 cell line through changing in gene expression of cell membrane transporters.

4.1 CYTOTOXIC ASSAY OPTIMISATION

MBFs are dissolved in DMSO. Therefore it was essential to determine the cytotoxic effect of DMSO on cells. Using the MTT cell proliferation assay it was demonstrated that DMSO infers toxicity only when present at concentrations higher than 2.5%. As the DMSO concentration decreased cell viability increased, this was observed as an increase in absorbance values, resulting from an increased number of cells reducing MTT to a measureable aqueous-soluble formazan. MBFs are dissolved in 200 mM DMSO which is below the level of DMSO shown to have cytotoxic effects. This data indicates that any changes observed in cell proliferation when adopting the binary weapon approach will be due to either the fragments enhancing the transportation efficiency of imatinib, or from the fragments themselves.

4.2 MTT ASSAY

As one of a number of measures of toxicity, we initially focussed on the MTT assay as a broad measure of cell proliferation and cytotoxicity in parallel to the transporter assays. The methodology was validated by looking at the impact of a short exposure to Triton X-100 (0.01%) upon the viability of SH-SY5Y and K562 cells. In a series of experiments repeated

3-4 times for each cell line sets for defining cell number and proper drug concentration by MTT.

0.3 μM exposure of imatinib for 24 hour was associated with 20% decrease in cell viability for both cell lines. Furthermore, 1 μM exposure of cisplatin for 48 hour was associated with 20% decrease in cell viability for both cell lines. The data indicate that K562 and SH-SY5Y exposure for 1 hour to imatinib concentrations of 3, 2 μM and above resulted in ≥ 50% cell death, respectively. These data are similar with those data from research by Bourgne et al (2012) that they found same imatinib concentrations and their cell viability ranges (95). Furthermore, MTT assays were performed for MBF screenings and test the cell cytotoxicity of them. Major ll, et al (2011)reported that some compounds of MBFs showed cell toxicity for some mammalian cell lines (80) .

Therefore, through screening of MBFs for K562 and two drugs (imatinib and cisplatin) one MBF was in common between these two treatment groups. MBF no.161 with chemical name of 2-(3-chlorophenoxy) ethanethioamide and molecular formula 8H8CINOS. However, SHSY5Y cells did not share any candidate MBF with K562, nor across the cisplatin or imatinib drugs group. .

Moreover, the chemical structure comparison between hits revealed that most of them have aromatic rings, including MBFs 161 and 94, which have 2 rings in their structures. . Additionally, these two MBFs showed less toxicity even in higher concentrations or more effects on transporter gene expressions (A table consist of hits chemical structures, formula Molecular weight and bioassay results were added to appendix No.5).

It should be highlighted that data from MTT assays were not reproducible which has some reasons, that can be categorized in 2 groups; 1. cancer cells are heterogeneous by nature, especially in our test group (K562)In fact, cancer cells do not show the same activities and

akin to most cell populations they are heterogeneous. This is known for K562 cells which are compromised from a mixture of two populations of adherent and non-adherent cells, so in the MTT assay for different biological replicates, the proportion of these cells vary and hence complete reproducible data cannot be routinely achieved. 2. The character of the MTT assay is not highly reproducible. However, in this project technical replicates (triplicate of samples in each experiment), 4 biological replications (repeat of each experiments) were designed to decrease the possibility of any mistakes and increase the number of replicates to help identify any outliers and the data confirmed the reproducibility of technical repeats of each day of experiments. Therefore, were shown to have standard deviations typically ranging between 8-20% in our intra- experimental replicates (replicates performed on the same day).

For the reproducibility and reliability of MTT assay In this regards, Alet van Tonder et al (2015) published a research study in which they compared the reproducibility of cytotoxicity data resulted from MTT assay with 4 other different cytotoxicity assays consisting of the neutral red uptake (NRU), resazurin reduction (RES) and sulforhodamine B (SRB) assays. It was concluded that the NRU, RES and SRB assays showed the smallest variability across the linear range, while the largest variation was observed for the MTT assay. This implies that these assays would more accurately detect small changes in cell number than the MTT assay. In total, data from MTT assay is not very reproducible (96).

4.3 RNA ANALYSIS

4.3.1 REFERENCE GENE ANALYSIS

Several researches reported the importance of finding the most stable reference gene and utilising them as an internal control of qPCR for comparing the expression level of targeted genes such as transporters in the current research. However, several studies suggest that the

expression of BCR-ABL is important in imatinib therapy investigation; its expression is altered since it is the target point for imatinib (97).

To compensate for non-biological variations in RNA extractions, stable reference genes were selected from 9 common tested reference genes through geNorm algorithm analysis. In this section of the study the most stable reference genes were found to be GAPDH (Glyceraldehyde 3-phosphate dehydrogenase) and ACTB (Beta-actin); however, it was concluded that ABL (Abelson) was also stably expressed and it was used as a control.

In the present study, GAPDH, ACTB genes were considered as suitably stable after an analysis of the K562 and SH-SY5Y cells using the geNorm algorithm.

4.4. TRANSPORTER GENE-EXPRESSION PROFILING USING RT-QPCR ANALYSIS

4.4.1 IDENTIFICATION OF REFERENCE GENES FOR RT-QPCR

The selection of stably expressed reference genes is an important precondition to a successful gene-expression profiling study design. This is because such housekeeping genes can be used as internal controls during RT-qPCR analysis in order to calculate the sensitivity of each measurement as well as to compensate for non-biological variations in RNA quality and quantity. This prevents the generation of false results, particularly when transcription rate variations between sample groups are small (88, 98).

The well-established and standardised tool, geNorm algorithm, which was specifically designed and validated for this purpose, and utilised in a number of other studies, was used to determine the most stable reference gene set for SH-SY5Y and K562 transporter gene-expression profiling. Overall, this algorithm involves the calculation of an internal control gene-stability measure [M], which represents a quantitative measure for the expression level variation of sets of control genes, with a greater M value indicating a greater contribution to

total expression level variance and an M value of 0 indicating identical expression level ratios. The combination of reference genes which is best amongst the total list of reference genes being screened is determined through the sequential exclusion of the least stable genes, re-calculating M for the remaining control genes (88).

The two most stably expressed reference genes for imatinib treated and untreated K562 and SH-SY5Y cells were GAPDH and ACTB also considered to be stably expressed, since these also fall below the stability threshold 'M', set as 0.4 (Figure 3.23,24,25). The two most stably expressed reference genes for cisplatin treated and untreated k562 cells were RPL32 and HPRT1. These housekeeping genes were used to normalise expression levels of transporter genes in drug treated and untreated K562 and SH-SY5Y cells.

4.4.2 IDENTIFICATION OF EXPRESSED CONSTANT INFLUX AND EFFLUX TRANSPORTER GENES IN K562 CELLS AND SH-SY5Y CELLS

Over the last decades, the molecular identification and functional characterization of drug transporters has been investigated. Following the drug administration, the expression and transport activity of drug transporters change, affecting the pharmacokinetics of substrate drugs (99). Moreover, it is widely accepted that membrane drug transporters contribute to the disposition of many drugs. Drug transport is controlled by two main super families of transporters; SLC and ABC (100).

RT-qPCR analyses were performed to determine which of the influx or efflux transporters of imatinib after treatment of selected MBFs will have changes in gene expression. Compared to the control group, when K562 cells were treated with MBFs (161 or 247), all transporters, efflux and influx, showed downregulation. However, treatment with imatinib and MBF 161 for 1 hour showed significant downregulation for ABCB10, BCR-ABL and SLCO1A2. However, the expression for other transporters were not dysregulated (no upregulation no

downregulation) showing the same expression with the control group. Moreover, treatment of K562 cells with imatinib and MBF 247, all influx and efflux transporters were downregulated significantly.

4.4.3 IMATINIB TREATMENT EFFECTS ON TRANSPORTER GENE EXPRESSION

With imatinib being mainly transported via proteinaceous membrane transporters or carriers (101), the expression of these influx and efflux transporters can be used to determine the drug's toxicity or its lack of efficacy.

In order to study whether imatinib treatment would affect the expression of influx transporter genes, RT-qPCR. The results shown in Figure 3.29 for K562 cells and 3.31 for SH-SY5Y cells, demonstrate that treatment with time points of imatinib treatment has alterations in the mRNA expression levels of ABCB1, ABCG2 and ABCC1 importers following either 1 or 5 h incubation periods for K562 cells, but all these efflux transporters beside SLC22A1 had downregulation. These results confirm previously published data by Kim et al. 2014 paper (102). It is proposed and hypothesised that imatinib at such low incubation time would cause up-regulations in the mRNA expression of influx transporters such as SLCO1A2. This would result in higher plasma concentrations of imatinib required to reach a maximum rate of intracellular imatinib triphosphate intracellularly. These data are similar to reported results by Hu et al (2008) that the 0.2 μM concentration of imatinib was used and it caused increased in expression of SLCO1A2, in contrary with data from Eechoute et al 2011, in which they reported that imatinib uptake is not related to SLCO1A2 expression (60). In the current research SLCO1A2 in all time courses of imatinib treatment withK562 except for 2 h significantly unregulated but after treatment with MBFs either 161 or 247 with imatinib or without imatinib was downregulated significantly.

Despite the successful therapeutic role of Imatinib, its failure to completely eradicate leukaemia cells has been observed (103).

In SH-SY5Y cells after imatinib treatment the expression of ABCB1, ABCC1 and SLC22A1 were stopped and ABCB10, ABCG2 and SLCO1A2SLCO1A2showed down regulation.

This study has endeavoured to determine the importance of MBF screening for the assessment of CML imatinib resistance. So K562 cells were treated with the two selected candidate active hits (161 and 247) with imatinib and without imatinib. Therefore, those samples treated with MBFs only (for both hits) showed downregulation for all transporters as well as BCR-ABL gene. Those cells treated with 161 and imatinib had no expression for ABCB1, ABCC1, ABCG2 and SLC22A1, however, the downregulation for ABCB10, SLCO1A2SLCO1A2and BCR-ABL were resulted. In addition, cells treated with 247 and imatinib showed down regulation for all investigated genes.

As a results, it is comprehensible that MBFs treatment with and without imatinib probably have effect on expression of transporters but since there is no similar work on K562 and imatinib with MBFs, it is not possible to compare data form the current study.

4.4.4 CISPLATIN TREATMENT EFFECTS ON TRANSPORTER GENE EXPRESSION

Cisplatin treatment was performed as a control for the results from imatinib treatment to check the alteration in gene expression of transporters were drug specific. The results shown in Figure 3.30 for K562 cells and 3.31 for SH-SY5Y cells, demonstrate that treatment with time points of cisplatin treatment has alterations in the mRNA expression levels of ABCB1 at the first hour of treatment decreased and then it increased for the other 3 time points. Similarly, Vilanova-Costa et al also reported up regulation for ABCB1 gene in K562 cells after cisplatin treatment. ABCG2 following 4 h of incubation periods for K562 cells, showed increasing for expression which had 100 times decreasing in expression after 1 h of cisplatin

and then it changed to up regulation after 4 h. However, all other transporters had downregulation. These results confirm previously published data by Cotovdorj et al. 2014 paper (104).

In SH-SY5Y cells after cisplatin treatment the expression of ABCB1, ABCC1 and SLC22A1 were stopped and ABCB10, BCR-ABL and SLCO1A2SLCO1A2showed upregulation but ABCG2 had lower expression.

Additionally, to determine the effect of MBF in the assessment of CML imatinib resistance were drug specific the same study design for imatinib was used with cisplatin. So K562 cells were treated with the two selected candidate active hits (161 and 94) with cisplatin and without cisplatin. Therefore, those samples treated with MBFs only (for both hits) showed downregulation for all transporters as well as BCR-ABL gene similar with those results from imatinib group. Those cells treated with 161 and cisplatin had no expression for ABCB1, ABCC1, ABCG2 and SLCO1A2, so the results for efflux transporters are similar to results from imatinib group. However, the downregulation for ABCB10, SLC22A1 and BCR-ABL were resulted. In addition, cells treated with 94 and cisplatin showed down regulation for all investigated genes except for ABCB1 had upregulation.

As a results, it is comprehensible that MBFs treatment with and without cisplatin probably have effect on expression of transporters. Moreover, the results for MBF (161) for imatinib compare to cisplatin showed a similar pattern of expression but with different values for efflux transporters and the different results for influx ones can probably confirm MBFs have different effect for different drugs.

4.5 CONCLUSION

Some 15 years of long-term treatment with imatinib and several years of experience with the next generation of TKIs, including nilotinib, dasatinib, bosutinib and ponatinib has revealed

many molecular parameters greatly impact the success of treatment of patients with CML. The progression of treatment for Ph^+ CML has been reviewed (see figure 1.4) . We suggest that with resistance against TKIs occurring as a result of low intracellular availability of the drug, and given that the intracellular availability of imatinib as well as other TKIs is a balance between influx and efflux transportation that the future treatment will rely on a polypharmaceutical approach including TKI's to help circumvent resistance to treatment. The whole field of drug development makes various assumptions of drug uptake which are largely based around Lipinski's (Pfizer) Rule of 5 that tentatively relates successful drugs to small size and lipid solubility (105, 106). The relationship is reasonably tenuous with several successfully administered drugs not remotely adhering to the suggested formula, and competing suggestions for drug uptake include the Kell rule of 0.5 which argues that the important facet of drug uptake relates to natural substance similarity which permits mimicry and thus uptake of the (alias) drug by existing transporter mechanisms (15, 17, 18). A possible prediction is that a future generation of TKI's may be more specifically tuned to active cell surface associated transporter uptake to not only combat MDR but also impact on therapeutic index since more TKI is directed to the target cells by using specific fragments.

In summary, in our test group (K562 and imatinib) by treatment with imatinib for 1, 2 and 3 hours all transporters showed downregulation, except for SLCO1A2SLCO1A2that showed significant upregulation after 1 and 3 hours. Moreover, comparison to K562 only control, MBF 247 showed a similar pattern of downregulation for all transporters with or without imatinib except for ABCB10 which had 10 times lower downregulation after treatment with MBF 247 and imatinib compared to MBF only. Whereas, the pattern of expression for K562 cells treated with MBF 161 showed all transporters, to be downregulated. Treatment with imatinib and MBF 161 only showed downregulation for ABCB10 and SLCO1A2. However, the expression for other transporters were not dysregulated, and thus matched the expression of

the control K562 cells. n the control group (K562 and cisplatin) through the first hour of cisplatin treatment, all genes showed significant downregulation. At 2, 3 and 4 hours ABCB1 showed significant upregulation (1000 times more). MBF 94 treated with or without cisplatin showed a similar pattern of gene expression dysregulation for all transporters except for ABCB1 which had 1000 times more gene expression and the pattern of downregulation changed to upregulation. However, the pattern of expression for MBF 161 showed complete differences when applying MBF only compared to MBF and cisplatin for all transporters either efflux or influx except for ABCB10 and SLCO1A2, in which they showed no dysregulation with 161 MBF and imatinib compared to 161 only. For ABCB10 and SLC22A1 the downregulation was increased 10 times.So based on the results, the difference between imatinib and cisplatin treatment on K562 was that cisplatin increased expression of ABCB1 and ABCG2 (efflux transporters). On the contrary, imatinib upregulated the expression of SLC22A1 and SLCO1A2 (influx transporters).

There are limited studies related to transporter gene-expression post drug treatment, and thus the correlation with the drug efficacy remains enigmatic. The possibility of transporter expression signatures being predicative biomarkers of drug response in patients is an exciting prospect. These studies are supportive of a binary weapon approach not only assisting with specific drug-uptake, but also the impact on associated transporters can be measured.

Any down-regulation in influx transporter expression or any up-regulations in the expression of efflux transporters would diminish the chemotherapeutic effect of imatinib, by accelerating its abolition from intracellular compartments. The assumption here is of course that protein expression is linked to transcript production, and the therapeutic effects for CML will be realised. Our data suggests that there is probably a relationship between MBF uptake and transporter genes expression. However, this exciting field needs further investigation.

4.6 FUTURE PERSPECTIVES

Because lack of time for an MPhil course of study we cannot continue this research in more depth. Below it is presented some possible routes to continue studies.

Following the screening of MBF, mass spectroscopy could be employed for identification of imatinb and MBFs inside the cell, as all the reported studies did not measure actual drug uptake, only their cytotoxic impact. Moreover, important cell signalling pathways should be investigated to find the origin of alteration in cell surface transporters. Furthermore, their Tanimoto indices will be determined through the use of Molecular ACCess System (MACCS) and KNIME, with the help of software experts. This will allow the study of variation of the Tanimoto similarity for MBFs with other metabolites, with the aim of determining any similarities which distinguish the fragments compatible with metabolites. In addition, the study can be involved the chemical synthesis of fragments with similar properties (in conjunction with algorithm experts), followed by further MBF screening, selecting fragments for imatinib over several iterative cycles (‘generations’) in the hope that improved variants can be created, eventually leading to the identification of natural metabolites with similar properties.

RT-qPCR studies include the investigation of efflux transporter gene expression changes following imatinib treatment, coupled with further studies of influx transporters expression for SH-SY5Y cells. Further RT-qPCR analysis will be performed to determine any significant expression changes in both influx and efflux transporters utilised by the selected fragments from the MBF, to further confirm the role of fragments in this binary weapon approach.

Therefore, in the current study the first library of MBFs was investigated in relation with imatinib and CML, consequently two candidates as active MBF hits were recognised.

Moreover the related effects of them on cell surface transporters showed that these hits caused changes in expression of efflux and influx transporters. But still further detailed studies are needed to understand this novel way.

REFERENCES

1. Caldemeyer L, Dugan M, Edwards J, Akard L. Long-Term Side Effects of Tyrosine Kinase Inhibitors in Chronic Myeloid Leukemia. Curr Hematol Malig Rep. 2016;11(2):71-9.
2. Chronic myeloid leukaemia [Internet]. Imperial College London. 2014.
3. Chen R, Chen B. The role of dasatinib in the management of chronic myeloid leukemia. Drug Design, Development and Therapy. 2015;9:773-9.
4. Trivedi D, Landsman-Blumberg P, Darkow T, Smith D, McMorrow D, Mullins CD. Adherence and persistence among chronic myeloid leukemia patients during second-line tyrosine kinase inhibitor treatment. J Manag Care Spec Pharm. 2014;20(10):1006-15.
5. Hoglund M, Sandin F, Simonsson B. Epidemiology of chronic myeloid leukaemia: an update. Ann Hematol. 2015;94 Suppl 2:S241-7.
6. Karimiani EG, Marriage F, Merritt AJ, Burthem J, Byers RJ, Day PJ. Single-cell analysis of K562 cells: an imatinib-resistant subpopulation is adherent and has upregulated expression of BCR-ABL mRNA and protein. Exp Hematol. 2013;42(3):183-91.e5.
7. P.G. S. Cytogenetic study in CML. Indian J Med Res. 2012;135(1):12-3.
8. Deininger MWN. Optimizing therapy of chronic myeloid leukemia. Experimental Hematology. 2007;35 144-54.
9. Verma M, Karimiani EG, Byers RJ, Rehman S, Westerhoff HV, Day PJ. Mathematical modelling of miRNA mediated BCR.ABL protein regulation in chronic myeloid leukaemia vis-a-vis therapeutic strategies. Integr Biol (Camb). 2013;5(3):543-54.
10. Markose P, Chendamarai E, Balasubramanian P, Velayudhan S, Srivastava V, Mathews V. Spectrum of BCR-ABL kinase domain mutations in patients with chronic myeloid leukemia from India with suspected resistance to imatinib-mutations are rare and have different distributions. Leuk Lymphoma. 2009;50(12):2092-5.
11. Wieczorek A, Uharek L. Management of Chronic Myeloid Leukemia Patients Resistant to Tyrosine Kinase Inhibitors Treatment. Biomark Insights. 2015;10(Suppl 3):49-54.
12. Mughal TI, Goldman JM. Chronic myeloid leukemia: current status and controversies. Oncology (Williston Park). 2004;18(7):837-44, 47; discussion 47-50, 53-4.
13. Huang X, Patel S, Ahmed N, Seiter K, Liu D. Severe toxicity of skin rash, fever and diarrhea associated with imatinib: case report and review of skin toxicities associated with tyrosine kinase inhibitors. Drug Design, Development and Therapy. 2008;2:215-9.
14. Bhamidipati PK, Kantarjian H, Cortes J, Cornelison AM, Jabbour E. Management of imatinib-resistant patients with chronic myeloid leukemia. Ther Adv Hematol. 2013;4(2):103-17.
15. Pricl S, Fermeglia M, Ferrone M, Tamborini E. T315I-mutated Bcr-Abl in chronic myeloid leukemia and imatinib: insights from a computational study. Mol Cancer Ther. 2005;4(8):1167-74.
16. Jorgensen HG, Holyoake TL. A comparison of normal and leukemic stem cell biology in Chronic Myeloid Leukemia. Hematol Oncol. 2001;19(3):89-106.
17. Visani G, Isidori A. Resistant chronic myeloid leukemia beyond tyrosine-kinase inhibitor therapy: which role for omacetaxine? Expert Opin Pharmacother. 2014;15(1):1-3.

18. Kurzrock R, Kantarjian HM, Druker BJ, Talpaz M. Philadelphia chromosome-positive leukemias: from basic mechanisms to molecular therapeutics. Ann Intern Med. 2003;138(10):819-30.
19. Chen Y, Peng C, Li D, Li S. Molecular and cellular bases of chronic myeloid leukemia. Protein Cell. 2010;1(2):124-32.
20. Bayraktar S, Goodman M. Detection of BCR-ABL Positive Cells in an Asymptomatic Patient: A Case Report and Literature Review. Case Reports in Medicine. 2010;2010.
21. Breed CD. Diagnosis, treatment, and nursing care of patients with chronic leukemia. Semin Oncol Nurs. 2003;19(2):109-17.
22. Chereda B, Melo JV. Natural course and biology of CML. Ann Hematol. 2015;94 Suppl 2:S107-21.
23. Meng Z, Li YH. [One of the Mechanisms in Blastic Transformation of Chronic Myeloid Leukemia: Epigenetics Abnormality]. Zhongguo Shi Yan Xue Ye Xue Za Zhi. 2016;24(1):250-3.
24. Hochhaus A, Kantarjian HM, Baccarani M, Lipton JH, Apperley JF, Druker BJ, et al. Dasatinib induces notable hematologic and cytogenetic responses in chronic-phase chronic myeloid leukemia after failure of imatinib therapy. Blood. 2007;109(6):2303-9.
25. Tokarski JS, Newitt JA, Chang CY, Cheng JD, Wittekind M, Kiefer SE, et al. The structure of Dasatinib (BMS-354825) bound to activated ABL kinase domain elucidates its inhibitory activity against imatinib-resistant ABL mutants. Cancer Res. 2006;66(11):5790-7.
26. Zaharieva MM, Amudov G, Konstantinov SM, Guenova ML. Modern Therapy of Chronic Myeloid Leukemia. In: Guenova PM, editor. Leukemia: InTech; 2013.
27. Intermesoli T, Castagnetti F, Soverini S, Bussini A, Spinelli O, Gnani A, et al. Durable molecular response despite F317L and E255K mutations: Successful treatment of chronic myeloid leukemia with sequential imatinib, nilotinib and dasatinib. Leuk Res. 2012;36(1):e10-1.
28. Yin CC. Detection and Molecular Monitoring of Minimal Residual Disease in Chronic Myelogenous Leukemia. J Clin Exp Pathol. 2012; 2(4):1000e110.
29. Oehler VG, Radich JP. Monitoring bcr-abl by polymerase chain reaction in the treatment of chronic myeloid leukemia. Curr Oncol Rep. 2003;5:426-35.
30. Pavlovsky C, Giere I, Moiraghi B, Pavlovsky MA, Aranguren PN, Garcia J, et al. Molecular monitoring of imatinib in chronic myeloid leukemia patients in complete cytogenetic remission: does achievement of a stable major molecular response at any time point identify a privileged group of patients? A multicenter experience in Argentina and Uruguay. Clin Lymphoma Myeloma Leuk. 2011;11(3):280-5.
31. Melo JV, Ross DM. Minimal residual disease and discontinuation of therapy in chronic myeloid leukemia: can we aim at a cure? Hematology Am Soc Hematol Educ Program. 2011;2011:136-42.
32. Okabe S, Tauchi T, Katagiri S, Tanaka Y, Ohyashiki K. Combination of the ABL kinase inhibitor imatinib with the Janus kinase 2 inhibitor TG101348 for targeting residual BCR-ABL-positive cells. J Hematol Oncol. 2014;7:37.
33. An X, Tiwari AK, Sun Y, Ding PR, Ashby CR, Jr., Chen ZS. BCR-ABL tyrosine kinase inhibitors in the treatment of Philadelphia chromosome positive chronic myeloid leukemia: a review. Leuk Res. 2010;34(10):1255-68.
34. Pavlů J, Szydlo RM, Goldman JM, Apperley JF. Three decades of transplantation for chronic myeloid leukemia: what have we learned? Blood. 2011;117(3):755-63.
35. Yokoo M, Kubota Y, Tabe Y, Kimura S. Comparative study of the anti-leukemic effects of imatinib mesylate, Glivec tablet and its generic formulation, OHK9511. Biol Pharm Bull. 2015;38(3):411-6.
36. Bain B. Lukemia Diagnosis. In: wiley@sons Aj, editor. fourth ed. l td2010. p. 1-2.
37. Trivedi R, Mithal A, Chattopadhyay N. Recent updates on the calcium-sensing receptor as a drug target. Curr Med Chem. 2008;15(2):178-86.

38. Burchert A, Saussele S, Eigendorff E, Müller M, Sohlbach K, Inselmann S, et al. Interferon alpha 2 maintenance therapy may enable high rates of treatment discontinuation in chronic myeloid leukemia. Leukemia. 2015 45:1-5.
39. Dusetzina SB, Winn AN, Abel GA, Huskamp HA, Keating NL. Cost sharing and adherence to tyrosine kinase inhibitors for patients with chronic myeloid leukemia. J Clin Oncol. 2014;32(4):306-11.
40. Jemal A, Siegel R, Xu J, Ward E. Cancer statistics, 2010. CA Cancer J Clin. 2010;60(5):277-300.
41. Watkins DB, Hughes TP, White DL. OCT1 and imatinib transport in CML: is it clinically relevant? Leukemia. 2015;29(10):1960-9.
42. Cashen A, Wildes T. The Washington Manual subspecialty consult series. Hematology and Oncology Subspeciality Consult.
43. Chahardouli B, Zaker F, Mousavi SA, Kazemi A, Ostadali M, Nadali F, et al. Evaluation of T315I mutation frequency in chronic myeloid leukemia patients after imatinib resistance. Hematology. 2013;18(3):158-62.
44. Branford S, Rudzki Z, Walsh S, Grigg A, Arthur C, Taylor K, et al. High frequency of point mutations clustered within the adenosine triphosphate-binding region of BCR/ABL in patients with chronic myeloid leukemia or Ph-positive acute lymphoblastic leukemia who develop imatinib (STI571) resistance. Blood. 2002;99(9):3472-5.
45. Cojbasic I, Macukanovic-Golubovic L, Mihailovic D, Vucic M, Lukic S. Improved prediction of clinical outcome in chronic myeloid leukemia. Int J Hematol. 2015;101(2):173-83.
46. Cortes J, Jabbour E, Kantarjian H, Yin CC, Shan J, O'Brien S, et al. Dynamics of BCR-ABL kinase domain mutations in chronic myeloid leukemia after sequential treatment with multiple tyrosine kinase inhibitors. Blood. 2007;110(12):4005-11.
47. Ai J, Tiu RV. Practical management of patients with chronic myeloid leukemia who develop tyrosine kinase inhibitor-resistant BCRABL1mutations. Ther Adv Hematol. 2014;5(4):107 -20.
48. Redaelli S, Piazza R, Rostagno R, Magistroni V, Perini P, Marega M. Activity of bosutinib, dasatinib, and nilotinib against 18 imatinibresistant BCR/ABL mutants. J Clin Oncol. 2009;27:469-71.
49. Assouline S, Lipton JH. Monitoring response and resistance to treatment in chronic myeloid leukemia. Current Oncology. 2011;18(2):e71-e83.
50. Stone RM. Optimizing treatment of chronic myeloid leukemia: a rational approach. Oncologist. 2004;9(3):259-70.
51. Zhang H, Chang G, Wang J, Lin Y, Ma L, Pang T. CUEDC2 sensitizes chronic myeloid leukemic cells to imatinib treatment. Leuk Res. 2013;37(11):1583-91.
52. Horvat I, Antolic MR, Zadro R, Sertić D, Labar B. Clinical significance of T315I ABL kinase domain mutation detection in patients resistant to imatinib mesylate therapy. Biochemia Medica. 2010;20(1):75-81.
53. Jabbour E, Cortes JE, Giles FJ, O'Brien S, Kantarjian HM. Current and Emerging Treatment Options in Chronic Myeloid Leukemia. CANCER. 2007;109(11):2171-81.
54. Sierra JR, Cepero V, Giordano S. Molecular mechanisms of acquired resistance to tyrosine kinase targeted therapy. Mol Cancer. 2010;9:75.
55. Shimada K, Tomita A, Minami Y, Abe A, Hind CK, Kiyoi H, et al. CML cells expressing the TEL/MDS1/EVI1 fusion are resistant to imatinib-induced apoptosis through inhibition of BAD, but are resensitized with ABT-737. Exp Hematol. 2012;40(9):724-37.e2.
56. Talati C, Ontiveros EP, Griffiths EA, EuniceS.Wang, MeirWetzler. How we will treat chronic myeloid leukemia in 2016. Blood Reviews. 2014;29 (2):137-42.
57. Balabanov S, Braig M, Brümmendorf TH. Current aspects in resistance against tyrosine kinase inhibitors in chronic myelogenous leukemia. Drug Discovery Today Technologies. 2014;11:89-99.
58. Nicolini FE, Mauro MJ, Martinelli G, Kim DW, Soverini S, Muller MC, et al. Epidemiologic study on survival of chronic myeloid leukemia and Ph(+) acute lymphoblastic leukemia patients with BCR-ABL T315I mutation. Blood. 2009;114(26):5271-8.

59. Szachowicz-Petelska B, Figaszewski Z, Lewandowski W. Mechanisms of transport across cell membranes of complexes contained in antitumour drugs. International Journal of Pharmaceutics. 2001;222:169–82.
60. Eechoute K, Franke RM, Loos WJ, Scherkenbach LA, Boere I, Verweij J, et al. Environmental and genetic factors affecting transport of imatinib by OATP1A2. Clinical pharmacology and therapeutics. 2011;89(6):816-20.
61. Dean M, Rzhetsky A, Allikmets R. The human ATP-binding cassette (ABC) transporter superfamily. Genome Res. 2001;11(7):1156-66.
62. Heaney NB, Holyoake TL. Therapeutic targets in chronic myeloid leukaemia. Hematol Oncol. 2007;25(2):66-75.
63. Widmer N, Colombo S, Buclin T, Decosterd LA. Functional consequence of MDR1 expression on imatinib intracellular concentrations. Blood. 2003;102(3):1142.
64. Ambudkar SV, Kim IW, Xia D, Sauna ZE. The A-loop, a novel conserved aromatic acid subdomain upstream of the Walker A motif in ABC transporters, is critical for ATP binding. FEBS Lett. 2006;580(4):1049-55.
65. Angelini S, Soverini S, Ravegnini G, Barnett M, Turrini E, Thornquist M, et al. Association between imatinib transporters and metabolizing enzymes genotype and response in newly diagnosed chronic myeloid leukemia patients receiving imatinib therapy. Haematologica. 2013;98(2):193-200.
66. Kathawala RJ, Gupta P, Ashby CR, Jr., Chen ZS. The modulation of ABC transporter-mediated multidrug resistance in cancer: a review of the past decade. Drug Resist Updat. 2015;18:1-17.
67. Skoglund K, Moreno SB, Baytar M, Jönsson J-I, Gréen H. ABCB1 haplotypes do not influence transport or efficacy of tyrosine kinase inhibitors in vitro. Pharmacogenomics and Personalized Medicine 2013;6:63-72.
68. Xia CQ, Smith PG. Drug efflux transporters and multidrug resistance in acute leukemia: therapeutic impact and novel approaches to mediation. Mol Pharmacol. 2012;82(6):1008-21.
69. Stromskaia TP, Rybalkina E, Turkina AG, Zabotina TN, Logacheva NP, Zakharova ES, et al. [Functional activity and expression of P-glycoprotein in chronic myeloid leukemia]. Ter Arkh. 2001;73(7):20-5.
70. Dobson PD, Kell DB. Carrier-mediated cellular uptake of pharmaceutical drugs: an exception or the rule? Nat Rev Drug Discov. 2008;7(3):205-20.
71. Cesar-Razquin A, Snijder B, Frappier-Brinton T, Isserlin R, Gyimesi G, Bai X, et al. A Call for Systematic Research on Solute Carriers. Cell. 2015;162(3):478-87.
72. Koczor CA, Torres RA, Lewis W. The role of transporters in the toxicity of nucleoside and nucleotide analogs. Expert Opin Drug Metab Toxicol. 2012;8(6):665-76.
73. Tiwari AK, Sodani K, Dai CL, Ashby CR, Jr., Chen ZS. Revisiting the ABCs of multidrug resistance in cancer chemotherapy. Curr Pharm Biotechnol. 2011;12(4):570-94.
74. Wu CP, Hsieh CH, Wu YS. The emergence of drug transporter-mediated multidrug resistance to cancer chemotherapy. Mol Pharm. 2011;8(6):1996-2011.
75. Hyde SC, Emsley P, Hartshorn MJ, Mimmack MM, Gileadi U, Pearce SR, et al. Structural model of ATP-binding proteins associated with cystic fibrosis, multidrug resistance and bacterial transport. Nature. 1990;346(6282):362-5.
76. Hagenbuch B, Stieger B. The SLCO (former SLC21) superfamily of transporters. Mol Aspects Med. 2013;34(2-3):396-412.
77. Hagenbuch B, Meier PJ. Organic anion transporting polypeptides of the OATP/ SLC21 family: phylogenetic classification as OATP/ SLCO superfamily, new nomenclature and molecular/functional properties. Pflugers Arch. 2004;447(5):653-65.
78. Lemos C, Jansen G, Peters GJ. Drug transporters: recent advances concerning BCRP and tyrosine kinase inhibitors. Br J Cancer. 2008;98(5):857-62.
79. Murray CW, Rees DC. The rise of fragment-based drug discovery. Nat Chem. 2009;1(3):187-92.

80. Major LL, Smith TK. Screening the MayBridge Rule of 3 Fragment Library for Compounds That Interact with the Trypanosoma brucei myo-Inositol-3-Phosphate Synthase and/or Show Trypanocidal Activity. Molecular Biology International. 2011;2011:14.
81. O' Hagan S, Swainston N, Handl J, Kell DB. A 'rule of 0.5' for the metabolite-likeness of approved pharmaceutical drugs. Metabolomics. 112015. p. 323-39.
82. Ciarimboli G, Deuster D, Knief A, Sperling M, Holtkamp M, Edemir B, et al. Organic Cation Transporter 2 Mediates Cisplatin-Induced Oto- and Nephrotoxicity and Is a Target for Protective Interventions. The American Journal of Pathology. 2010;176(3):1169-80.
83. Dahlin JL, Walters MA. The essential roles of chemistry in high-throughput screening triage. Future medicinal chemistry. 2014;6(11):1265-90.
84. Rees DC, Congreve M, Murray CW, Carr R. Fragment-based lead discovery. Nature Reviews Drug Discovery 2004;3:660-72.
85. Strober W. Trypan blue exclusion test of cell viability. Curr Protoc Immunol. 2001;Appendix 3:Appendix 3B.
86. Mosmann T. Rapid colorimetric assay for cellular growth and survival: application to proliferation and cytotoxicity assays. Journal of immunological methods. 1983;65(1-2):55-63.
87. Riss TL, Moravec RA. Use of multiple assay endpoints to investigate the effects of incubation time, dose of toxin, and plating density in cell-based cytotoxicity assays. Assay and drug development technologies. 2004;2(1):51-62.
88. Hellemans J, Vandesompele J. Selection of reliable reference genes for RT-qPCR analysis. Methods in molecular biology (Clifton, NJ). 2014;1160:19-26.
89. Salesse S, Verfaillie CM. BCR/ABL: from molecular mechanisms of leukemia induction to treatment of chronic myelogenous leukemia. Oncogene. 2002;21(56):8547-59.
90. Branford S, Rudzki Z, Walsh S, Parkinson I, Grigg A, Szer J. Detection of BCR-ABL mutations in patients with CML treated with imatinib is virtually always accompanied by clinical resistance, and mutations in the ATP phosphate-binding loop (P-loop) are associated with a poor prognosis. Blood. 2003;102:276-83.
91. Dvorak P, Lysak D, Vokurka S. Discontinuation of tyrosine kinase inhibitors in chronic myeloid leukemia patients - worldwide battlefield. Neoplasma. 2015;62(2):167-71.
92. Baccarani M, Castagnetti F, Gugliotta G, Rosti G. A review of the European LeukemiaNet recommendations for the management of CML. Ann Hematol. 2015;94 Suppl 2:S141-7.
93. Mahon F-X. Is going for cure in chronic myeloid leukemia possible and justifiable? American Society of Hematology. 2012:122-8.
94. Rees MG, Seashore-Ludlow B, Cheah JH, Adams DJ, Price EV, Gill S, et al. Correlating chemical sensitivity and basal gene expression reveals mechanism of action. nature CHEMICAL BIOLOGY. 2016;12:109-18.
95. Bourgne C, Bamdad M, Janel A, Libert F, Gagnieu MC, Rapatel C, et al. Measurement of imatinib uptake by flow cytometry. Cytometry A. 2012;81(11):996-1004.
96. van Tonder A, Joubert AM, Cromarty AD. Limitations of the 3-(4,5-dimethylthiazol-2-yl)-2,5-diphenyl-2H-tetrazolium bromide (MTT) assay when compared to three commonly used cell enumeration assays. BMC Research Notes. 2015;8:47.
97. Kantarjian HM, Giles F, Gattermann N, Bhalla K, Alimena G, Palandri F, et al. Nilotinib (formerly AMN107), a highly selective BCR-ABL tyrosine kinase inhibitor, is effective in patients with Philadelphia chromosome–positive chronic myelogenous leukemia in chronic phase following imatinib resistance and intolerance. Blood. 2007;110(10):3540-6.
98. Bustin SA. Quantification of mRNA using real-time reverse transcription PCR (RT-PCR): trends and problems. Journal of molecular endocrinology. 2002;29(1):23-39.
99. Terada T, Inui K-i. Gene expression and regulation of drug transporters in the intestine and kidney. b i ochemical pharmacology 2 0 07 7(3):4 40 – 4 9.

100. EA B, MT E, Z D, Y L, H L, KS B, et al. Rifampin Regulation of Drug Transporters Gene Expression and the Association of MicroRNAs in Human Hepatocytes. Front Pharmacol. 2016 26(7):111.
101. Yamakawa Y, Hamada A, Nakashima R, Yuki M, Hirayama C, Kawaguchi T, et al. Association of genetic polymorphisms in the influx transporter SLCO1B3 and the efflux transporter ABCB1 with imatinib pharmacokinetics in patients with chronic myeloid leukemia. Therapeutic drug monitoring. 2011;33(2):244-50.
102. Kim YK, Lee SS, Jeong SH, Ahn JS, Yang DH, Lee JJ, et al. OCT-1, ABCB1, and ABCG2 Expression in Imatinib-Resistant Chronic Myeloid Leukemia Treated with Dasatinib or Nilotinib. Chonnam medical journal. 2014;50(3):102-11.
103. Alvarado Y, Kantarjian H, O'Brien S, Faderl S, Borthakur G, Burger J, et al. Significance of suboptimal response to imatinib, as defined by the European LeukemiaNet, in the long-term outcome of patients with early chronic myeloid leukemia in chronic phase. Cancer. 2009;115(16):3709-18.
104. Gotovdorj T, Lee E. 2,3,7,8-Tetrachlorodibenzo-p-dioxin induced cell-specific drug transporters with acquired cisplatin resistance in cisplatin sensitive cancer cells. 2014;29(9):1188-98.
105. Breccia M, Molica M, Alimena G. How tyrosine kinase inhibitors impair metabolism and endocrine system function: a systematic updated review. Leuk Res. 2014;38(12):1392-8.
106. Marin D, Milojkovic D, Olavarria E, Khorashad JS, de Lavallade H, Reid AG, et al. European LeukemiaNet criteria for failure or suboptimal response reliably identify patients with CML in early chronic phase treated with imatinib whose eventual outcome is poor. Blood. 2008;112(12):4437-44.

APPENDIX 1

Another way to present the results obtained from pooled-screening experiments. However, in table1 where the percentage of cell viability of each well is independently. As described before each experimental set compromised two 96-well plates and were considered as a one biological replicate.

Table-A1: Represents the data from MBF screening in pooled condition for K562 cells and imatinib treatment

	MBF Only	MBF+Imatinib	MBF Only	MBF+Imatinib	MBF Only	MBF+Imatinib	MBF Only	MBF+Imatinib
1	103.15	80.87	103.12	77.64	65.6	39.33	113.12	58.44
2	101.59	101.45	111.01	97.13	99.71	28.25	113.42	67.53
3	103.28	101.7	103.24	97.37	107.14	47.63	107.54	59.82
4	117.25	93.55	116.94	89.65	111.24	51.84	105.24	60.13
5	107.42	71.04	116.89	68.33	107.35	53.03	110.71	61.59
6	106.27	103.04	111.86	98.63	113.27	62.72	111.09	62.1
7	111.77	92.05	111.52	88.23	63.53	44.12	112.51	61.11
8	99.65	91.88	99.65	88.07	101.43	43.54	115.94	60.03
9	104.98	96.29	114.59	92.24	108.51	58.75	113.4	53.39
10	116	114.63	115.6	109.61	117.47	57.14	112.08	48.53
11	111.89	103.8	111.31	99.35	116.52	59.39	110.66	59.63
12	96.07	81.49	96.11	78.23	112.45	58.66	114.28	63.35
13	105.85	95.99	105.79	91.96	76.46	50.16	119.8	55.19
14	119.75	100.74	119.19	96.46	101.92	49.08	103.81	66.11
15	116.21	115.04	116.03	110	101.24	58.35	103.52	65.95
16	111.15	102.59	110.8	98.21	111.7	70.82	106.94	63.56
17	117.43	83.96	117.12	80.57	83.47	34.41	117.02	65.09
18	110.64	84.94	110.29	81.5	105.61	56.83	111.68	60.74
19	113.77	80.46	113.5	77.25	84.28	45.49	111.59	62.02
20	95.99	85.48	96.04	82.01	66.81	39.31	113.3	63
21	110.91	103.69	110.79	99.25	112.14	56.52	119.25	52.28
22	100.72	87.66	100.71	84.07	100.67	57.47	114.64	51.82

23	111.08	101.34	110.5	97.03	113.01	62.26	114.63	60.8
24	90.01	99.19	90.13	94.99	105.09	66.92	100.53	56.57
25	116	110.23	115.82	105.44	91.62	56.03	110.2	65.81
26	118.35	114.13	117.57	109.14	92.72	54.62	113.33	73.01
27	115.42	117.8	115.25	112.61	101	59.34	110.43	59.21
28	110.78	118.92	110.43	113.14	117.14	66.52	110.48	66.35
29	117.15	80.18	116.73	76.99	95.75	49.15	113.68	66.98
30	116.57	83.41	116.38	80.05	113.61	58.04	114.83	57.84
31	106.07	103.36	106	98.94	93.13	58.68	111.87	67.86
32	95.35	83.28	95.41	79.93	99.18	59.99	106.55	74.47
33	115.7	116.22	115.53	111.12	123.59	61.27	117.44	55.06
34	115.85	89.93	105.45	86.22	107.84	54.76	111.87	58.72
35	119.82	44.16	119.6	42.88	51.62	24.59	110.96	52.08
36	113.97	97.9	113.81	93.77	111.24	61.31	98.05	58.7
37	82.75	99.85	82.94	95.62	50.57	37.39	83.53	43.6
38	116.07	119.11	105.21	113.85	115.34	57.4	100.82	67.01
39	118.12	103.06	117.69	111.07	88.85	56.35	116.93	65.01
40	125.38	105.23	105.09	119.12	114.66	77.81	108.79	69.29
41	116.12	77.11	105.6	74.08	96.96	46.41	118.21	72.18
42	96.02	77.13	96.06	74.11	114.85	40.01	117.8	61.99
43	111.09	85.21	110.97	81.75	91.73	48.49	120.98	62.92
44	92.43	81.54	92.52	78.27	100.08	66.28	90.85	66.1
45	116.31	108.84	105.9	104.13	100.01	46.39	115.25	47.02
46	99.32	70.52	99.32	67.85	80.9	51.58	115.41	60.16
47	118.1	73.94	117.55	71.08	84.52	36.75	105.54	53.21
48	119.17	97.06	118.95	92.97	116.88	67.93	95.29	65.06
49	109.75	108.53	109.64	103.84	86.84	57.95	98.24	55.03
50	119.41	110.83	118.51	106.01	113.42	58.55	118.18	65.14
51	110.64	112.63	110.18	116.12	115.87	68.19	113.69	68.94
52	117.56	119.15	117.37	112.3	114.09	78.92	108.91	61.73
53	110.14	76.22	119.46	73.24	99.4	60.3	114.77	64.09
54	82.51	45.81	82.71	44.45	82.8	20.35	104.05	60.31
55	110.74	87.22	110.5	83.66	89.88	49.48	111.24	63.79

56	70.81	80.9	71.14	77.67	90.62	62.39	103.8	64.17
57	78.14	81.23	78.38	77.98	76.46	41.65	91.97	21.98
58	87.12	74.98	87.27	72.06	113.78	63.91	115.07	54.56
59	103.75	68.6	103.71	66.02	111.38	49.86	111.32	62.07
60	119.21	92.9	118.99	89.03	111.5	70.84	101.92	55.09
61	105.57	107.71	105.51	103.06	103.95	55.82	114.64	61.22
62	115.08	111.37	114.12	115.99	119.42	64.93	116.18	65.58
63	115.65	111.29	115.48	115.92	119.07	69.12	115.55	63.11
64	98.11	116.98	98.13	110.24	117.43	73.71	98.43	40.92
65	111.56	77.8	110.75	74.74	109.61	58.97	109.58	62.55
66	115.18	76.33	114.9	73.34	113.36	54.58	117.24	57.26
67	110.53	93.63	110.41	89.72	71.59	44.41	116.82	76.05
68	102.32	89.17	102.3	85.51	90.84	88.83	95.85	68.83
69	105.41	110.07	105.35	114.76	115	61.07	117.18	46.76
70	103.08	71.82	103.04	69.07	112.05	78.37	85.62	39.37
71	110.2	74.64	110.08	71.75	111.72	62.08	84.91	42.96
72	117.83	78.85	117.63	75.73	112.85	57.82	96.91	68.15
73	84.64	114.78	84.81	118.69	92.1	71.51	114.26	58.46
74	113.24	100.06	112.86	95.81	116.23	59.96	97.47	58.72
75	76.54	89.3	76.81	85.63	104.06	62.12	98.17	68.47
76	82.48	114.87	82.68	118.25	110.22	83.15	105.99	63.05
77	88.66	76.89	88.79	73.87	110.6	62.32	114.23	64.51
78	60.6	35.6	61.05	34.77	63.73	33.75	79.29	47.29
79	86.34	90.14	86.5	86.42	78.45	51.03	113.2	66.31
80	82.2	82.81	82.4	79.48	85.24	92.09	102.13	68.6
81	96.28	98.94	96.33	94.76	104.36	57.89	112.5	53.84
82	76.91	55.47	77.17	53.59	103.95	81.92	115.6	43.25
83	89.96	66.58	90.08	64.11	111.31	65.9	118.57	52.86
84	95.9	86.36	95.95	82.85	110.26	71.51	94.99	65.63

	MBF Only	MBF+Cisplatin	MBF Only	MBF+Cisplatin	MBF Only	MBF+Cisplatin	MBF Only	MBF+Cisplatin
1	65.60	95.70	99.58	72.34	68.91	88.94	111.71	73.98
2	99.71	78.98	91.69	80.74	76.99	88.05	80.70	84.80
3	107.14	88.24	86.90	85.08	81.17	90.73	88.18	97.28
4	111.24	85.58	85.02	97.33	92.96	95.68	82.36	91.70
5	107.35	79.43	97.62	99.96	95.48	79.96	96.55	96.83
6	133.27	79.87	89.78	94.72	90.45	75.97	87.71	73.03
7	63.53	84.19	90.94	91.18	87.04	86.36	94.99	90.26
8	101.43	85.85	93.74	95.15	90.86	77.61	66.42	85.20
9	108.51	74.62	107.96	97.31	92.93	93.95	103.34	86.46
10	117.47	75.36	115.03	106.33	101.62	81.49	82.20	85.69
11	126.52	85.90	97.59	97.64	93.25	91.69	95.89	76.83
12	142.45	96.79	100.54	106.25	101.55	81.98	90.70	85.91
13	76.46	90.50	96.88	76.49	72.90	85.26	100.18	78.97
14	101.92	80.93	83.86	84.23	80.35	80.43	82.13	79.71
15	101.24	93.33	83.62	86.45	82.49	83.00	73.60	91.09
16	131.70	84.62	86.40	81.69	77.90	92.63	66.47	94.88
17	83.47	90.43	102.77	79.41	75.71	94.75	76.29	86.05
18	105.61	85.01	90.26	88.48	84.44	87.86	96.15	82.73
19	84.28	89.43	104.85	97.97	93.58	90.77	102.61	89.28
20	66.81	86.77	91.58	99.92	95.45	77.39	92.35	84.39
21	112.14	85.09	104.58	84.24	80.36	100.42	96.33	84.42
22	100.67	84.75	100.82	104.91	100.25	88.00	98.76	94.15
23	113.01	77.51	92.67	89.73	85.64	87.46	85.04	71.80
24	145.09	86.25	81.18	91.70	87.54	74.68	86.88	84.59
25	91.62	97.06	89.06	86.23	82.27	99.02	102.56	84.76
26	92.72	87.55	91.61	93.96	89.72	100.32	83.51	76.46
27	101.00	93.95	89.25	87.21	83.22	89.87	88.53	88.86
28	117.14	87.40	89.29	83.34	79.49	96.28	84.45	95.75
29	95.75	94.46	100.04	89.52	85.44	103.03	98.34	92.39
30	113.61	79.48	92.84	93.80	89.56	87.12	88.54	83.06
31	93.13	98.56	98.56	89.52	85.44	88.26	106.29	92.15
32	99.18	83.30	86.09	86.75	82.77	84.08	83.70	90.13
33	123.59	80.50	94.96	93.24	89.03	93.69	90.71	92.10
34	107.84	81.14	90.42	105.36	100.69	91.59	78.29	81.18
35	51.62	71.05	105.98	100.79	96.29	85.57	80.54	72.17
36	141.24	78.74	79.16	99.93	95.46	83.22	86.72	74.29
37	50.57	42.74	67.33	55.83	53.01	64.19	52.04	41.88
38	135.34	77.78	81.42	75.16	71.62	90.24	81.28	66.62
39	88.85	81.77	94.54	85.48	81.55	82.18	62.65	83.08
40	124.66	71.97	87.91	85.71	81.77	85.10	71.89	77.10
41	96.96	82.47	95.59	78.89	75.21	96.79	90.10	85.30
42	114.85	89.52	95.25	99.41	94.96	88.44	93.26	78.75
43	91.73	89.98	97.85	90.90	86.77	91.19	85.56	84.01
44	100.08	78.91	73.30	87.29	83.30	81.32	72.57	84.08
45	100.01	85.17	93.17	91.06	86.92	97.19	86.40	84.16
46	80.90	90.92	93.30	96.08	91.76	86.94	89.99	82.12
47	84.52	55.21	85.27	88.73	84.68	72.19	72.45	61.89
48	116.88	87.92	76.91	107.08	102.34	88.58	96.10	83.03

49	86.84	64.39	79.31	73.54	70.06	72.83	67.15	69.74
50	133.42	78.95	95.56	83.82	79.95	96.64	79.91	66.28
51	135.87	88.12	100.05	80.90	77.15	94.32	81.19	89.95
52	124.09	83.49	88.01	89.41	85.33	85.99	85.16	90.40
53	99.40	84.23	100.93	91.66	87.50	91.88	94.54	80.07
54	82.80	84.57	84.05	85.19	81.27	76.18	87.67	83.40
55	89.88	87.75	98.06	84.08	80.21	80.52	88.53	84.24
56	90.62	86.09	83.84	86.91	82.93	88.36	84.69	88.77
57	76.46	51.91	74.21	56.24	53.41	62.24	57.26	53.09
58	113.78	92.63	93.03	88.09	84.07	89.74	94.73	91.14
59	111.38	78.53	98.12	85.99	82.04	83.85	85.17	80.22
60	131.50	89.47	82.32	79.61	75.90	81.37	95.75	76.16
61	103.95	89.56	100.82	90.57	86.45	97.73	101.89	86.53
62	129.42	76.61	93.93	80.00	76.27	98.38	87.75	68.19
63	129.07	78.32	93.42	78.85	75.17	86.83	76.37	83.53
64	117.43	80.75	79.47	81.02	77.26	84.28	69.07	87.95
65	109.61	80.37	88.55	83.86	79.99	89.13	70.02	79.35
66	133.36	86.03	94.79	103.06	98.47	97.91	92.43	81.57
67	71.59	94.31	94.45	78.52	74.85	86.56	92.99	89.70
68	90.84	77.91	77.37	78.17	74.52	83.41	88.40	78.47
69	115.00	96.09	102.90	82.27	78.47	108.79	99.80	82.94
70	112.05	75.25	69.03	67.23	63.98	61.74	66.43	69.32
71	111.72	77.65	68.46	59.68	56.72	54.56	82.36	76.40
72	132.85	89.27	78.23	94.43	90.17	80.85	96.25	83.36
73	92.10	91.40	108.67	78.08	74.43	93.99	98.95	94.43
74	116.23	72.33	78.69	73.96	70.47	89.90	82.14	76.12
75	104.06	81.93	79.26	67.92	64.65	92.33	83.11	86.12
76	120.22	84.67	85.63	84.18	80.30	89.87	86.37	92.18
77	120.60	74.55	108.64	87.76	83.75	81.84	80.57	73.30
78	63.73	43.86	63.88	61.04	58.02	63.63	55.70	27.33
79	78.45	84.63	99.65	76.20	72.62	93.01	93.47	94.06
80	85.24	72.53	82.49	84.92	81.02	80.25	74.50	85.70
81	104.36	94.34	107.23	85.75	81.81	104.37	108.99	90.12
82	103.95	86.77	93.46	90.18	86.08	86.68	93.50	93.72
83	111.31	77.82	95.88	84.91	81.00	85.28	100.39	83.21
84	110.26	98.60	76.67	85.74	81.80	80.29	97.10	87.36

Table-A2: Represents the data from MBF screening in pooled condition for K562 cells and cisplatin treatment

	MBF Only	MBF+Imatinib	MBF Only	MBF+Imatinib	MBF Only	MBF+Imatinib
1	66.80	55.28	32.97	74.55	30.26	83.00
2	99.72	55.21	32.88	90.90	30.17	62.32

3	106.89	59.00	72.39	94.30	71.27	108.36
4	110.84	53.55	69.19	98.99	67.95	86.51
5	107.09	56.05	81.80	112.86	81.07	95.10
6	122.11	62.42	89.79	96.69	89.38	115.89
7	64.80	56.70	81.98	90.90	81.25	108.13
8	101.38	48.18	81.44	102.57	80.70	100.18
9	108.21	60.97	233.80	109.46	110.19	103.14
10	116.86	57.04	64.93	90.54	63.52	88.73
11	120.60	50.91	92.01	106.25	91.69	114.96
12	120.98	44.25	84.82	68.67	84.21	102.03
13	77.28	52.82	62.09	67.84	60.56	75.52
14	101.86	58.26	88.72	91.55	88.27	65.09
15	101.20	59.53	87.84	81.26	87.35	112.93
16	120.60	54.40	100.98	90.44	101.02	107.48
17	84.04	53.94	83.58	99.63	82.91	83.28
18	105.42	60.28	88.19	100.28	87.72	76.45
19	84.82	56.49	76.12	89.43	75.15	87.81
20	67.97	49.55	72.03	92.65	70.91	110.34
21	111.72	57.92	88.64	105.97	88.18	110.62
22	100.65	50.64	81.18	101.84	80.42	102.31
23	112.55	51.55	89.88	88.15	89.47	93.63
24	123.52	51.28	80.29	76.57	79.50	96.67
25	91.91	52.66	80.47	81.26	79.68	95.29
26	92.98	58.29	103.82	85.57	103.97	107.85
27	100.97	58.68	88.55	76.94	88.08	113.37
28	116.54	57.18	101.78	102.66	101.85	116.14
29	95.89	59.43	80.47	98.81	79.68	112.93
30	113.14	60.14	96.27	97.89	96.12	87.72
31	93.37	55.94	101.42	103.31	101.48	107.48
32	99.21	54.35	89.52	95.13	89.10	97.51
33	122.77	60.85	76.03	101.65	75.06	108.91
34	107.57	59.59	69.19	96.51	67.95	95.38
35	53.30	54.98	85.08	85.76	84.48	95.84
36	129.80	53.96	78.51	73.45	77.65	93.81
37	52.29	47.54	64.13	49.28	62.68	74.32
38	124.11	55.71	95.74	92.65	95.57	101.57
39	89.24	60.08	78.34	83.19	77.46	116.72
40	123.80	57.13	77.27	97.61	76.35	103.23
41	97.07	63.66	87.22	95.77	86.70	113.83
42	114.33	57.94	82.15	91.45	81.43	55.30
43	92.01	59.32	94.23	109.83	94.00	104.06
44	100.08	55.18	93.96	89.89	93.72	98.15
45	100.01	65.15	76.29	83.55	75.34	84.67
46	81.57	57.43	70.61	84.66	69.43	102.31
47	85.06	49.56	96.98	72.89	96.86	108.68
48	116.29	47.15	60.49	86.22	58.90	104.71

49	87.30	52.82	64.66	71.61	63.24	79.86
50	122.26	51.87	90.68	76.66	90.30	98.06
51	124.62	56.74	90.59	74.92	90.21	117.92
52	123.25	59.71	71.50	103.58	70.35	100.37
53	99.42	60.76	88.55	84.10	88.08	116.90
54	83.40	61.70	84.11	87.32	83.47	117.09
55	90.23	59.38	96.80	91.36	96.67	85.96
56	90.95	51.14	99.73	90.90	99.72	108.31
57	77.28	47.81	73.45	44.41	72.38	36.73
58	113.30	52.98	86.33	94.67	85.78	95.57
59	110.99	58.15	94.85	84.01	94.64	104.66
60	130.40	46.82	76.03	83.74	75.06	94.64
61	103.81	53.94	60.85	48.36	59.27	71.83
62	128.39	46.61	100.53	78.68	100.55	86.70
63	128.06	58.01	82.78	67.38	82.08	107.20
64	116.82	48.73	64.75	79.69	63.33	89.93
65	109.28	55.20	86.42	82.36	85.87	52.52
66	122.20	69.51	71.68	90.26	70.54	51.23
67	72.58	55.43	82.69	88.97	81.99	70.81
68	91.16	46.75	86.95	89.80	86.42	81.90
69	114.48	61.43	93.70	102.76	93.44	49.48
70	111.63	50.71	72.39	147.23	71.27	75.80
71	111.31	49.05	92.28	83.19	91.96	89.84
72	121.70	56.97	86.77	90.26	86.24	100.37
73	92.37	50.96	46.91	73.17	44.77	77.83
74	115.67	47.85	60.94	67.20	59.36	81.07
75	103.92	58.84	95.47	86.58	95.29	77.37
76	119.51	60.93	73.10	77.49	72.01	58.44
77	119.89	65.27	101.24	85.39	101.29	101.02
78	65.00	39.52	70.97	12.71	69.80	69.24
79	79.20	63.57	77.72	69.49	76.82	83.28
80	85.75	46.48	120.60	74.36	110.31	93.26
81	104.21	48.55	99.02	80.25	98.98	74.32
82	103.81	57.53	74.34	98.81	73.31	82.36
83	110.92	47.26	90.77	70.78	90.39	94.00
84	109.90	42.32	82.51	68.12	81.80	83.56

Table-A3: Represents the data from MBF screening in pooled condition for SH-Y5Y cells and imatinib treatment.

	MBF Only	MBF+Cisplatin	MBF Only	MBF+Cisplatin	MBF Only	MBF+Cisplatin
1	91.82	52.42	96.81	80.91	100.54	94.97
2	101.47	63.77	100.49	80.35	116.92	88.7
3	117.65	71.54	106.66	87.95	115.55	92.59
4	103.16	57.96	109.54	82.10	108.91	80.5
5	105.71	60.28	108.33	72.44	93.42	77.29
6	99.82	51.19	83.17	88.51	111.49	89.66
7	108.71	57.31	106.22	85.09	100.74	74.37
8	89.88	72.11	99.72	83.96	107.52	89.56
9	91.18	48.84	94.23	88.57	97.42	82.29
10	86.33	53.46	99.42	90.50	100.28	83.56
11	100.22	50.36	90.44	84.53	100.77	66.48
12	64.80	45.60	94.09	76.43	106.3	66.72
13	88.78	52.42	105.15	74.03	103.43	92.94
14	103.31	63.77	98.35	74.78	112.2	84.32
15	110.11	71.54	109.44	75.37	114.19	82.22
16	106.01	57.96	100.83	75.99	105.59	75.05
17	96.32	60.28	107.36	72.29	94.98	76.81
18	98.82	51.19	85.42	93.87	113.42	87.94
19	105.96	57.31	107.96	81.79	99.55	70.61
20	100.27	72.11	112.12	83.06	111.95	79.12
21	95.87	48.84	91.58	87.05	87.2	75.71
22	100.97	53.46	109.27	88.95	89.36	85.63
23	87.73	50.36	89.74	83.90	92.79	67.92
24	70.80	45.60	78.85	67.40	92.62	86.91
25	101.71	61.63	113.52	92.25	103.32	90.25
26	102.51	60.76	104.11	76.80	108.8	89.77
27	105.31	56.35	108.36	76.43	112.18	80.81
28	106.11	56.48	110.37	76.40	114.47	83.08
29	94.37	46.13	111.41	77.86	102.13	78.74
30	100.37	50.15	79.22	92.81	108.63	78.57
31	104.81	55.82	110.94	89.72	114.99	77.09
32	108.46	65.04	114.49	88.76	115.07	88.29
33	90.68	52.02	97.21	90.78	104.09	81.26
34	81.88	53.64	111.51	92.31	103.63	84.12
35	88.98	54.91	93.99	85.68	101.25	61.96
36	60.91	47.79	86.35	78.61	99.91	81.02
37	86.63	51.19	112.82	86.02	97.36	86.63
38	98.27	54.21	104.91	72.97	110.81	80.12
39	97.87	54.60	103.00	76.27	117.2	76.95
40	96.92	60.49	115.77	86.42	100.79	83.74
41	109.41	58.62	113.79	74.78	104.12	79.84
42	99.62	49.62	86.92	95.49	111.61	87.84
43	89.53	61.50	111.21	92.37	103.09	81.57
44	109.01	58.44	105.82	84.31	117.85	94.76
45	84.33	38.70	84.61	61.39	73.95	58.17
46	94.82	59.97	109.37	95.14	102.75	82.08
47	96.42	53.11	88.33	89.29	100.94	70.33
48	74.69	36.39	89.54	78.58	98.52	88.77
49	87.48	52.07	108.73	87.92	96.25	89.04

50	96.12	51.54	94.43	71.91	110.67	86.73
51	114.45	51.02	102.57	77.61	109.03	84.15
52	95.07	53.20	98.78	77.33	102.95	88.42
53	95.07	50.41	109.74	77.08	99.4	75.74
54	82.98	46.91	64.11	82.35	99.74	80.91
55	92.37	53.64	112.45	91.06	99.4	85.77
56	106.81	53.51	111.08	82.59	117.23	90.7
57	24.84	16.04	21.76	16.09	8.69	4.01
58	100.27	60.76	110.94	92.00	94.32	88.56
59	94.67	58.22	95.03	96.86	96.65	68.2
60	70.90	42.63	84.04	78.05	89.44	84.29
61	99.62	58.79	112.15	82.03	97.11	91.42
62	94.92	60.89	93.62	79.85	103.15	87.32
63	102.21	59.27	89.37	78.17	106.95	83.91
64	102.06	57.44	100.32	86.61	94.64	76.02
65	91.87	45.91	108.83	78.92	87.48	55.93
66	90.33	40.41	73.19	82.38	107.41	90.59
67	100.07	47.57	110.98	87.92	96.05	82.53
68	112.75	49.84	107.02	86.24	109.39	92.08
69	88.13	46.87	97.51	90.60	86.46	76.16
70	96.32	63.20	103.87	97.42	103.75	75.43
71	89.58	64.95	113.49	87.92	100.79	80.22
72	60.46	56.00	90.11	89.23	106.56	99.07
73	97.72	46.96	99.12	104.83	94.83	80.57
74	100.27	54.73	90.51	78.11	100.85	84.46
75	87.73	58.70	95.13	78.67	100.37	88.73
76	94.82	62.55	116.27	88.23	97.81	76.12
77	95.22	44.64	90.01	82.35	100.28	69.99
78	8.81	13.55	8.13	7.21	10.31	-1.5
79	84.73	44.73	108.23	77.21	90.46	69.68
80	98.27	49.32	105.15	84.09	114.16	84.81
81	78.69	44.38	98.08	101.65	93.61	87.6
82	100.47	66.78	107.09	68.89	114.82	90.39
83	79.09	56.74	91.51	93.21	100.65	65.96
84	52.16	43.55	84.28	67.87	104.48	85.63

Table-A4: Represents the data from MBF screening in pooled condition for SH-Y5Y cells and cisplatin treatment

APPENDIX 2

Another way to present the results obtained from single-screening experiments. Howevre, in table1 where the percentage of cell viability of each well is independently. As described before each experimental set compromised two 96-well plates and were considered as a one biological replicate.

Table-A5: Represents the data from MBF screening in single condition for K562 cells and imatinib treatment

	MBF Only	MBF+Imatinib	MBF Only	MBF+Imatinib	MBF Only	MBF+Imatinib
1	89.65	82.67	82.34	81.06	75.14	36.86
2	73.59	68.48	80.45	62.15	78.21	19.03
3	87.21	88.32	98.02	71.92	64.22	41.17
4	75.17	76.89	93.03	65.40	70.53	33.78
5	100.21	86.10	88.38	66.60	81.63	34.47
6	90.54	74.65	84.79	84.59	73.53	51.31
7	91.56	88.87	96.52	73.60	59.19	36.40
8	94.17	57.48	79.60	55.95	70.16	28.81
9	113.17	75.86	87.09	67.75	78.29	53.86
10	75.01	77.00	80.56	77.62	71.93	51.03
11	62.27	56.15	88.67	65.44	64.93	23.14
12	89.20	92.87	83.09	56.15	81.35	50.16
13	80.04	87.31	81.88	68.48	72.22	75.71
14	73.69	66.74	76.81	69.10	70.43	50.08
15	73.92	70.49	86.86	63.33	64.03	56.78
16	83.43	71.20	103.88	68.37	65.58	63.80
17	86.18	93.00	80.17	63.65	63.09	58.71
18	91.89	67.33	82.62	75.42	62.27	56.90
19	89.20	69.78	110.42	75.38	27.25	26.22
20	88.20	74.26	86.96	80.44	63.19	55.01
21	87.83	92.50	89.68	78.41	72.87	58.42
22	71.74	59.10	68.13	49.76	57.40	28.72
23	103.91	86.28	90.79	64.50	68.03	47.74
24	115.25	68.54	103.00	86.55	64.98	34.15
25	84.09	93.12	87.43	79.74	72.82	67.25
26	80.60	64.25	83.61	70.85	67.16	47.74
27	87.05	98.83	101.15	76.15	62.69	51.77
28	68.25	81.05	105.95	80.36	68.58	56.57
29	89.43	85.94	83.92	58.37	75.95	45.69
30	98.79	64.50	94.27	78.73	68.58	55.87
31	93.41	78.76	99.31	72.00	58.38	58.30
32	94.13	82.44	104.79	79.44	68.11	51.93

33	20.27	7.44	10.35	14.50	6.15	12.09
34	47.01	38.92	54.31	38.54	56.09	27.94
35	63.20	52.34	69.81	63.73	64.56	39.69
36	17.45	19.58	23.16	16.79	9.96	0.00
37	59.19	82.15	83.97	64.89	47.98	43.47
38	76.47	69.73	77.72	59.65	55.64	52.96
39	74.39	77.57	77.82	67.04	47.17	49.14
40	77.54	75.54	85.62	85.53	59.45	46.71

Table-A6: Represents the data from MBF screening in single condition for K562 cells and cisplatin treatment

	MBF Only	MBF+Cisplatin	MBF Only	MBF+Cisplatin	MBF Only	MBF+Cisplatin
1	106.37	58.08	63.78	61.21	90.76	60.22
3	92.38	50.52	87.83	44.94	84.38	47.31
4	87.43	52.88	89.29	52.04	68.92	37.78
5	96.96	69.29	87.50	41.70	57.20	39.83
6	96.81	69.26	85.97	62.29	57.01	39.30
7	36.72	38.39	27.85	41.67	51.46	43.78
8	118.07	73.96	86.36	83.87	93.53	63.71
9	107.01	55.28	51.79	57.30	74.87	49.06
10	76.54	69.99	60.71	53.69	62.10	42.58
11	101.30	71.08	81.33	39.47	46.49	36.01
12	82.84	90.26	77.00	61.76	41.62	37.66
13	68.56	74.71	76.51	56.47	58.77	44.69
14	99.51	57.13	66.02	68.04	68.92	55.69
15	93.24	64.64	89.50	62.09	73.08	53.34
16	91.03	44.06	73.19	51.58	77.26	41.09
17	104.19	54.30	93.24	48.40	77.11	41.56
18	91.77	65.36	80.81	43.23	59.21	37.97
19	94.22	73.26	100.34	69.82	47.73	42.40
21	79.38	51.29	63.83	53.34	21.52	16.78
22	80.92	54.11	82.30	56.85	67.02	48.18
23	91.33	60.25	54.77	64.20	85.53	54.86
24	84.30	63.81	55.16	56.91	68.85	36.27
25	100.19	49.14	60.83	46.20	76.46	38.25
26	95.57	40.88	73.35	43.84	70.79	39.61
27	92.03	56.93	74.55	44.18	51.79	34.06
28	133.23	58.96	59.60	62.25	49.41	40.13
29	95.75	44.15	70.02	62.91	77.29	54.10
30	110.17	75.83	78.02	67.95	84.49	42.88
31	62.26	54.42	89.57	63.04	74.97	45.32
32	133.74	64.74	82.80	48.03	55.61	35.83
33	84.38	65.97	97.29	63.95	58.00	37.03
34	96.83	61.51	75.75	56.13	69.49	45.34
35	7.68	5.19	7.58	11.28	11.87	12.75

36	97.92	75.82	77.43	64.01	77.27	53.72
37	13.89	3.87	12.29	9.46	4.44	0.71
38	103.59	57.51	90.04	59.42	74.57	42.26
39	76.25	56.95	74.24	69.13	56.11	43.19
40	83.32	54.50	63.71	46.60	62.50	54.19

Table-A7: Represents the data from MBF screening in single condition for SH-Y5Y cells and imatinib treatment

	MBF Only	MBF+Imatinib	MBF Only	MBF+Imatinib	MBF Only	MBF+Imatinib
1	95.64	106.83	83.92	71.21	91.68	80.56
2	83.67	109.64	81.02	66.54	123.23	114.01
3	96.94	101.16	76.90	78.34	126.07	104.98
4	100.93	95.95	83.77	86.46	110.60	105.02
5	83.29	95.99	98.50	105.91	107.35	116.83
6	91.08	93.68	86.61	80.41	102.33	98.01
7	94.97	102.84	80.19	85.99	111.77	107.60
8	105.16	99.30	81.71	82.75	104.11	86.81
9	85.79	89.01	98.15	89.45	120.90	123.32
10	101.27	101.21	84.36	86.48	110.85	96.92
11	85.35	98.67	84.86	92.82	105.38	77.78
12	91.94	89.56	88.74	91.08	103.55	104.86
13	99.63	48.07	97.32	96.96	112.78	103.61
14	98.14	93.59	80.03	81.23	101.52	94.06
15	80.83	81.61	82.89	91.31	123.23	74.68
16	123.38	93.74	80.99	89.10	115.77	96.68
17	108.52	86.73	99.34	93.35	136.67	98.13
18	56.23	53.28	86.56	80.75	126.88	97.73

Table-A7: Represents the data from MBF screening in single condition for SH-Y5Y cells and cisplatin treatment

	MBF Only	MBF+Cisplatin	MBF Only	MBF+Cisplatin	MBF Only	MBF+Cisplatin
1	62.59	8.65	79.60	88.79	75.14	36.86
2	91.00	89.07	84.49	67.83	78.21	19.03
3	88.52	81.56	82.31	64.97	64.22	41.17
4	84.47	63.46	76.40	77.72	70.53	33.78
5	86.95	58.03	73.60	66.04	81.63	34.47
6	91.17	73.01	66.38	76.51	73.53	51.31
7	85.16	67.92	92.26	86.13	59.19	36.40
8	83.54	80.11	83.22	101.10	70.16	28.81
9	97.49	84.45	80.44	104.30	78.29	53.86
10	59.96	9.40	74.84	76.39	71.93	51.03
11	92.17	81.87	86.38	79.22	64.93	23.14
12	93.48	68.95	88.81	81.32	81.35	50.16
13	82.18	72.54	70.19	79.07	72.22	75.71
14	86.30	76.23	87.21	88.58	70.43	50.08
15	76.43	77.65	76.24	83.62	64.03	56.78
16	83.33	71.33	70.44	90.03	65.58	63.80
17	74.18	13.13	93.32	93.58	63.09	58.71
18	84.74	73.19	84.95	77.94	62.27	56.90

APPENDIX 3

CHEMICAL STRUCTURES OF TKIS

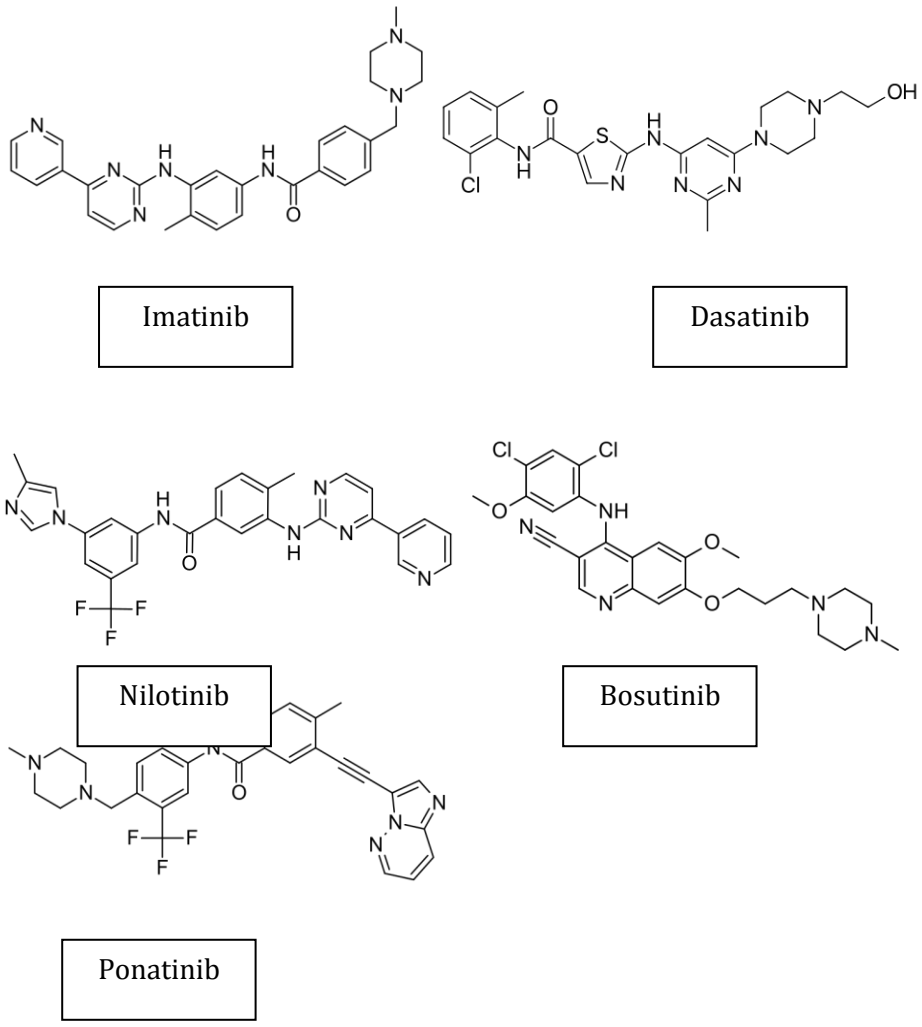

Figure A-1 TKIs chemical structures

APPENDIX 4

STATISTICAL ANALYSIS

In section 2.7.5 the statistical analysis method was described completely, so the test for analysis, used for different gene expressions were different based on their normal distribution. Three following tables categorised the statistical test for each gene. The fist table the gene expression in K562 cells and imatinib treatments (for figure 3.29, section 3.5.3), the second table is for K562 cells and cisplatin treatment (for figure 3.30, section 3.5.4) and the last one is for SH-SY5Y cells and drug treatment (for figure 3.31, section 3.5.5).

Transporter	Statistical test
ABCB1	ANOVA- (Tukey HSD)
ABCB10	ROBUST tests of equality of means- (Tukey HSD)
ABCC1	ANOVA- (Tukey HSD)
ABCG2	ANOVA- (Tukey HSD)
SLCO1A2	ROBUST tests of equality of means- (Tukey HSD)
	ROBUST tests of equality of means- (Tukey HSD)
BCR-ABL	ROBUST tests of equality of means- (Tukey HSD)

Table A9- The statistical test for each gene this table is related to section 3.5.3; Identification of expression for cell transporters by with imatinib and candidate MBFs in K562 cells

Transporter	Statistical test
ABCB1	ROBUST tests of equality of means- Games of HOWELL
ABCB10	ROBUST tests of equality of means- Games of HOWELL
ABCC1	ANOVA- Games of HOWELL
ABCG2	ANOVA- Games of HOWELL
SLCO1A2	ANOVA- Games of HOWELL
SLC22A1	ANOVA- Games of HOWELL
BCR-ABL	ANOVA- Games of HOWELL

Table A10- The statistical test for each gene this table is related to section 3.5.4. Identification of expression for cell transporters by with cisplatin and candidate MBFs in K562 cells

Transporter	Statistical test
ABCB1	ANOVA- Games of HOWELL
ABCB10	ROBUST tests of equality of means- Games of HOWELL
ABCC1	ANOVA- Games of HOWELL
ABCG2	ANOVA- Games of HOWELL
SLCO1A2	ANOVA- Games of HOWELL
SLC22A1	ANOVA- Games of HOWELL
BCR-ABL	ANOVA- Games of HOWELL

Table A11- The statistical test for each gene this table is related to section 3.5.5. Identification of expression for cell transporters by with cisplatin and imatinib in SH-SY5Y cells

APPENDIX 5

CHEMICAL STRUCTURES OF SELECTED MBFS (HITS)

The following table shows the chemical structure of MBFs, most of these selected MBFs have aromatic cycles in their structures.

Library No. of MBF	Chemical structure	Formula	MW g/mol	Bioassay Results
161	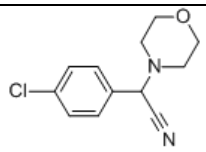	2-(4-chlorophenyl)-2-morpholinoacetonitrile C12H13ClN2O	236.7	Multiplexed high-throughput screen for small molecule regulators of RGS family protein interactions, specifically RGS7-Galphao
329	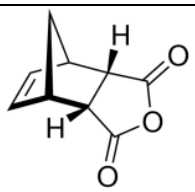	2,5-dimethyl-3-furoic acid C7H8O3	140.14	qHTS Assay for Inhibitors of the Human Apurinic/apyrimidinic Endonuclease 1 (APE1)
249	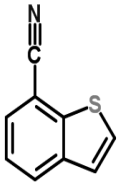	Benzo[b] thiophene-7-Carbonitrile C9H5NS	159.21	Inhibition of CYP2A6 in human liver microsomes assessed as inhibition of coumarin 7-hydroxylation after 10 mins by plate reader
258	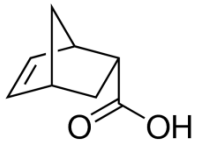	5-Norbornene-2-carbonitrile, mixture of endo and exo C8H10O2	138.16	NCI In Vivo Anticancer Drug Screen. Data for tumour model L1210 Leukaemia (intraperitoneal) in CD2F1 (CDF1) mice.

213	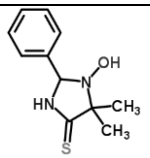	1-hydroxy-5,5-dimethyl-2-phenyltetrahydro-4H-imidazole-4-thione C11H14N2OS	222.31	Evaluated for inhibition of specific [3H] 5-HT receptor binding in rat cortex.
245	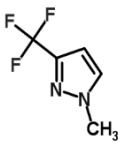	1-methyl-3-(trifluoromethyl)-1H-pyrazole C5H5F3N2	150.104	Multiplexed high-throughput screen for small molecule regulators of RGS family protein interactions, specifically RGS7-Galphao.
247	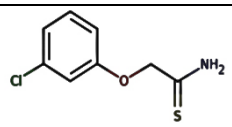	2-(3-chlorophenoxy)ethanethioamide C8H8ClNOS	201.67	Bioassay name: p450-cyp1a2
323	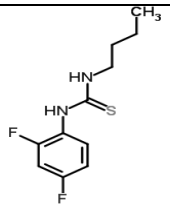	N-butyl-N'-(2,4-difluorophenyl)thiourea C11H14F2N2S	244.30	Fluorescence Polarization Cell-Free Homogeneous Primary HTS to Identify Inhibitors of the LANA Histone H2A/H2B Interaction.
94	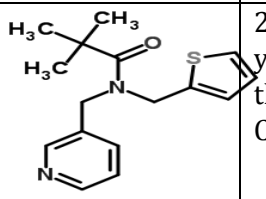	2,2-dimethyl-N-(pyridin-3-ylmethyl)-N-(2-thienylmethyl)propanamide C19H32BNO2	381.27	No results
319	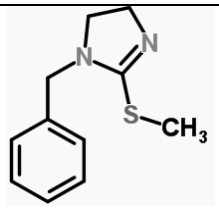	1-benzyl-2-(methylthio)-4,5-dihydro-1H-imidazole hydroiodide C11H15	334.220	Inhibition of inosine/L-alanine-induced Bacillus anthracis Sterne 34F2 spore germination pre-treated for 15 mins before inosine/L-alanine challenge.

357	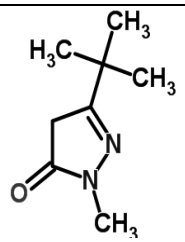	3-(tert-butyl)-1-methyl-4,5-dihydro-1H-pyrazol-5-one C8H14N2O	154.2	NCI Yeast Anticancer Drug Screen. Data for the rad50 strain.
365	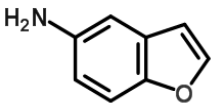	1-benzofuran-5-amine C8H7NO	133.15	Aqueous Solubility from MLSMR Stock Solutions.
292	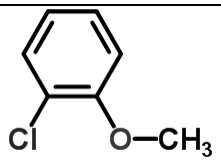	2-Chloroanisole ClC6H4OCH3	142.58	NCI In Vivo Anticancer Drug Screen. Data for tumour model L1210 Leukaemia (intraperitoneal) in B6D2F1 (BDF1) mice.

Table A12- Represents the chemical structures of MBFs